On Relating Aspects of Tropical Geometry, Cluster Algebras, and Zonotopal Algebras

vorgelegt von
Diplom-Mathematiker
Sarah Brodsky
Evanston

Von der Fakultät II – Mathematik und Naturwissenschaften
der Technischen Universität Berlin
zur Erlangung des akademischen Grades

Doktor der Naturwissenschaften
Dr. rer. nat.

genehmigte Dissertation

Promotionsausschuss

Vorsitzender: Prof. Dr. Martina Hofmanova
Berichterin: Prof. Dr. Olga Holtz
Berichter: Prof. Dr. Michael Joswig
Berichter: Prof. Dr. Felipe Rincón

Tag der wissenschaftlichen Aussprache: 29. September 2016

Berlin 2016

Abstract

Each chapter of this dissertation touches upon subjects which at first glance may not seem related. Upon subtle inspection, aspects of tropical geometry, cluster algebras, and zonotopal algebra all relate to the combinatorics of the associahedra and are used to study mirror symmetry, scattering amplitudes, and other aspects of quantum mechanics. This dissertation is a collection of works which aim to strengthen the connections between the mathematical fields of tropical geometry, cluster algebras, and zonotopal algebra, as well as to strengthen their utility in the toolboxes of quantum mechanical studies.

We begin with cluster algebras. It has been established in recent years how to approach acyclic cluster algebras of finite type using subword complexes. In chapter I, we continue this study by showing that the extended part of the mutation matrix coincides with the root configuration in the root space, and by starting to describe the Newton polytopes of the F-polynomials in the weight space. This chapter is based on unpublished work with Christian Stump.

Next we move on to where cluster algebras and tropical geometry meet; in chapter II, we show that the number of combinatorial types of clusters of type D_4 modulo reflection-rotation is exactly equal to the number of combinatorial types of tropical planes in $\mathbb{TP}^5$. This follows from a result of Sturmfels and Speyer which classifies these tropical planes into seven combinatorial classes using a detailed study of the tropical Grassmannian $\mathrm{Gr}(3,6)$. Speyer and Williams show that the positive part $\mathrm{Gr}^+(3,6)$ of this tropical Grassmannian is combinatorially equivalent to a small coarsening of the cluster fan of type D_4. We provide a structural bijection between the rays of $\mathrm{Gr}^+(3,6)$ and the almost positive roots of type D_4 which makes this connection more precise. This bijection allows us to use the pseudotriangulations model of the cluster algebra of type D_4 to describe the equivalence of "positive" tropical planes in $\mathbb{TP}^5$, giving a combinatorial model which characterizes the combinatorial types of tropical planes using automorphisms of pseudotriangulations of the octagon. This chapter is based on work with Cesar Ceballos and Jean-Philippe Labbé [14].

Next we go a bit deeper into tropical geometry, and study the moduli space of metric graphs that arise from tropical plane curves in chapter III. There are far fewer such graphs than tropicalizations of classical plane curves. For fixed genus g, our moduli space is a stacky fan whose cones are indexed by regular unimodular triangulations of Newton polygons with g interior lattice points. It has dimension $2g + 1$ unless $g \leq 3$ or $g = 7$. We compute these spaces explicitly for $g \leq 5$. This chapter is based on joint published work with Michael Joswig, Ralph Morrison, and Bernd Sturmfels [13].

Lastly, we touch upon zonotopal algebras in chapter IV, linking the machinery of zonotopal algebra with two particular polytopes: the Stanley-Pitman polytope and the regular simplex $\mathfrak{Sim}_n(t_1, ..., t_n)$ with parameters $t_1, ..., t_n \in \mathbb{R}_+^n$, defined by the inequalities $\sum_{i=1}^n r_i \leq \sum_{i=1}^n t_i$, $r_i \in \mathbb{R}_+^n$, where the $(r_i)_{i \in [n]}$ are variables. Specifically, we will discuss the central Dahmen-Micchelli space of the broken wheel graph BW_n and its dual, the $\mathcal{P}$-central space. We will observe that the $\mathcal{P}$-central space of BW_n is monomial, with a basis given by the BW_n-parking functions. We will show that the volume polynomial of the the Stanley-Pitman polytope lies in the central Dahmen-Micchelli space of BW_n and is precisely the polynomial in a particular basis of the central Dahmen-Micchelli space which corresponds to the monomial $t_1 t_2 \cdots t_n$ in the dual monomial basis of the $\mathcal{P}$-central space. We will then define the generalized broken wheel graph $GBW_n(T)$ for a given rooted tree T on n vertices. For every such tree, we can construct 2^{n-1} directed graphs, which we will refer to as *generalized broken wheel graphs*. Each generalized broken wheel graph constructed from T will give us a polytope, its volume polynomial, and a *reference monomial*. The 2^{n-1} polytopes together give a polytopal subdivision of $\mathfrak{Sim}_n(t_1, ..., t_n)$, their volume polynomials together give a basis for the subspace of homogeneous polynomials of degree n of the corresponding central Dahmen-Micchelli space, and their reference monomials together give a basis for its dual. This chapter is based on unpublished work with Amos Ron.

Zusammenfassung

Jedes Kapitel dieser Dissertation behandlet Themenbereiche welche auf den ersten Blick unzusammenhängend erscheinen mögen. Bei genauerer Betrachtung jedoch stellt man fest, dass tropische Geometrie, die Theorie der Cluster Algebren und Zonotopische Algebra enge Verbindungen zur Kombinatorik von Assoziaedern vorweisen und das jene Gebiete Anwendung in der Untersuchung von Spiegelsymmetrie, Streuamplituden und weiterer Aspekten der Quantenmechanik finden. Diese Dissertation ist eine Sammlung von Arbeiten, deren Ziel es ist einerseits die Zusammenhänge der mathematischen Gebiete der tropischen Geometrie, der Theorie der Cluster Algebren und zonotopaler Algebra zu vertiefen und andererseits den Nutzen genau dieser Gebiete als Werkzeuge der Quantenmechanik zu stärken.

Wir beginnen mit Cluster Algebren. In den letzten Jahren stellte sich heraus wie azyklische Cluster Algebren endlichen Typs mit Hilfe von Teilwortkomplex is the literal translation untersucht werden können. In Kapitel I führen wir diese Bemühungen fort, indem wir zeigen, dass der erweiterte Teil der Mutationsmatrix mit der Wurzelkonfiguration im Wurzelraum übereinstimmt und indem wir beginnen die Newtonpolytope der F-Polynome im Gewichtsraum zu beschreiben. Dieses Kapitel basiert auf bisher unveröffentlichter Arbeit mit Christian Stump.

Im nächsten Themenkomplex treffen sich Cluster Algebren und tropische Geometrie; in Kapitel II zeigen wir, dass die Zahl der kombinatorischen Typen von Clustern des Typs D_4 modulo Drehspiegelungen der Anzahl kombinatorischer Typen von tropischen Ebenen in $\mathbb{TP}^5$ entspricht. Dies folgt aus einem Resultat von Sturmfels und Speyer, welches – mittels einer detaillierten Untersuchung der tropischen Grassmannschen $\mathrm{Gr}(3,6)$ – diese tropischen Ebenen in sieben kombinatorische Klassen einteilt. Speyer und Williams zeigten, dass der positive Teil $\mathrm{Gr}^+(3,6)$ dieser tropischen Grassmannschen kombinatorisch äquivalent zu einer leichten Vergröberung des Clusterfächers vom Typ D_4 ist. Wir geben eine strukturelle Bijektion zwischen den Strahlen von $\mathrm{Gr}^+(3,6)$ und den fast positiven Wurzel vom Typ D_4 an, welche diese Verbindungen präzisiert. Diese Bijektion erlaubt es uns das Pseudotriangulierungsmodell für Cluster Algebren des Typs D_4 zu nutzen, um die Äquivalenz „positiver"tropischer Ebenen in $\mathbb{TP}^5$ zu beschreiben, womit wir ein kombinatorisches Modell erhalten, das die kombinatorischen Typen tropischer Ebenen mittels Automorphismen von Pseudotriangulieren des Oktagons charakterisiert. Diese Kapitel basiert auf gemeinsamer Arbeit mit Cesar Ceballos und Jean-Philippe Labbé [14].

Als nächstes beschäftigen wir uns näher mit tropischer Geometrie und untersuchen in Kapitel III den Modulraum der metrischen Graphen, die als tropische ebene Kurven auftreten. Es gibt weit weniger Graphen dieser Form als Tropikalisierungen klassischer ebener Kurven. Für festes Geschlecht g ist unser Modulraum ein stacky Fächer, dessen Kegel von regulären unimodularen Triangulierungen von Newtonpolygonen mit g inneren Gitterpunkten indiziert sind. Er hat Dimension $2g+1$, außer für $g \leq 3$ und $g = 7$. Wir berechnen diese Räume explizit für $g \leq 5$. Dieses Kapitel basiert auf gemeinsamer Arbeit mit Michael Joswig, Ralph Morrison und Bernd Sturmfels [13].

Zuletzt betrachten wir zonotaple Algebren in Kapitel IV, indem wir die Maschinerie zonotapler Algebren mit zwei speziellen Polytopen verknüpfen: Das Stanley-Pitman Polytop und der reguläre Simplex $\mathfrak{Sim}_n(t_1,...,t_n)$ mit Parametern $t_1,...,t_n \in \mathbb{R}^n_+$, definiert durch die Ungleichungen $\sum_{i=1}^n r_i \leq \sum_{i=1}^n t_i$, $r_i \in \mathbb{R}^n_+$, wobei $(r_i)_{i\in[n]}$ Variablen sind. Insbesondere werden wir den zentralen Dahmen-Micchelli Raum des Broken Wheel Graph BW_n und dessen dualen Graphen untersuchen. Wir werden sehen, dass der $\mathcal{P}$-zentrale Raum von BW_n monomial ist, wobei die Basis gegeben ist durch die BW_n-parking Funktionen. Wir werden zeigen, dass das Volumenpolynom des Stanley-Pitman Polytops im zentralen Dahmen-Micchelli Raum von BW_n liegt und mit dem Polynom in einer gewissen Basis des zentralen Dahem-Micchelli Raums übereinstimmt, welches zu dem Monom $t_1 t_2 \cdots t_n$ in der dualen monomialen Basis des $\mathcal{P}$-zentralen Raums korrespondiert. Wir werden den verallgemeinerten Broken Wheel Graph $GBW_n(T)$ für einen gegeben Baum T mit n Knoten definieren. Für jeden solchen

Baum können wir 2^{n-1} gerichtete Graphen definieren, welche wir verallgemeinerte Broken Wheel Graphen nennen werden. Für jeden solchen verallgemeinerten Broken Wheel Graph erhalten wir ein Polytop, sein Volumenpolynom und ein *Referenzmonom*. Die 2^{n-1} Polytope gemeinsam betrachtet liefern eine polytopale Unterteilung von $\mathfrak{Sim}_n(t_1, ..., t_n)$, ihre Volumenpolynome ergeben zusammen eine Basis des Unterraums der homogenen Polynome von Grad n des korrespondierenden zentral Dahmen-Micchelli Raums und ihre Referenzmonome ergeben zusammen eine Basis des Dualen. This Kapitel basiert auf unveröffentlichter Arbeit mit Amos Ron.

Preface

The research presented in this dissertation lies in the fields of tropical geometry, cluster algebras, and zonotopal algebras, and has the intention of making the boundaries between theses fields more clear. I am interested in studying various aspects of these fields and how they link together in relation to the work of Alexander B. Goncharov, Alexander Postnikov, and others on scattering amplitudes and the positive Grassmannian [3]. Their work sets a mathematical framework for understanding the movements of massless particles and their potential for interacting with one another. The behaviour of massless particles is calculated via directed graphs, called *plabic graphs*, with bicolors vertices, in which an integral system is associated. These plabic graphs can be mapped into the positroid stratification of the Grassmannian, with an inverse map given by ⅃-diagrams of Postnikov [93]. The plabic graphs of each fiber of this map are related by a set of particular *moves* which change the vertex colors and directions of the edges; these moves are described by Postnikov in [93]. When a move is performed on a plabic graph, the coordinates of its associated integrable system change. The relations describing these changes are exactly those of a cluster algebra.

Specifically, the cluster algebras which appear in the study of plabic graphs are those which relate to the postive part of the Grassmannian. There are such cluster algebras of both *finite* and *infinite* type whose underlying geometric structure is that of a Grassmannian. The connection between certain cluster algebras of finite type and the Grassmannian was first introduced by Sergey Fomin and Andrei Zelevinsky [42]. Speyer and Williams [102] were the first to show a connection between certain cluster algebras of finite type and the positive part of the tropical Grassmannian, suggesting that the tropicalization of the positive part of the Grassmannian more accurately fits the combinatorial structure of the cluster algebras in question. They provide a parameterization for the positive part of the tropical Grassmannian as well as describe a fan which combinatorially captures the maximal cells of the positive part of the tropical Grassmannian.

The box spline is a multivariate function $\mathbb{R}^d \to \mathbb{R}$ used widely in approximation and interpolation theory. The box spline is very much an object of "applied" mathematics, frequently being used for problems such as surface modeling and multidimensional signal processing. Behind this very practical mathematical object is a wealth of pure mathematics. Box splines are piecewise polynomial functions of several variables which have many well-studied algebraic and combinatorial objects associated to it: matroids, hyperplane arrangements, toric arrangements, polytopes, and zonotopal spaces, which were introduced by Amos and Holtz in [59].

These algebraic and combinatorial objects associated to box splines are also found, in particular, in the study of Lie groups and cluster algebras. As every cluster algebra is also related to a generalized associahedra, by working backwards and uncovering the zonotopal structure of the associahedra, a connection between box splines and cluster algebras can be made, thus establishing a potential link between box splines and the physics captured by scattering amplitudes. This link could help physicists make measurements on the physical spaces captured by cluster algebras they study and analyze probability distributions and other data they associate to cluster algebras. Furthermore, some of the zonotopal spaces associated to box splines capture certain solution sets to systems of differential equations. Thus, this link could also shed some light on the differential equations needed to model the physical behaviour modeled by scattering amplitudes.

This dissertation is composed of four works whose motivation comes from the story just told. They are more or less unchanged, with some modifications where appropriate.

Chapter I is based on an unpublished project with Christian Stump. My role in this project was in working closely with Christian to prove the results presented in this chapter.

Chapter II is based on a project with Cesar Ceballos and Jean-Philippe Labbé [14] which has been submitted to the journal *Beiträge zur Algebra und Geometrie*. My role in this project was in working with Cesar and Jean-Philippe to prove the results presented in this chapter as well as working with Jean-Philippe on all computations needed.

Chapter III is based on a project with Michael Joswig, Ralph Morrison, and Bernd Sturmfels [13] which has been published in *Research in the Mathematical Sciences*. My role in this project was to work closely with Michael Joswig on performing the computations needed and documenting the computational methods used.

Chapter IV is based on an unpublished project with Amos Ron. My role in this project was to work with Amos to prove and write-up all results presented in this chapter.

Acknowledgements. I realize in hindsight that I have been a mathematician for a significant part of my life now. During this time, I have met many people in my personal and academic life who have kept me strong, passionate, and curious. It is hard to know exactly where or with whom to begin to acknowledge. With quite some thought I have managed to go back to the beginning of my memories of my mathematical journey and comb through them to find many particular individuals and groups of people I hold a deep appreciation for during this time. Let me start from the beginning of my time as a mathematician and work my way forward.

I started to become a mathematician along side Henry Tucker. Henry, thank you for being such a good person and friend. You were a motivating force in my decision to pursue mathematics and I thank you for it.

The frequenters of the Haste House will also always have a place in my heart. Josh Abramson, George Melvin, Alex Paulin, Ingrid Melvær Paulin, Josh Abbott, Zach Bowen, and Jane Tivol. It was a very good, unforgettable time that we all had together. Thank you for adding a lot of richness to my Berkeley life, though the good times and the bad. And for supporting me throughout.

I would not have really discovered my passion for mathematics if it was not for Bernd Sturmfels. Bernd, thank you for having so much faith and confidence in me, even when I did not have it for myself. Thank you for encouraging me and challenging me. Thank you for all the opportunities you enabled for me. Thank you for always caring, though the good times and the bad. I will never forget all that you have done to support me during my mathematical journey. I cannot thank you enough.

Melody Chan, Alex Fink, and Felipe Rincón. Thank you guys for being such solid friends and mentors. You guys are just so amazing! And make me feel like I can be amazing too. Especially during the times when I needed to be reminded of this the most. Thank you.

Thank you Kris Nairn. Without you I would have never broken free from my Grizzly Peak prison and have found the courage in myself to pursue what I want and what makes me happy. You gave me the extra kick I needed to follow my passion and become a mathematician.

Thank you Hannah Markwig, Thomas Markwig, and Andreas Gathmann. For Kaiserslautern. For giving me an opportunity to experience life and mathematics in Germany for the first time. Thank you for being so kind and supportive towards me. Thank you for accepting me as your own and giving me so many opportunities to grow, both personally and intellectually. My experience in Kaiserslautern was profound and unforgettable; I cannot thank you enough for giving it to me.

Kim Laine, Andy Voellmer, and Daniel Appel. Thank you for being such amazing friends. You guys made me feel accepted and like I had a place in a community I struggled to fit into. Kim, it was so incredibly fun to spend endless hours in Evans solving commutative algebra problems with you. Andy and Dan, you were the best officemates anybody could ever ask for!

With you two I never felt like a misfit. Speaking to you guys about everything mathematical, philosophical, and personal are highlights of my time in Evans.

Maria G. Martinez and Anastasia Chavez. You guys are such strong, incredible women. I am in awe of your courage, your drive, and your ability to stand against all odds, and all those you encounter to are blinded by their own ignorance. Again and again. I respect you both so much.

Yael Degany, you are perhaps the smartest, wisest, and most thoughtful person I know. Every conversation I have had with you has been a deep and profound one. Thank you for your words. Thank you for your advice. Thank you for encouraging me. For accepting me. Thank you for your attention and your patience. Thank you for always reminding me to stay focused; for what I focus on grows.

Thank you HiP House for showing me what a family feels like. Thank you for giving me space to be myself and to grow into the person I am today. Thank you Tim Ruckle, Kim Lucas, and Jennie Zhao, in particular. Thank you for being there with me through all the anxiety.

Thank you Team China Doll: Aga Czeszumska, Anastasia Victor, John Faichney, Nathan Boley, Carolyn Cotterman, Dave Lu, Steven Brummond, Win Mixter, and Trevor Owens. I love you guys! I don't know how I would have made it through without you guys around helping me to keep the colors bright and my spirits high.

I could not have asked for a more amazing person to be my advisor than Olga Holtz. Olga, thank you so much for believing in me. For listening to me and understanding me. Thank you for having faith in me when even I had none. Thank you for your support, your wisdom, and all of our conversations, both mathematical and otherwise. Thank you for giving me the courage to explore, while still being there to advice me on any matter when I needed it. You are an amazing person and a role model. I am honored to be your mathematical descendant.

Thank you to my two mathematical brothers, Matthias Lenz and Bryan Gillespie, for being so kind, helpful, and positive. I am so grateful to have such good people as mathematical siblings.

Heather Heintzel, thank you for being my friend and always being there for me. To listen. To advise. To just have a nice chat. You really brightened my days.

Thank you to my tropical geometry community for being so awesome! In particular, Spencer Backman, Ralph Morrison, Yoav Len, Tif Shen, Nathan Pflueger, Tyler Foster, Farbod Shokrieh, Philipp Vollmer, Marvin Hahn, and Binglin Li. Any time I started to lose my passion for mathematics, I knew that all I needed was a conference with you guys to remind me of how awesome my community is and the work that we all do.

Thank you Michael Joswig for being my mentor, for working with me, and for treating me as a student of your own. Thank you Kristin Shaw, Fatemeh Mohammadi, Kathlén Kohn, and Carlos Améndola for always including me and making me feel welcome. Your kindness made all the difference in the world to me.

Jean-Philippe Labbé, Cesar Ceballos, and Christian Stump. Thank you guys for all the awesome mathematics! I have so much fun with you guys talking about mathematics and I always really looked forward to meeting with you all to talk about our projects. I am so happy to have found people I really like to do mathematics with.

Helga Zeike, Cori Dressler, and Danielle Keiser. Thank you three for being such grounding friends of mine. You guys are such positive, rational forces in my life.

And my Shandy Bisqwuits: Kyra Edeker, Michael Gomez, Lisa Kirchner, Flora Petersen, Gregor Sohn, Woutr Jaspers, Karin Weissenbrunner, Jamie Morrow, Marianne Jungmaier, and Thilo Maluch. Thank you all for being my family. For being so chill and together. For building things with me. For giving me so much love. For making me feel at home. I am so lucky to have you all in my life.

Finally I would like to thank my dissertation committee, Martin Henk, Olga Holtz, Michael Joswig, and Felipe Rincón for reviewing and supporting this dissertation, Marvin Hahn for translating my abstract into German, and the NSF graduate student fellowship, Berkeley Chancellor's fellowship, the ERC starting grant awarded to Olga Holtz, and the BMS graduate student grant for supporting me financially during this process.

Berlin, July 2016

Sarah Brodsky

Contents

Cluster Algebras

Let (W, S) be a finite crystallographic Coxeter system of rank n with simple system S, and let $c \in W$ be a standard Coxeter element for (W, S); *i.e.* $c = s_1 \cdots s_n$ is the product of all elements in S in some order. Let $A = (a_{st})_{s,t \in S}$ be a crystallographic Cartan matrix for (W, S); *i.e.* an integral matrix $(a_{st})_{s,t \in S}$ such that $a_{ss} = 2$, $a_{st} \leq 0$, $a_{st}a_{ts} = 4\cos^2(\frac{\pi}{m_{st}})$ and $a_{st} = 0 \Leftrightarrow a_{ts} = 0$ for all $s \neq t \in S$ where m_{st} is the order of st in W, and let $\Delta \subseteq \Phi^+ \subseteq \Phi_{\geq -1} \subseteq \Phi \subseteq L = \mathbb{Z}\Delta$ be the resulting root system with simple roots $\Delta = \{\alpha_s \,:\, s \in S\}$, positive roots Φ^+, and almost positive roots $\Phi_{\geq -1} = \Phi^+ \sqcup -\Delta$. For convinience, we also set $\alpha_i := \alpha_{s_i}$. As $a_{st} = 0$ if and only if $st = ts$, we think of a the standard Coxeter element c as an acyclic orientation of the Dynkin diagram by orienting an edge $s \to t$ if s comes before t in any given but *fixed* reduced word $\mathsf{c} = \mathsf{s}_1\mathsf{s}_2 \cdots \mathsf{s}_n$.

Associating an initial seed of a cluster algebra of finite type with principal coefficients to this data is well established; we refer to [**39**] (and also to [**37, 38**]) for all needed background on cluster algebras: for a given such orientation of the Dynkin diagram, define the skew-symmetrizable matrix $\mathsf{M}_c = (b_{st})_{s,t \in S}$ by

$$b_{st} = \begin{cases} -a_{st} & \text{if } s \to t, \\ a_{st} & \text{if } s \leftarrow t, \\ 0 & \text{else.} \end{cases}$$

The initial cluster seed is then given by $(\widetilde{\mathsf{M}}_c, \mathbf{x}, \mathbf{y})$ where the (extended) exchange matrix $\widetilde{\mathsf{M}}_c$ is the $(2n \times n)$-matrix $\begin{bmatrix} \mathsf{M}_c \\ \mathbb{1}_n \end{bmatrix}$ with principal part M_c and extended part $\mathbb{1}_n$ being an identity matrix, $\mathbf{x} = (x_1, \ldots, x_n)$ are the cluster variables (the cluster of the seed), and $\mathbf{y} = (y_1, \ldots, y_n)$ are the frozen variables (the coefficients of the seed). One should think of the variables x_k and y_k as being indexed by α_k for all $1 \leq k \leq n$, so they are indexed in a way that is consistent with the order of the simple reflections in the given Coxeter element c. Let $\mathcal{A}(W, c) := \mathcal{A}(\widetilde{\mathsf{M}}_c)$ be the cluster algebra generated from this initial seed.

It is known that every cluster variable $u(\mathbf{x}, \mathbf{y}) \in \mathcal{A}(W, c)$ lives inside the ring

$$\mathbb{Z}[x_1^{\pm 1}, \ldots, x_n^{\pm 1}; y_1, \ldots, y_n];$$

i.e. $u(\mathbf{x}, \mathbf{y}) = p(\mathbf{x}, \mathbf{y}) / \mathrm{m}(\mathbf{x})$ where $p(\mathbf{x}, \mathbf{y})$ is a polynomial in $\mathbf{x}, \mathbf{y}$ with integer coefficients and $\mathrm{m}(\mathbf{x})$ in a monomial in $\mathbf{x}$, see [**39**, Proposition 3.6]. The *d-vector* $d(u)$ of $u(\mathbf{x}, \mathbf{y})$ is the exponent vector of the denominator monomial $\mathrm{m}(\mathbf{x})$, *i.e.*, $d(u) = (d_1, \ldots, d_n)$ for $\mathrm{m}(\mathbf{x}) = x_1^{d_1} \cdots x_n^{d_n}$ and should be thought of as a vector in the basis Δ, *i.e.*, $d(u) = d_1\alpha_1 + \ldots + d_n\alpha_n \in L$. Under this identification, it was shown in [**38**, Theorem 1.9], that the map $u \mapsto d(u)$ is a bijection between all cluster variables in $\mathcal{A}(W, c)$ and the almost positive roots $\Phi_{\geq -1}$, and that furthermore, $d(u) = -\alpha_i \in -\Delta \Leftrightarrow u(\mathbf{x}, \mathbf{y}) = x_i^{-1}$. We will regularly use this bijection in indexing objects. For example, set $F_u(\mathbf{y}) = F_\beta(\mathbf{y}) = u(\mathbf{1}, \mathbf{y}) = p(\mathbf{1}, \mathbf{y})$ to be the *F-polynomial* associated to $u(\mathbf{x}, \mathbf{y}) \in \mathcal{A}(W, c)$ and to $\beta \in \Phi_{\geq -1}$ with $d(u) = \beta$. (As $F_\beta(\mathbf{y}) = 1$ for $\beta \in -\Delta$, one often considers F-polynomials only associated to positive roots.)

We also think of any exchange matrix $\widetilde{\mathsf{M}} = \begin{bmatrix} \mathsf{M}^{pr} \\ \mathsf{M}^{ex} \end{bmatrix}$ of a cluster seed of $\mathcal{A}(W, c)$ with cluster $\{u_1, \ldots, u_n\}$ as being indexed as follows: Row and column i of M^{pr} are both indexed by the almost positive root associated to u_i. Equally, column i of M^{ex} is indexed by this almost

positive root, while row i of M^{ex} is indexed by the simple root α_i. The *c-vector* $c(u) = c(\beta) \in L$ with $\beta = d(u)$ *inside the cluster* $\{u_1, \ldots, u_n\}$ is then given by the column vector of M^{ex} in the column indexed by the almost positive root β, written as a linear combination of the simple roots,

$$c(u) = c(\beta) = [\mathsf{M}^{ex}]_{\alpha_1, \beta} \alpha_1 + \ldots + [\mathsf{M}^{ex}]_{\alpha_n, \beta} \alpha_n,$$

where we emphasize that this not only depends on the variable $u(x, y)$ but on the actual seed.

Every cluster seed is uniquely determined by its cluster, and the *cluster complex* of $\mathcal{A}(W, c)$ is the simplicial complex with ground set being the set of cluster variables, and with facets being the clusters. Cluster complexes of finite type with the initial seed coming from a bipartite Coxeter element (*i.e.*, those where every vertex in the corresponding orientation of the Dynkin diagram is a sink or a source) were studied and completely described in terms of compatibility of d-vectors in [**38**]. Polytopal realizations of the cluster complex of type $\mathcal{A}(W, c)$ were first obtained by F. Chapoton, S. Fomin, and A. Zelevinsky in [**25**] for bipartite Coxeter elements, and by C. Hohlweg, C. Lange, and H. Thomas in [**57**] for general Coxeter elements.

Despite the nice combinatorial descriptions of the cluster complex and its polytopal realization in terms of the corresponding root system given by sending a cluster variable to its denominator vector, to the best of our knowledge there has not been any successful attempt to describe the numerator of the cluster variables from that perspective. In particular, no explicit construction of the cluster variables for finite type cluster algebras is known that does not use the defining iterative procedure (which we recall in Section 2).

> *The aim of this chapter is to start the program to describe the cluster variables*
> *in finite types in terms of combinatorial data from root systems.*

With this aim, we follow the recently introduced subword complex approach to finite type cluster algebras. These subword complexes were introduced by A. Knutson and E. Miller in the context of Gröbner geometry of Schubert varieties in [**70, 69**]. Their appearance in the context of finite type cluster algebras was established by C. Ceballos, J.-P. Labbé, V. Pilaud, and C. Stump in various collaborations. In particular, it was given

- ▷ a description of the cluster complex of the cluster algebra $\mathcal{A}(W, c)$ [**18**, Theorem 2.2],
- ▷ a new and rather simple description of its polytopal realization [**89**, Theorem 6.4],
- ▷ a proof that the barycenter of this realization equals the barycenter of the corresponding permutahedron [**90**, Theorem 1.1],
- ▷ an explicit description of the principal parts of the exchange matrices of the clusters [**89**, Theorem 6.20], and
- ▷ and an explicit description of the d-vectors with respect to any initial seed [**19**, Corollary 3.4].

In the present chapter, we provide the following two constructions in terms of subword complexes towards this aim. First, we show in Theorem 1.7 that the extended part of the mutation matrices of the cluster algebra $\mathcal{A}(W, c)$ coincides with the root configuration, and second, we start the development of understanding the F-polynomials for $\mathcal{A}(W, c)$ in Theorem 1.10 and Theorems 1.11 and 1.12) by describing their (partially conjectured) Newton polytopes.

Observe that the first part also implies that one obtains as well the g-vectors by considering the coroot configuration instead together with inverting the corresponding matrix. A combinatorial description of the F-polynomials would therefore be the last step to provide a complete description of the cluster variables as it is well known how to recover these from the the g-vectors and the F-polynomials, see [**39**].

Two further remarks about previous work is in order:

(i) As we will later use, R. Schiffler gave an explicit description of the cluster variables of type A_n via *T-paths* on triangulations on the regular $(n+3)$-gon [99], and G. Musiker and R. Schiffler generalized that description to cluster variables for cluster algebras associated to *unpunctured surfaces* with arbitrary coefficients [86].

(ii) N. Reading and D. Speyer provide a general combinatorial framework for cluster algebras to obtain information about exchange matrices, principal coefficients, and g-vectors in [97], see Theorems 1.5 and 1.9 for further details. As we will see there, the two approaches are closely related. The two main differences currently are that our approach has not been extended beyond finite type, while their approach only uses (their versions of) the root and the coroot configurations, while they do not use the complete (co-)root and (co-)weight functions. We will (in parts conjecturely) see in Theorem 1.10 how one can extract information about F-polynomials using the weight function.

To later see the close relationship between F-polynomials and the combinatorics of subword complexes, we provide the following well understood running example of type A_2.

EXAMPLE 0.1. The cluster variables in the cluster algebra generated from the initial seed of type A_2 with principal coefficients and their d-vectors and F-polynomials are given by:

$u(\mathbf{x}, \mathbf{y})$	$d(u) \in \Phi_{\geq -1}$	$F_u(\mathbf{y})$
$x_1 = \frac{1}{x_1^{-1}}$	$-\alpha_1$	1
$x_2 = \frac{1}{x_2^{-1}}$	$-\alpha_2$	1
$\frac{x_2 + y_1}{x_1}$	α_1	$y_1 + 1$
$\frac{x_1 y_1 y_2 + x_2 + y_1}{x_1 x_2}$	$\alpha_1 + \alpha_2$	$y_1 y_2 + y_1 + 1$
$\frac{x_1 y_2 + 1}{x_2}$	α_2	$y_2 + 1$

Any two cluster variables in cyclically consecutive rows form a cluster. The five cluster seeds and the cluster complex are thus given by:
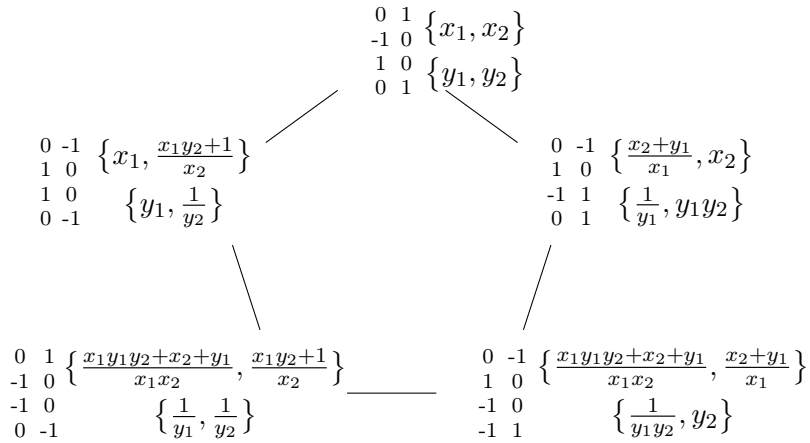
Observe that between the two clusters $\left\{ \frac{x_2 + y_1}{x_1}, x_2 \right\}$ and $\left\{ \frac{x_1 y_1 y_2 + x_2 + y_1}{x_1 x_2}, \frac{x_2 + y_1}{x_1} \right\}$, we switched the position of the common variable in the sense that the two columns and the first two rows of the mutation matrices switched. This is unavoidable and has to be done within this 5-cycle; to better keep track of this, we prefer—as mentioned—to think of the columns and rows being indexed by almost positive roots and simple roots rather than by the linear ordering in which rows/columns of matrices usual thought of.

1. Definitions and main results

We start with recalling several notions from finite roots systems and the theory of subword complexes and their relations to the cluster algebra $\mathcal{A}(W, c)$. We refer to [**89**] for a detailed treatment of these notions and further background.

Consider the finite crystallographic Coxeter system (W, S) acting essentially on a Euclidean vector space $\left(V, \langle \cdot \,|\, \cdot \rangle\right)$ of dimension n, with simple roots $\Delta = \{\alpha_s \ : \ s \in S\}$ and simple coroots $\Delta^\vee = \{\alpha_s^\vee \ : \ s \in S\}$. We then have that $\alpha_s^\vee = 2\alpha_s / \langle \alpha_s \,|\, \alpha_s \rangle$, and that the crystallographic Cartan matrix $A = (a_{st})_{s,t \in S}$ is given by $a_{st} = \langle \alpha_t \,|\, \alpha_s^\vee \rangle$. The fundamental weights $\nabla = \{\omega_s \ : \ s \in S\}$ and fundamental coweights $\nabla^\vee = \{\omega_s^\vee \ : \ s \in S\}$ are the bases dual to the simple coroots and to the simple roots, respectively. This is, $\langle \omega_s \,|\, \alpha_t^\vee \rangle = \langle \alpha_s \,|\, \omega_t^\vee \rangle = \delta_{s=t}$. It is then easy to check that $\alpha_s = \sum_{t \in S} a_{ts}\omega_t$ and $\alpha_s^\vee = \sum_{t \in S} a_{st}\omega_t^\vee$, and that moreover, $s(\omega_t) = \omega_t - \delta_{s=t}\alpha_s$ for $s \in S$. Given the Coxeter element c with fixed reduced word $\mathsf{c} = \mathsf{s}_1 \cdots \mathsf{s}_n$, we will often write $\alpha_i = \alpha_{s_i}$, $\alpha_i^\vee = \alpha_{s_i}^\vee$, $\omega_i = \omega_{s_i}$, and $\omega_i^\vee = \omega_{s_i}^\vee$ for simplicity. Denote by $\Phi = W(\Delta) = \left\{w(\alpha_s) \ : \ w \in W, s \in S\right\}$ the root system for (W, S), by $\Phi^+ = \Phi \cap \mathbb{R}_{\geq 0}\Delta$ the positive roots, and by $\Phi_{\geq -1} = \Phi^+ \sqcup -\Delta \subseteq \Phi$ the set of almost positive roots. We will often write $|\Phi^+| = N$, so that $|\Phi_{\geq -1}| = n + N$.

Now let Q be a word in the simple generators S and let $\rho \in W$. The *subword complex* $\mathcal{SC}(\mathsf{Q}, \rho)$ is the simplicial complex of subwords of Q whose complement contains a reduced expression of ρ (we refer to Theorem 1.6 for a detailed example). In this paper, we are only interested in the case that $\rho = w_\circ$ is the unique longest element in W with respect to the weak order, and Q being one specific word constructed from the Coxeter element c, see below. We thus write $\mathcal{SC}(\mathsf{Q})$ for $\mathcal{SC}(\mathsf{Q}, w_\circ)$ and assume that Q does indeed contain a reduced expression for $w_\circ$. Define I_g and I_ag to be the lexicographically first and last facets of $\mathcal{SC}(\mathsf{Q})$, respectively. These are called *greedy facet* and *antigreedy facet*.

For $\mathsf{Q} = \mathsf{q}_1 \cdots \mathsf{q}_m$, associate to any facet I of the subword complex $\mathcal{SC}(\mathsf{Q})$ a *root function* $\mathsf{r}(I, \cdot) : [m] \to W(\Delta)$ and a *weight function* $\mathsf{w}(I, \cdot) : [m] \to W(\nabla)$ defined by

$$\mathsf{r}(I, k) = \Pi\mathsf{Q}_{[k-1] \smallsetminus I}(\alpha_{q_k}) \quad \text{and} \quad \mathsf{w}(I, k) = \Pi\mathsf{Q}_{[k-1] \smallsetminus I}(\omega_{q_k}),$$

where $\Pi\mathsf{Q}_X$ denotes the product of the simple reflections $q_x \in \mathsf{Q}$, for $x \in X$, in the order given by Q. For later convenience, we as well define the *coroot function* $\mathsf{r}^\vee(I, \cdot) : [m] \to W(\Delta^\vee)$ and a *coweight function* $\mathsf{w}^\vee(I, \cdot) : [m] \to W(\nabla^\vee)$ by

$$\mathsf{r}^\vee(I, k) = \Pi\mathsf{Q}_{[k-1] \smallsetminus I}(\alpha_{q_k}^\vee) \quad \text{and} \quad \mathsf{w}^\vee(I, k) = \Pi\mathsf{Q}_{[k-1] \smallsetminus I}(\omega_{q_k}^\vee).$$

The root function locally encodes the flip property in the subword complex: each facet adjacent to I in $\mathcal{SC}(\mathsf{Q})$ is obtained by exchanging an element $i \in I$ with the unique element $j \notin I$ such that $\mathsf{r}(I, j) \in \{\pm\mathsf{r}(I, i)\}$. If $i < j$ such a flip is called *increasing*, and *decreasing* otherwise. Observe moreover that the greedy facet and the antigreedy facet are the unique facets such that every flip is increasing and decreasing, respectively.

After this exchange, the root function and the weight function is updated by a simple application of $s_{\mathsf{r}(I,i)}$, see Theorem 2.2. The root function is used to define the *root configuration* of the facet I as the multiset

$$\mathsf{R}(I) = \left\{\!\left\{ \mathsf{r}(I, i) \ : \ i \in I \right\}\!\right\}, \tag{I.1}$$

and the coroot function is used to define the *coroot configuration* of the facet I as the multiset

$$\mathsf{R}^\vee(I) = \left\{\!\left\{ \mathsf{r}^\vee(I, i) \ : \ i \in I \right\}\!\right\}. \tag{I.2}$$

For later convenience, we denote by $\mathsf{r}(I, i)_j = \left\langle \mathsf{r}(I, i) \,\middle|\, \omega_j^\vee \right\rangle$ the coefficient of α_j in the root $\mathsf{r}(I, i)$.

On the other hand, the weight function is used to define the *brick vector* of I as

$$\mathsf{B}(I) = \sum_{k \in [m]} \mathsf{w}(I, k),$$

and the *brick polytope* of Q is defined to be the convex hull of the brick vectors of all facets of the subword complex $\mathcal{SC}(\mathrm{Q})$,

$$\mathcal{B}(\mathrm{Q}) = \mathrm{conv}\left\{\mathsf{B}(I) \ : \ I \text{ facet of } \mathcal{SC}(\mathrm{Q})\right\}.$$

It was shown in [89] that the brick polytope $\mathcal{B}(\mathrm{Q})$ is the Minkowski sum of Coxeter matroid polytope in the sense of [11].

THEOREM 1.1 ([89, Proposition 1.5]). *For any word* Q *in* S *of length* m *containing a reduced expression for* $w_\circ$ *we have that*

$$\mathcal{B}(\mathrm{Q}) = \sum_{k\in[m]}\mathcal{B}(\mathrm{Q},k)$$

where $\mathcal{B}(\mathrm{Q},k) = \mathrm{conv}\left\{\mathsf{w}(I,k) \ : \ I \text{ facet of } \mathcal{SC}(\mathrm{Q})\right\}$.

For the Coxeter element c with the fixed reduced word $\mathrm{c} = \mathrm{s}_1\cdots\mathrm{s}_n$, the *Coxeter sorting word* (or c-*sorting word*) $\mathrm{c}(\rho)$ of an element $\rho \in W$ is given by the lexicographically first subword of c^∞ that is a reduced expression for ρ. Observe that the word $\mathrm{c}(\rho)$ depends on the reduced expression and should thus thought of being associated to the Coxeter element c and being defined up to commutations of consecutive commuting letter. This notion was defined by N. Reading in [96] and plays an important role in the combinatorial descriptions of finite type cluster algebras and in particular in the description of cluster complexes in terms of subword complexes. In particular, the main results in [18] and [89] provide the following description of the combinatorics of the cluster complex of $\mathcal{A}(W,c)$:

THEOREM 1.2 ([18, Theorem 2.2]). *The cluster complex of the cluster algebra* $\mathcal{A}(W,c)$ *is isomorphic to the subword complex* $\mathcal{SC}\big(\mathrm{cw}_\circ(\mathrm{c})\big)$.

We thus refer to $\mathcal{SC}\big(\mathrm{cw}_\circ(\mathrm{c})\big)$ as the c-*cluster complex* (where we again abuse notation and use the fixed reduced expression for c). One identifies positions in $\mathrm{cw}_\circ(\mathrm{c})$ and almost positive roots by sending the kth letter s_k of the initial copy of c to the negative simple root $-\alpha_{s_k}$, and the kth letter q_k of $\mathrm{c}(w_\circ)$ to the positive root $q_1\cdots q_{k-1}(\alpha_{q_k})$. See Theorem 2.2 that this indeed is a bijection, and observe that this equals the root function of the greedy facet outside of it,

$$q_1\cdots q_{k-1}(\alpha_{q_k}) = \mathsf{r}(I_\mathrm{g}, n+k). \tag{I.3}$$

This identification yields the isomorphism in Theorem 1.2 by sending a cluster to the positions inside the word $\mathrm{cw}_\circ(\mathrm{c})$ corresponding to the almost positive roots of the d-vectors of the cluster. To make this explicit, we use th following notations: Let $I = \{i_1 < \ldots < i_n\}$ be a facet of the cluster complex $\mathcal{SC}\big(\mathrm{cw}_\circ(\mathrm{c})\big)$. We then denote by $S(I) = \big(\widetilde{\mathsf{M}}(I), \mathbf{u}(I), \mathbf{f}(I)\big)$ with

$$\widetilde{\mathsf{M}}(I) = \begin{bmatrix} \mathsf{M}^{pr}(I) \\ \mathsf{M}^{ex}(I) \end{bmatrix}$$
$$\mathbf{u}(I) = \big(u_{i_1}(I), \ldots, u_{i_n}(I)\big)$$
$$\mathbf{f}(I) = \big(f_{i_1}(I), \ldots, f_{i_n}(I)\big)$$

the cluster seed of $\mathcal{A}(W,c)$ corresponding to I under the given isomorphism between cluster variables, almost positive roots, and positions in the word $\mathrm{cw}_\circ(\mathrm{c})$. The columns of $\widetilde{\mathsf{M}}(I)$ are then also indexed by the positions $i_1, \ldots, i_n$ as are the rows of $\mathsf{M}^{pr}(I)$, while the rows of $\mathsf{M}^{ex}(I)$ are indexed by the positions $1, \ldots, n$. We also denote by $c(I,i)$ the c-vector coming from column $i \in I$ of $\mathsf{M}^{ex}(I)$.

Polar polytopal realizations of the cluster complex were first obtained by F. Chapoton, S. Fomin, and A. Zelevinsky in [25] for bipartite Coxeter elements, and by C. Hohlweg, C. Lange, and H. Thomas in [57] for general Coxeter elements. As one obtains for type A_n classical constructions of associahedra, such a polytopal realization is called c-*associahedron*. The subword complex approach and the brick polytope construction provide a rather simple construction.

THEOREM 1.3 ([**89**, Theorem 4.9]). *The cluster complex is realized by the polar of the brick polytope $\mathcal{B}(\mathrm{cw}_\circ(\mathrm{c}))$. In other words, the brick polytope $\mathcal{B}(\mathrm{cw}_\circ(\mathrm{c}))$ is a c-associahedron.*

Indeed, this vertex description of a polytopal realization is equal to the construction in [**57**] up to a translation, see [**89**, Corollary 6.10].

THEOREM 1.4 ([**89**, Theorem 6.40]). *Let I be a facet of $\mathcal{SC}(\mathrm{cw}_\circ(\mathrm{c}))$. The principal part of the exchange matrix $\widetilde{\mathsf{M}}(I)$ is then given by*

$$\mathsf{M}^{pr}(I)_{ij} = \begin{cases} -\big\langle\, \mathsf{r}(I,j) \,\big|\, \mathsf{r}^\vee(I,i) \,\big\rangle & \text{if } i < j \\[4pt] \big\langle\, \mathsf{r}(I,j) \,\big|\, \mathsf{r}^\vee(I,i) \,\big\rangle & \text{if } i > j \\[4pt] 0 & \text{if } i = j \end{cases}$$

where $\mathsf{Q} = \mathsf{q}_1 \cdots \mathsf{q}_{n+N} = \mathrm{cw}_\circ(\mathrm{c})$ and $i, j \in I$.

The following remark starts to clarify the connection between the subword complex approach to finite type cluster algebras and the approach using N. Reading and D. Speyer's combinatorial frameworks [**97**].

REMARK 1.5. The central structures in their combinatorial frameworks are the *labels* and *colabels*. We have seen in [**89**, Proposition 6.20] that the labels in finite types are the root configurations defined in (I.1), and we obtain by duality that the colabels in finite types are the coroot configurations defined in (I.2). Given this connection in finite types, we immediately obtain that Theorem 1.4 is the same description as given in [**97**, Theorem 3.25]. See also Theorem 1.9 for the relation of the subword complex approach and [**97**, Theorem 3.26].

Before presenting the results of this paper, we would like to expain them in great detail in the example of type A_2, as we hope that this makes them easier to understand.

EXAMPLE 1.6. This example shows the construction of the c-cluster complex $\mathcal{SC}(\mathrm{cw}_\circ(\mathrm{c}))$ of type A_2, and its *close similarity* to the type A_2 cluster algebra in Theorem 0.1. Let W be the symmetric group $A_2 = \mathfrak{S}_3$ with simple transpositions $S = \{s_1 = (12), s_2 = (23)\}$, Coxeter element $c = s_1 s_2 = (123)$, simple roots $\Delta = \{\alpha_1 = e_1 - e_2, \alpha_2 = e_2 - e_3\}$, and fundamental weights $\nabla = \{e_1, e_1 + e_2\}$. The word $\mathsf{Q} = \mathrm{cw}_\circ(\mathrm{c})$ is then given by

$$\mathsf{q}_1\mathsf{q}_2\ \mathsf{q}_3\mathsf{q}_4\mathsf{q}_5 = \underbrace{\mathsf{s}_1\mathsf{s}_2}_{\mathrm{c}}\ \underbrace{\mathsf{s}_1\mathsf{s}_2\mathsf{s}_1}_{\mathrm{c}(\mathrm{w}_\circ)},$$

and the facets of $\mathcal{SC}(\mathrm{cw}_\circ(\mathrm{c}))$ are thus

$$\{\mathsf{q}_1, \mathsf{q}_2\}, \{\mathsf{q}_2, \mathsf{q}_3\}, \{\mathsf{q}_3, \mathsf{q}_4\}, \{\mathsf{q}_4, \mathsf{q}_5\}, \{\mathsf{q}_1, \mathsf{q}_5\}.$$

The following table records the root function of $\mathcal{SC}(\mathrm{cw}_\circ(\mathrm{c}))$ indexed both by almost positive roots and positions in the word Q:

I	$-\alpha_1$ 1	$-\alpha_2$ 2	α_1 3	$\alpha_1 + \alpha_2$ 4	α_2 5
$I_{\mathrm{g}} = \{\mathsf{q}_1, \mathsf{q}_2\}$	$(1,-1,0)$	$(0,1,-1)$	$(1,-1,0)$	$(1,0,-1)$	$(0,1,-1)$
$\{\mathsf{q}_2, \mathsf{q}_3\}$	$(1,-1,0)$	$(1,0,-1)$	$(-1,1,0)$	$(1,0,-1)$	$(0,1,-1)$
$\{\mathsf{q}_3, \mathsf{q}_4\}$	$(1,-1,0)$	$(1,0,-1)$	$(0,1,-1)$	$(-1,0,1)$	$(0,-1,1)$
$I_{\mathrm{ag}} = \{\mathsf{q}_4, \mathsf{q}_5\}$	$(1,-1,0)$	$(1,0,-1)$	$(0,1,-1)$	$(-1,1,0)$	$(0,1,-1)$
$\{\mathsf{q}_1, \mathsf{q}_5\}$	$(1,-1,0)$	$(1,-1,0)$	$(1,0,-1)$	$(1,-1,0)$	$(0,-1,1)$

Observe that the root configuration of a facet I (indicated in grey) written in simple roots coincides with the columns of the extended parts of the mutation matrices in Theorem 0.1. E.g., the facet $\{\mathsf{q}_3, \mathsf{q}_4\}$ corresponds to the cluster seed where the d-vectors are the almost positive roots $(\alpha_1, \alpha_1 + \alpha_2)$. It has (ordered) root configuration $(\alpha_2, -\alpha_1 - \alpha_2)$ which corresponds to the two columns $c(\alpha_1) = (0,1)$ and $c(\alpha_1 + \alpha_2) = (-1,-1)$ in the extended part

of the mutation matrix for that cluster (indexed by the cluster variables). This phenomenon will be explained in all finite types in Theorem 1.7.

Similarly, the following table records the weight function of $\mathcal{SC}\big(\mathrm{cw_\circ}(c)\big)$:

I	$-\alpha_1$ 1	$-\alpha_2$ 2	α_1 3	$\alpha_1 + \alpha_2$ 4	α_2 5	B(I)
$I_g = \{q_1, q_2\}$	$(1,0,0)$	$(1,1,0)$	$(1,0,0)$	$(1,1,0)$	$(0,1,0)$	$(4,3,0)$
$\{q_2, q_3\}$	$(1,0,0)$	$(1,1,0)$	$(0,1,0)$	$(1,1,0)$	$(0,1,0)$	$(3,4,0)$
$\{q_3, q_4\}$	$(1,0,0)$	$(1,1,0)$	$(0,1,0)$	$(0,1,1)$	$(0,1,0)$	$(2,4,1)$
$I_{ag} = \{q_4, q_5\}$	$(1,0,0)$	$(1,1,0)$	$(0,1,0)$	$(0,1,1)$	$(0,0,1)$	$(2,3,2)$
$\{q_1, q_5\}$	$(1,0,0)$	$(1,1,0)$	$(1,0,0)$	$(1,0,1)$	$(0,0,1)$	$(4,1,2)$

This yields that the brick polytope is given by

$$\mathcal{B}(\mathrm{cw_\circ}(c)) = \mathrm{conv}\left\{430, 340, 241, 232, 412\right\}$$
$$= \mathrm{conv}\{100\} + \mathrm{conv}\{110\} + \mathrm{conv}\{100, 010\}$$
$$+ \mathrm{conv}\{110, 011, 101\} + \mathrm{conv}\{010, 001\}.$$

There are multiple things to be observed in this table which will be explained in this paper. Most importantly, one shifts all weights inside a column by the weight in the row of the antigreedy facet I_{ag} and expresses the result in terms of the simple roots to obtain in each column the exponent vectors of the monomials in the F-polynomials for the corresponding cluster variable:

	$-\alpha_1$	$-\alpha_2$	α_1	$\alpha_1 + \alpha_2$	α_2	B(I) − B(I_{ag})
$I_g = \{q_1, q_2\}$	$(0,0)$	$(0,0)$	$(1,0)$	$(1,1)$	$(0,1)$	$(2,2)$
$\{q_2, q_3\}$	$(0,0)$	$(0,0)$	$(0,0)$	$(1,1)$	$(0,1)$	$(1,2)$
$\{q_3, q_4\}$	$(0,0)$	$(0,0)$	$(0,0)$	$(0,0)$	$(0,1)$	$(0,1)$
$I_{ag} = \{q_4, q_5\}$	$(0,0)$	$(0,0)$	$(0,0)$	$(0,0)$	$(0,0)$	$(0,0)$
$\{q_1, q_5\}$	$(0,0)$	$(0,0)$	$(1,0)$	$(1,0)$	$(0,0)$	$(2,0)$
$F_\beta(\mathbf{y})$	1	1	$1+$ y_1	$1+$ y_1+ $y_1 y_2$	$1+$ y_2 y_2	

We will prove this phenomenon in type A_n, while we will only conjecture generalizations thereof in other types.

Nevertheless, the following properties of the columns perfectly match properties of F-polynomials in general and hold for general finite type c-cluster complexes:

(i) Inside the columns the weight is constant within the entries inside the facets (the entries in grey) and this weight also coincides with the weight in the row of the antigreedy facet.

(ii) When shifting all weights inside the columns by this entry, all entries inside the facets become 0 and the first row coincides with the first row for the table of the root function in the positions corresponding to the positive roots.

(iii) Every other entry is obtained from the entry in the first (last) row by subtracting (adding) simple roots.

The second item corresponds to the facts that the F-polynomials have a constant term 1 and a monomial with exponent vector equal to the d-vector, and the third item corresponds to the fact that this monomial is the unique monomial of hightest degree and is divided by every other monomial in the F-polynomial.

The first result shows the close relationship between the extended part of the mutation matrix in finite type cluster algebras and the root function of the corresponding subword complex.

THEOREM 1.7. *Let I be a facet of the c-cluster complex $\mathcal{SC}(\mathrm{cw}_\circ(\mathrm{c}))$ corresponding to the seed $S(I)$ in the cluster algebra $\mathcal{A}(W, c)$. Then the columns of $\mathsf{M}^{ex}(I)$ are given by the root configuration, i.e.,*

$$c(I, i) = \mathsf{r}(I, i).$$

As a direct consequence, we get the following description of the frozen variables in terms of the roof configuration. Recall that $\mathsf{r}(I, i)_j = \left\langle \mathsf{r}(I, i) \,\middle|\, \omega_j^\vee \right\rangle$ denotes the coefficient of α_j in $\mathsf{r}(I, i)$.

COROLLARY 1.8. *In the situation of Theorem 1.7, we obtain*

$$f_i(I) = y_1^{\mathsf{r}(I,i)_1} \cdots y_n^{\mathsf{r}(I,i)_n}.$$

PROOF. The theorem gives that $[\mathsf{M}^{ex}]_{ji} = \mathsf{r}(I, i)_j$. The corollary will thus follow with the well known Theorem 2.1 below. $\square$

REMARK 1.9. We have seen in Theorem 1.5 how the description of the mutation matrix through subword complexes relates to the description through N. Reading and D. Speyer's combinatorial frameworks. Indeed, Theorem 1.7 is the subword complex counterpart of [**97**, Theorem 3.26]. Our theorem above is exactly their Theorem 3.26(1), and their parts (2)–(5) as well follow by the same arguments:

   (i) Every c-vector is a root in the root system and thus has a definite sign.
  (ii) The g-vectors are the basis vectors given by the dual basis of the coroot configuration, as obtained from the fact that the c-vectors and the g-vectors are related this way.
 (iii) The g-vectors form a basis for the weight lattice as the root configuration forms a basis of the root lattice and the coroot configuration forms a basis for the coroot lattice, which follows directly from their well-known recursive descriptions (see [**89**, Proposition 6.20].
 (iv) all F-polynomials in finite type have constant term 1, as this follows from (i) via [**39**, Proposition 5.6].

We have now seen how to obtain properties from the root and coroot configuration. Indeed, we have *not* used the root and coroot functions outside of the facets to derive data. This does not seem very surprising in light of Theorem 2.2 which recalls that the root function on the complement of a given facet is always the complete set of positive roots.

Next, we look at properties of the cluster algebra that can be studied using the weight function, this time both inside and also outside of a given facet. To state these, we define (in the usual way) the *Newton polytope* of an F-polynomial $F_\beta(\mathbf{y})$ as the convex hull of its exponent vectors in the root basis. This is,

$$\mathrm{Newton}\left(F_\beta(\mathbf{y})\right) = \mathrm{conv}\left\{\lambda_1 \alpha_1 + \ldots + \lambda_n \alpha_n \ : \ y_1^{\lambda_1} \cdots y_n^{\lambda_n} \text{ monomial in } F_\beta(\mathbf{y})\right\}.$$

CONJECTURE 1.10. *Let $F_\beta(\mathbf{y})$ be the F-polynomial associated to the positive root β for the cluster algebra $\mathcal{A}(W, c)$. Let i be the index $1 \le i \le N$ associated to β in Equation (I.3). Then*

$$\mathrm{Newton}\left(F_\beta(\mathbf{y})\right) = \mathrm{conv}\left\{\mathsf{w}(F, n + i) - \mathsf{w}(I_{\mathrm{ag}}, n + i) \ : \ F \text{ facet of } \mathcal{SC}\left(\mathrm{cw}_\circ(\mathrm{c})\right)\right\}.$$

THEOREM 1.11. *Conjecture 1.10 holds for $\mathcal{A}(W, c)$ with W of type A_n.*

This theorem will be proved in Section 3 by relating it to the combinatorial model of type A_n cluster algebras of R. Schiffler [**99**] using its description given by G. Musiker and R. Schiffler in [**86**]. Observe moreover that this property for the *linear Coxeter element* $c = (1, \ldots, n + 1)$ in A_n was indeed already found by A. Postnikov in [**91**], see Corollary 8.2 and the following two paragraphs, where he in particular showed that this Minkowski sum of Newton polytopes is exactly the realization given by J.-L. Loday in [**76**].

THEOREM 1.12. *Conjecture 1.10 holds for $\mathcal{A}(W, c)$ and in all exceptional types.*

PROOF. This was obtained via explicit computer explorations using various Sage packages written by Christian Stump and his collaborators. $\square$

This conjecture would have the following immediate corollary.

COROLLARY 1.13. *If Theorem 1.10 holds for $\mathcal{A}(W, c)$, then the c-associahedron $\mathcal{B}(\mathrm{cw}_\circ(\mathrm{c}))$ coincides up to translation with the Minkowski sum of the Newton polytopes of the F-polynomials of $\mathcal{A}(W, c)$.*

PROOF. This then follows from the Minkowski decomposition of any brick polytope into Coxeter matroid polytopes given in Theorem 1.1. $\square$

COROLLARY 1.14. *If Theorem 1.10 holds for $\mathcal{A}(W, c)$, then any F-polynomial $F_\beta(\mathbf{y})$ has a unique monomial of maximal degree whose exponent vector equals β, and such that any of its monomials divides this monomial of maximal degree.*

PROOF. This will follow from Theorem 2.7. $\square$

2. Proof of 1.7

In this section, we prove Theorem 1.7 and also provide several auxillary results for general finite type c-cluster complexes. These will be then used in Section 3 to show the close relationship of the F-polynomial and the weight vectors.

We start with recalling cluster mutations on cluster seeds. Let $S = (\widetilde{\mathsf{M}}, \mathbf{u}, \mathbf{f})$ with $\widetilde{\mathsf{M}} = \begin{bmatrix} \mathsf{M}^{pr} \\ \mathsf{M}^{ex} \end{bmatrix}$ be a cluster seed as above. Given that we have indexed colums of $\widetilde{\mathsf{M}}$ and the rows of M^{pr} both by the d-vectors of the cluster variables $\mathbf{u} = (u_1, \ldots, u_n)$, we now mutate S at $\beta \in \Phi_{\geq -1}$ such that $\beta = d(u_i)$. The *seed mutation* $\mu_i = \mu_\beta$ in *direction* β defines a new seed $\mu_i(S) = (\widetilde{\mathsf{M}}', \mathbf{x}', \mathbf{y}')$ defined by the following *exchange relations*, written for better readability in the indices $\{1, \ldots, n\}$ of $\{u_1, \ldots, u_n\}$ rather than in their d-vectors:

(1) The entries of $\widetilde{\mathsf{M}}' = (b'_{k\ell})$ are given by
$$b'_{k\ell} = \begin{cases} -b_{k\ell} & \text{if } k = i \text{ or } \ell = i \\ b_{k\ell} + b_{ki}b_{i\ell} & \text{if } b_{ki} > 0 \text{ and } b_{i\ell} > 0 \\ b_{k\ell} - b_{ki}b_{i\ell} & \text{if } b_{ki} < 0 \text{ and } b_{i\ell} < 0 \\ b_{k\ell} & \text{otherwise.} \end{cases}$$

(2) The cluster variables u'_k of the cluster $\mathbf{u}' = \{u'_1, \ldots, u'_n\}$ are given by $u'_k = u_k$ for $k \neq i$ and
$$u'_i = \frac{f_i \prod u_k^{\max\{b_{ki}, 0\}} + \prod u_k^{\max\{-b_{ki}, 0\}}}{(f_i \oplus 1) u_i}$$

(3) The frozen variables f'_ℓ of the coefficients $\mathbf{f} = \{f'_1, \ldots, f'_n\}$ are given by
$$f'_\ell = \begin{cases} f_i^{-1} & \text{if } \ell = i \\ f_\ell f_i^{\max\{b_{i\ell}, 0\}} (f_i \oplus 1)^{-b_{i\ell}} & \text{if } \ell \neq i \end{cases}.$$

As usual, we use in (2) and (3) the tropical notation $\oplus$ which is defined for monomials by $\left(\prod_i y_i^{a_i} \right) \oplus \left(\prod_i y_i^{b_i} \right) = \prod_i y_i^{\min\{a_i, b_i\}}$.

COROLLARY 2.1 ([**39**, (2.13)]). *The frozen variables are given by*
$$f_i = y_1^{[\mathsf{M}^{ex}]_{1i}} \cdots y_n^{[\mathsf{M}^{ex}]_{ni}}.$$

To prove Theorem 1.7, we will show that the entries in the root configuration behave as described in the matrix mutation in (1) for the c-vectors. In order to properly set this up,

it will be convenient to use that one can extract the coefficient of α_j in the root $r(I, i)$ using the inner product with the fundamental coweights, as we need to show that

$$\left[\mathsf{M}^{ex}(I)\right]_{ji} = r(I, i)_j = \left\langle\, r(I, i) \,\middle|\, \omega_j^\vee \,\right\rangle.$$

The argument will follow the same lines as the proof of Theorem 1.4 in [**89**]. We will frequently make use of the following lemma:

LEMMA 2.2 ([**18**, Lemma 3.3 & Lemma 3.6], [**89**, Lemma 3.3 & Lemma 4.4]). *Let I and J be two adjacent facets of the subword complex $\mathcal{SC}(Q)$ with $I \setminus i = J \setminus j$. Then*

   (1) The map $r(I, \cdot) : k \mapsto r(I, k)$ is a bijection between the complement of I and Φ^+.
   (2) The position j is the unique position in the complement of I for which $r(I, j) \in \{\pm r(I, i)\}$. Moreover, $r(I, j) = r(I, i) \in \Phi^+$ if $i < j$, while $r(I, j) = -r(I, i) \in \Phi^-$ if $j < i$.
   (3) The map $\mathsf{r}(J, \cdot)$ is obtained from $\mathsf{r}(I, \cdot)$ by

$$r(J, k) = \begin{cases} s_{r(I,i)}(r(I, k)) & \text{if } \min\{i, j\} < k \leq \max\{i, j\}, \\ r(I, k) & \text{otherwise.} \end{cases}$$

   (4) The map $\mathsf{w}(J, \cdot)$ is obtained from $\mathsf{w}(I, \cdot)$ by

$$\mathsf{w}(J, k) = \begin{cases} s_{\mathsf{r}(I,i)}(\mathsf{w}(I, k)) & \text{if } \min(i, j) < k \leq \max(i, j), \\ \mathsf{w}(I, k) & \text{otherwise.} \end{cases}$$

   (5) For $k' \notin I$, we have $\left\langle\, \mathsf{r}(I, k') \,\middle|\, \mathsf{w}(I, k) \,\right\rangle$ is non-negative if $k' \geq k$, and non-positive if $k' < k$.

The initial condition is satisfied by definition:

LEMMA 2.3. *Let I_g be the greedy facet of $\mathcal{SC}(cw_\circ(c))$. Then*

$$\left[\mathsf{M}^{ex}(I_\mathrm{g})\right]_{ji} = \left\langle\, \mathsf{r}(I_\mathrm{g}, i) \,\middle|\, \omega_j^\vee \,\right\rangle.$$

PROOF. This is the case as both sides are clearly equal to $\left\langle\, \alpha_i \,\middle|\, \omega_j^\vee \,\right\rangle$.   □

LEMMA 2.4. *Let I, J be two faces of $\mathcal{SC}(cw_\circ(c))$ with $I \setminus i = J \setminus j$, and let $k \in I \setminus i$ and $\ell \in \{1, \ldots, n\}$. Then $\mathsf{r}(J, j) = -\mathsf{r}(I, i)$ and*

$$r(J, k)_\ell = \begin{cases} r(I, k)_\ell + r(I, i)_\ell \cdot \left[\mathsf{M}^{pr}(I)\right]_{ik} & \text{if } r(I, i)_\ell \geq 0, \left[\mathsf{M}^{pr}(I)\right]_{ik} \geq 0, \\ r(I, k)_\ell - r(I, i)_\ell \cdot \left[\mathsf{M}^{pr}(I)\right]_{ik} & \text{if } r(I, i)_\ell \leq 0, \left[\mathsf{M}^{pr}(I)\right]_{ik} \leq 0, \\ r(I, k)_\ell & \text{otherwise.} \end{cases}$$

PROOF. The property that $\mathsf{r}(J, j) = -\mathsf{r}(I, i)$ holds in general for facets $I \setminus i = J \setminus j$ in subword complexes. It is a direct consequence of Theorem 2.2(2).

It thus remains to show that $\mathsf{r}(J, k)_\ell$ is obtained from $\mathsf{r}(I, k)_\ell$ as desired. For simplicity, observe that we can assume that $i < j$ as every facet of any subword complex $\mathcal{SC}(Q)$ can be obtained from the greedy facet by a sequence of increasing flips. This implies, again by Theorem 2.2(2), that $r(I, i) \in \Phi^+$ and thus $r_(I, i)_\ell \geq 0$. The case of a decreasing flip $i > j$ could as well be computed in the exact same way.

The first case is $i < k < j$. It follows from [**89**, Lemma 6.43] that also $\left[\mathsf{M}^{pr}\right]_{ik} \geq 0$. And, as desired, we obtain

$$\begin{aligned} r(J, k)_\ell &= \left\langle\, \Pi Q_{[k]\setminus J}(\alpha_{q_k}) \,\middle|\, \omega_\ell^\vee \,\right\rangle \\ &= \left\langle\, \Pi Q_{[i]\setminus I} \cdot q_i\big(\Pi Q_{[i,k]\setminus I}(\alpha_{q_k})\big) \,\middle|\, \omega_\ell^\vee \,\right\rangle \\ &= \left\langle\, \Pi Q_{[i]\setminus I} \cdot \Big(\Pi Q_{[i,k]\setminus I}(\alpha_{q_k}) - \left\langle\, \Pi Q_{[i,k]\setminus I}(\alpha_{q_k}) \,\middle|\, \alpha_{q_i}^\vee \,\right\rangle \alpha_{q_i}\Big) \,\middle|\, \omega_\ell^\vee \,\right\rangle \\ &= \left\langle\, \Pi Q_{[k]\setminus I}(\alpha_{q_k}) \,\middle|\, \omega_\ell^\vee \,\right\rangle - \left\langle\, \Pi Q_{[i,k]\setminus I}(\alpha_{q_k}) \,\middle|\, \alpha_{q_i}^\vee \,\right\rangle \cdot \left\langle\, \Pi Q_{[i]\setminus I}(\alpha_{q_i}) \,\middle|\, \omega_\ell^\vee \,\right\rangle \\ &= r(I, k)_\ell + r(I, i)_\ell \cdot \left[\mathsf{M}^{pr}(I)\right]_{ik}. \end{aligned}$$

The second equality is obtained as we do the flip from $i \in I$ to $j \in J$, the third equality is the definition of the application of the simple reflection q_i to $\Pi Q_{[i,k] \setminus I}(\alpha_{q_k})$, and the fourth equality is the linearity of the inner product.

The second case is $k \notin [i, j]$. It follows from [**89**, Lemma 6.43] that $\left[\mathsf{M}^{pr}\right]_{ik} \leq 0$, while $\mathsf{r}(I,i)_\ell \geq 0$. And indeed, the flip from i to j does not effect the root function at k, and we obtain that $\mathsf{r}(I,k)_\ell = \mathsf{r}(J,k)_\ell$, as desired. $\qquad \square$

We are now in the situation to deduce Theorem 1.7.

PROOF OF THEOREM 1.7. It follows from (1) and Theorem 2.4 that

$$\left[\mathsf{M}^{ex}(I)\right]_{\ell k} = \mathsf{r}(I,k)_\ell \implies \left[\mathsf{M}^{ex}(J)\right]_{\ell k'} = \mathsf{r}(J,k')_\ell$$

for $I \setminus i = J \setminus j$ and either $k = k' \neq i$ or $k = i$ and $k' = j$. As Theorem 2.3 provides the equality for the initial mutation matrix, we obtain $\left[\mathsf{M}^{ex}(I)\right]_{\ell i} = \mathsf{r}(I,i)_\ell$ for all $i \in I$, implying the theorem. $\qquad \square$

LEMMA 2.5. *Let I, J be two facets of $\mathcal{SC}(cw_\circ(c))$ with $k \in I \cap J$. Then $w(I,k) = w(J,k)$.*

PROOF. This is a direct consequence of Theorem 2.2(3) and the two observations that
   ▷ $\langle \mathsf{r}(I,k) \,|\, \mathsf{w}(I,k') \rangle = 0$ for $k, k' \in I$ (see [**89**, Proposition 6.6]), and
   ▷ all facets of $\mathcal{SC}\big(\mathrm{cw}_\circ(\mathrm{c})\big)$ containing k are connected by flips (see [**89**, Corollary 3.11]).
Indeed, this property of the weight function was already used in the proof of [**89**, Proposition 6.8]. $\qquad \square$

The following lemma is a direct consequence of Theorem 2.2(4) and (5).

LEMMA 2.6 ([**89**]). *Let $I \setminus i = J \setminus j$ with $i < j$ be two facets of $\mathcal{SC}\big(\mathrm{cw}_\circ(\mathrm{c})\big)$. For any $k \in [n + N]$ we then have*

$$\mathsf{w}(J,k) = \mathsf{w}(I,k) - \lambda \mathsf{r}(I,i) \text{ for } \lambda \in \mathbb{R}_{\geq 0} \text{ and } \mathsf{r}(I,i) \in \Phi^+.$$

The following lemma has not been considered before and will serve as the starting point of understanding F-polynomials in terms of the weight function.

LEMMA 2.7. *For $k \in \{n + 1, \ldots, n + N\}$, we have that*

$$\mathsf{w}(I_\mathrm{g}, k) - \mathsf{w}(I_\mathrm{ag}, k) = \mathsf{r}(I_\mathrm{g}, k).$$

Observe that, as we have seen in Equation (I.3), this is also closely related to the bijection relating cluster algebras and subword complexes.

PROOF OF THEOREM 2.7. Starting with the greedy facet I_g, we flip the first position $k - n$ times without changing the weight function at k (as we do not pass position k) and obtain, up to commutations of consecutive commuting letters,

$$\mathsf{w}(I_\mathrm{g}, k) = \mathsf{w}(\{k - n, \ldots, k - 1\}, k).$$

We also obtain, up to commutations of consecutive commuting letters,

$$\mathsf{w}(I_\mathrm{ag}, k) = \mathsf{w}(\{k, \ldots, k + n - 1\}, k) = \mathsf{w}(\{k - n + 1 \ldots, k\}, k).$$

The first equality holds for the same reason as above as these $N - k$ flips of the last position starting with I_ag do not pass position k. The second equality follows from Theorem 2.5 as k is now contained in both facets. With these observations, we finally obtain for $c(\mathrm{w}_\circ) = \mathsf{q}_1 \cdots \mathsf{q}_N$ that

$$\begin{aligned}
\mathsf{w}(I_\mathrm{g}, k) - \mathsf{w}(I_\mathrm{ag}, k) &= \mathsf{w}(\{k - n, \ldots, k - 1\}, k) - \mathsf{w}(\{k - n + 1 \ldots, k\}, k) \\
&= q_1 \cdots q_{k-1}(\omega_{q_k}) - q_1 \cdots q_k(\omega_{q_k}) \\
&= q_1 \cdots q_{k-1}(\omega_{q_k}) - q_1 \cdots q_{k-1}(\omega_{q_k} - \alpha_{q_k}) \\
&= q_1 \cdots q_{k-1}(\alpha_{q_k}) \\
&= \mathsf{r}(I_\mathrm{g}, k)
\end{aligned}$$
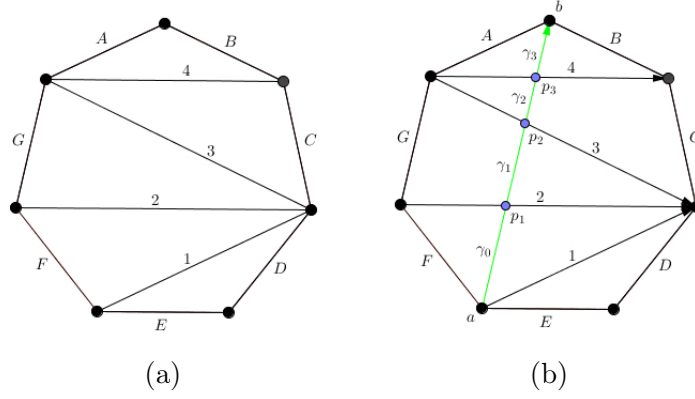
as desired. $\qquad \square$

FIGURE 1. A path in a triangulation of the 7-gon.

3. Proof of 1.11

Before we start recalling the Musiker-Schiffler construction and prove the theorem, we quickly set the needed notations for the reflection group of type A_n. In this type, we have that W is the symmetric group $\mathfrak{S}_{n+1}$ acting on $\mathbb{R}^{n+1}$, whose generators S are the set of simple transpositions $S = \{\tau_1, \ldots, \tau_n\}$ for $\tau_i = (i, i+1)$. Thus, the Coxeter element c is given by the product of all simple transpositions in some order. For consecutive simple transpositions, we write $\tau_i < \tau_{i-1}$ if τ_i appears to the left of τ_{i-1} in c, and $\tau_i > \tau_{i-1}$ if τ_i appears to the right of τ_{i-1}. We will say that a sequence $\tau_{i_k}, \ldots, \tau_{i_1}$ is a *suffix of c* if there is a reduced word c for c ending in $\tau_{i_k}, \ldots, \tau_{i_1}$. If all $\tau_{i_k}, \ldots, \tau_{i_1}$ are inside the interval $\{\tau_i, \ldots, \tau_j\}$ for $i < j$, we moreover say that it is a *suffix of c restricted to the interval $[i, j]$* if the suffix property holds after removing all letters not in $\{\tau_i, \ldots, \tau_j\}$ from c. The simple roots are moreover given by $\Delta = \{e_i - e_{i+1} \ : \ 1 \leq i \leq n\}$, the positive roots by $\Phi^+ = \{e_i - e_j \ : \ 1 \leq i < j \leq n+1\}$, and the fundamental weights by $\nabla = \{e_1 + \ldots + e_i \ : \ 1 \leq i \leq n\}$.

3.1. F-polynomials from T-paths. R. Schiffler derived in [**99**] an explicit formula for the cluster variables of type A_n via *T-paths* which are certain paths on the diagonals of triangulations of a regular $(n+3)$-gon. G. Musiker and R. Schiffler then extended that description and obtained in [**86**] an explicit formula for cluster variables in a similar fashion for cluster algebras associated to unpunctured surfaces with arbitrary coefficients. In this section, we will review this construction for type A_n to establish the needed notions to relate their description to the weight function in order to derive Theorem 1.11.

Let T be a triangulation of a regular $(n+3)$-gon, with boundary diagonals (or edges) labelled by $B_1, \ldots, B_{n+3}$ and with proper diagonals labelled by $1, \ldots, n$. (In examples, we use $A, B, \ldots$ instead of $B_1, \ldots, B_{n+3}$ for convenience.) An example can be found in Figure 1(a). Let $\gamma \notin T$ be another proper diagonal connecting non-adjacent vertices a and b, oriented from a to b. Denote the intersection points of γ with the proper diagonals in T along its orientation by $p_1, \ldots, p_d$, and the corresponding diagonals in T by $t_1, \ldots, t_d$. Let γ_k denote the segment of γ from point p_k to point p_{k+1}, where we use $p_0 = a$ and $p_{d+1} = b$. Each γ_k lies in exactly one triangle $\triangle_k$, and we orient the diagonal t_k in T by the orientation induced from the counterclockwise orientation of $\triangle_k$.

A *T-path* ζ from a to b in T is a path $\zeta = (\zeta_1, \ldots, \zeta_{2d+1})$ in T which uses the diagonals t_k in the even positions. In symbols, $\zeta_{2k} = t_k$ for $1 \leq k \leq d$. Observe that such a T-path is uniquely determined by the directions in which the diagonals $t_1, \ldots, t_d$ in the even position are followed. If the direction of ζ coincides along the diagonal t_k with the direction induced by the counterclockwise orientation of the triangle $\triangle_k$, we write that ζ travels t_k in *positive direction*, and it travels t_k in *negative direction* otherwise. It is not hard to see that there is always a unique T-path that travels all t_k's in positive direction. We call this path the *greedy T-path*,

and denote it by ζ_g. Similarly, we denote by ζ_{ag} the *antigreedy T-path* that travels all t_k's in negative direction. For instance, the greedy T-path in Figure 1(b) is $(F, 2, 3, 3, 3, 4, B)$ and the antigreedy T-path is $(1, 2, 2, 3, 4, 4, A)$.

We say that a T-path ζ is *flipped* to a T-path ζ' if ζ and ζ' only differ in two odd positions $2k - 1$ and $2k + 1$ for some k. In other words, t_k is the unique diagonal which is travelled by ζ and ζ' in opposite directions, while all others are travelled in the same direction. We thus also say that t_k *is flipped* between ζ and ζ'. In Figure 1(b), flipping t_6 in the T-path $(F, 2, 3, 3, 3, 4, B)$ yields the T-path $(F, 2, 3, 3, B_3, 4, A)$.

To a T-path $\zeta = (\zeta_1, \ldots, \zeta_{2d+1})$, one associates the monomial $m[\zeta]$ given by the product of variables y_k such that $\zeta_{2k} = t_k$ is travelled in positive direction. For instance, the greedy T-path $\zeta_g = (F, 2, 3, 3, 3, 4, B)$ yields the monomial $m[\zeta_g] = y_2 y_3 y_4$, while the antigreedy T-path $\zeta_{ag} = (1, 2, 2, 3, 4, 4, A)$ yields $m[\zeta_{ag}] = 1$. Moreover, all monomials obtained from T-paths for the diagonal γ in the example are given by

ζ	$m[\zeta]$
$(F, 2, 3, 3, 3, 4, B)$	$y_2 y_3 y_4$
$(F, 2, 3, 3, C, 4, A)$	$y_2 y_3$
$(1, 2, G, 3, 3, 4, B)$	$y_3 y_4$
$(1, 2, G, 3, C, 4, A)$	y_3
$(1, 2, 2, 3, 4, 4, A)$	1

This combinatorial model now provides a description of the F-polynomials for the cluster algebra where the initial datum is the fixed given triangulation T of a regular $(n+3)$-gon. It is well-known that these F-polynomials are now indexed by diagonals $\gamma \notin T$, see [**86**].

THEOREM 3.1 ([**99**, Theorem 4.6]). *Let T be a triangulation of the regular $(n+3)$-gon, and let $\gamma \notin T$ from a to b. Then*

$$F_\gamma(\mathbf{y}) = \sum m[\zeta],$$

where the sum ranges over all T-paths ζ from a to b.

Next, we recall how to associate a triangulation T_c of the regular $(n+3)$-gon to a standard Coxeter element c in type A_n.

(1) Pick a fixed vertex of the $(n + 3)$-gon, labelled v_1, and draw an edge connecting the two vertices adjacent to v_1. Label the new edge by 1.
(2) Let $i = 2$.
(3) While $i \leq n$:

If $\tau_i < t_{i-1}$, then label the vertex clockwise from v_{i-1} by v_i, draw an edge connecting the two vertices adjacent to v_i which are not v_{i-1}, and label the new edge i. Let $i = i + 1$.

If $\tau_i > \tau_{i-1}$, then label the vertex counter-clockwise from v_{i-1} by v_i, draw an edge connecting the two vertices adjacent to v_i which are not v_{i-1}, and label the new edge i. Let $i = i + 1$.

A simple example is given in the following figure in type A_3 with $c = (1234) = \tau_1 \tau_2 \tau_3$:
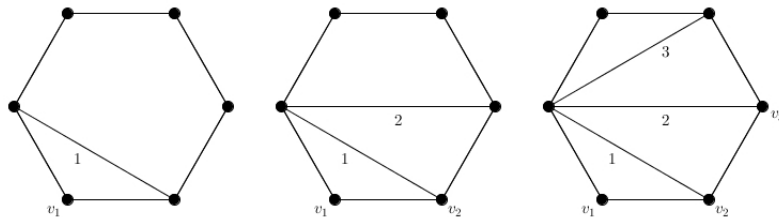
We make the following elementary observation.

LEMMA 3.2. *Let c be a Coxeter element in type A_n, and let $1 \leq i \leq j \leq n$. Then there is a unique diagonal $\gamma \notin T_c$ that crosses exactly the diagonals labelled by $i, i+1, \ldots, j$, and every diagonal not in T_c can be obtained this way.*

PROOF. The triangulations that can be obtained from a Coxeter element by the procedure are exactly the triangulations that do not have inner triangles, *i.e.*, no triangles for which all three sides are proper diagonals. The statement follows.   □

We have the following corollary of the above Theorem 3.1, which we will then use to deduce Theorem 1.11.

COROLLARY 3.3. *Let c be a standard Coxeter element in type A_n and let $\beta = e_i - e_j$ be a positive root. The F-polynomials for the cluster algebra $\mathcal{A}(W, c)$ are then given by*

$$F_\beta(\mathbf{y}) = \sum m[\zeta],$$

where the sum ranges over all T-paths ζ from a to b where a and b are given such that the path γ from a to b is the unique path that crosses exactly the diagonals labelled $a, \ldots, b-1$.

PROOF. This follows from the well known connection between $\mathcal{A}(W, c)$ and the triangulation T_c as described above.   □

In order to prove our results in the following sections, we need the following proposition regarding possible flips in triangulations with respect to a Coxeter element c:

PROPOSITION 3.4. *Let T_c be the triangulation associated to a Coxeter element c, and let $\gamma \notin T_c$ be another proper diagonal from a to b which crosses exactly the diagonals $\{i, i+1, \ldots, i+d-1\}$. Then for any suffix $(i_k, i_k+1), \ldots, (i_1, i_1+1)$ of c restricted to $\{\tau_i, \ldots, \tau_{i+d-1}\}$, one can flip the diagonals $i_1, \ldots, i_k$ in this order in the greedy T_c-path from a to b. Moreover, every T_c-path from a to b is obtained this way.*

PROOF. We start with explicitly describing the four possible restrictions for directions in which T_c-paths can travel. To this end, consider the situation that t_{i-1} and t_i are oriented towards their shared vertex in T_c, or, equivalently, that $(i, i+1) < (i-1, i)$. Then, a T_c-path ζ from a to b

> ▷ that travels the diagonal $\zeta_{2i} = t_i$ in *positive* direction must also travel $\zeta_{2i-2} = t_{i-1}$ in *positive* direction, and
> ▷ that travels the diagonal $\zeta_{2i} = t_i$ in *negative* direction must also travel $\zeta_{2i} = t_i$ in *negative* direction.

The situation where t_{i-1} and t_i are oriented away from their shared vertex in T_c, or, equivalently, that $(i, i+1) > (i-1, i)$ is the same with the roles of positive and negative direction interchanged.

But this is nothing else but saying that the T_c-path is obtained from the greedy T_c-path ζ_g (which travels all the diagonals in positive direction) by flipping diagonals $i_1, \ldots, i_k$ in this order for a suffix $(i_k, i_k + 1), \ldots, (i_1, i_1 + 1)$ of c, as desired.   □

3.2. F-polynomials from subword complexes. The first step to use the above construction to obtain the F-polynomials from the weight vectors of $\mathcal{SC}(\mathrm{cw}_\circ(\mathrm{c}))$, we provide a property of the weight vectors of $\mathcal{SC}(\mathrm{cw}_\circ(\mathrm{c}))$ which parallels Theorem 3.4. This is indeed the heard of the proof.

PROPOSITION 3.5. *Consider a cluster algebra $\mathcal{A}(W, c)$ of type A_n. Given any index k and facet I, the weight $w(I, k)$ is obtained from $w(I_g, k)$ by flipping an initial segment of c, up to commutations.*

PROOF. Let $c = q_1 \cdots q_n$. If the simple transposition s_i is to the left of s_{i+1} in c, we will write $s_i < s_{i+1}$ and if s_i is to the right of s_{i+1} in c, we will write $s_i > s_{i+1}$.

We know by lemma 2.7 that $w(I_g, k) - w(I_{ag}, k) = \alpha_k = e_i - e_j$ for some $i, j \in [n+1]$. Together, we know that $w(I_g, k)$ and $w(I_{ag}, k)$ are of the form

$$w(I_g, k) = (***, 1, ***, 0, ***) \text{ and } w(I_{ag}, k) = (***, 0, ***, 1, ***),$$

where the ith entry of $w(I_g, k)$ and the jth entry of $w(I_{ag}, k)$ are 1, the jth entry of $w(I_g, k)$ and the ith entry of $w(I_{ag}, k)$ are 0, and the other entries of $w(I_g, k)$ and $w(I_{ag}, k)$ are equal and either 0 or 1.

First let us prove that for $m < i$ and $m > j$, the mth entries of $w(I_g, k)$ (and thus of $w(I_{ag}, k)$) are equal. Observing that $cw(I_g, k) = w(I_{ag}, k)$, we notice that if this wasn't the case, then when we apply c to $w(I_g, k)$, there will exist an entry m, $m < i$ or $m > j$, equal to 1 which will be flipped with an entry equal to 0. Then the mth entry of $w(I_g, k)$ and $w(I_{ag}, k)$ will not be equal, a contradiction.

For the entries $m < i$ of $w(I_g, k)$ (and thus of $w(I_{ag}, k)$), we need to ensure that the swap between the $i - 1^{th}$ and i^{th} entry does not change the entry in position $i - 1$; this can only be ensured if the entries $m < i$ are equal to 0 if $s_{i-1} < s_i$ and are equal to 1 if $s_{i-1} > s_i$. Similarly, for the entries $m > j$ of $w(I_g, k)$ (and thus of $w(I_{ag}, k)$) we need to also ensure that the swap between the jth and $j + 1^{th}$ entry does not change the entry in position $j + 1$; this can only be ensured if the entries $m > j$ are equal to 0 if $s_{j-1} > s_j$ and are equal to 1 if $s_j > s_{j-1}$.

For entries $i < m < j$ of $w(I_g, k)$ (and thus of $w(I_{ag}, k)$), we need to ensure that a 1 is moved into the jth position, a 0 is moved into the ith position, and that every entry $i < m < j$ is the same in I_g and I_{ag}. Keeping in mind that every position is swapped exactly once, the only way we can ensure such conditions is if each entry $i < m < j$ is equal to 0 if $s_{m-1} > s_m$ and equal to 1 if $s_{m-1} < s_m$.

The conditions on each entry m we just described tell us that c dictates which entries are 0 and which are 1 in $w(I_g, k)$ and $w(I_{ag}, k)$, and the order in which each simple transposition must be applied so that $w(I_g, k) - w(I_{ag}, k) = \alpha_k$. This order is exactly the order in which the simple transpositions appear in c, up to commutation. Thus, every possible weight $w(I, k)$ must be obtained from $w(I_g, k)$ by flipping an initial segment of c, up to commutations. □

With this, we are finally in the position to obtain the desired properties.

PROOF OF THEOREM 1.11. We start with a cluster algebra $\mathcal{A}(W, c)$ of type A_n and construct the triangulation T_c. We pick an almost positive root $\alpha_{i_1} + \alpha_{i_2} + \cdots + \alpha_{i_d}$, which we will identify with its corresponding d-vector $d(u)$. Let $\gamma \notin T_c$ be the diagonal which crosses the diagonals $i_1, \ldots, i_d \in T_c$.

The greedy T_c-path gives us the term $y_{i_1} \cdots y_{i_d}$ of $F_u(\mathbf{y})$. Proposition 3.4 tells us that if we start flipping from the greedy T_c-path in the order $i_d, \ldots, i_1$, up to commutations, then we obtain every T_c-path. Starting with the greedy T_c-path, as we flip in the order $i_d, \ldots, i_1$, up to commutations, we are effectively removing each variable from the term $y_{i_1} \cdots y_{i_d}$ one at a time.

Let k be the index such that $w(I_g, k) - w(i_{ag}, k) = d(u)$, which is the exponent vector of $y_{i_1} \cdots y_{i_d}$. Proposition 3.5 tells us that if we start flipping from the greedy facet in the order $i_d, \ldots, i_1$, up to commutations, then we obtain every possible weight of index k. Starting with the greedy facet, as we flip in the order $i_d, \ldots, i_1$, up to commutations, we are subtracting $\alpha_{i_d}, \alpha_{i_{d-1}}, \ldots, \alpha_{i_1}$ one at a time in this order, up to commutations, from $w(I_g, k) - w(I_{ag}, k)$. Which is effectively the same as removing each variable from the term $y_{i_1} \cdots y_{i_d}$ one at a time.

So flipping from the greedy T_c-path and flipping from the greedy facet yield the same set of terms; i.e. the set $\{y_{i_1} \cdots y_{i_d}, y_{i_1} \cdots y_{i_{d-1}}, \ldots, y_{i_1}\}$, whose sum is the desired F-polynomial. □

CHAPTER II

Where Cluster Algebras and Tropical Geometry Meet

Cluster algebras are commutative rings generated by a set of cluster variables, which are grouped into overlapping sets called clusters. They were introduced by S. Fomin and A. Zelevinsky in the series of papers [**41, 42, 44, 45**], and since then have shown fascinating connections with diverse areas such as Lie theory, representation theory, Poisson geometry, algebraic geometry, combinatorics and discrete geometry. One important family of examples is the family of cluster algebras of finite type, which were classified in [**42**] using the Cartan–Killing classification for finite crystallographic root systems. Among them are the cluster algebras of type D_n which are one of the main objects of study in this chapter. We focus on the cluster algebra of type D_4 and the combinatorial structures related to its cluster complex. Cluster complexes are simplicial complexes that encode the mutation graph of the cluster algebra, i.e., the graph describing how to pass from a cluster to another. They were introduced by Fomin and Zelevinsky [**43**] in connection with their proof of the Zamolodchikov's periodicity conjecture for algebraic Y-systems. One remarkable connection of cluster complexes with tropical geometry was discovered by Speyer and Williams in [**102**]. They study the positive part $\mathrm{Gr}^+(d,n)$ of the tropical Grassmannian $\mathrm{Gr}(d,n)$, and show that $\mathrm{Gr}^+(2,n)$ is combinatorially isomorphic to the cluster complex of type A_{n-3}, and that $\mathrm{Gr}^+(3,6)$ and $\mathrm{Gr}^+(3,7)$ are closely related to the cluster complexes of type D_4 and E_6. The tropical Grassmannian $\mathrm{Gr}(d,n)$ was first introduced by Speyer and Sturmfels [**101**] as a parametrization space for tropicalizations of ordinary linear spaces. The tropicalization of an ordinary linear space gives a tropical linear space in $\mathbb{TP}^{n-1}$ in the sense of Speyer [**103, 104**], but not all tropical linear spaces are realized in this way in general. In the case $\mathrm{Gr}(3,6)$, all tropical planes in $\mathbb{TP}^5$ are realized by the Grassmannian [**101**]. Speyer and Sturmfels [**101**] explicitly studied all tropical planes in $\mathbb{TP}^5$ and found that there are exactly 7 different combinatorial types. On the other hand, one may also classify clusters of type D_4 up to combinatorial type, from which we deduce that there are exactly 7 different combinatorial types of clusters modulo reflection and rotation. This leads to two natural questions:

(1) How are the 7 combinatorial types of tropical planes in $\mathbb{TP}^5$ and the 7 combinatorial types of type D_4 clusters related?
(2) Which of the 7 combinatorial types of tropical planes in $\mathbb{TP}^5$ are realized in the positive part $\mathrm{Gr}^+(3,6)$ of the tropical Grassmannian $\mathrm{Gr}(3,6)$?

This chapter gives precise answers to these questions. Surprisingly, the 7 combinatorial types of tropical planes and the 7 combinatorial types of clusters are not bijectively related as one might expect. We show that only 6 of the 7 combinatorial types of tropical planes are achieved by the positive tropical Grassmannian $\mathrm{Gr}^+(3,6)$, and use the pseudotriangulation model of cluster algebras of type D_4 to compare them with the combinatorial types of clusters of type D_4. In particular, we obtain that

> *if two pseudotriangulations are related by a sequence of reflections of the octagon preserving the parity of the vertices, and possibly followed by a global exchange of central chords, then their corresponding tropical planes in $\mathbb{TP}^5$ are combinatorially equivalent.*

The combinatorial classes of positive tropical planes are then obtained by taking unions of the classes generated by this finer equivalence on pseudotriangulations.

Section 1 recalls the notion of cluster algebras of type D_n and their cluster complexes, and shows that the clusters of type D_4 are divided into 7 combinatorial classes. Section 2 recalls the necessary notions in tropical geometry, tropical Grassmannians and their positive parts, as well as the Speyer–Sturmfels classification of tropical planes in $\mathbb{TP}^5$ into 7 combinatorial classes. In section 3, we present a precise connection between the cluster complex of type D_4 and the positive part $\mathrm{Gr}^+(3,6)$ of the tropical Grassmannian $\mathrm{Gr}(3,6)$. We compute the combinatorial types of tropical planes in $\mathbb{TP}^5$ corresponding to the clusters of type D_4 in section 4. Finally, in section 5 we describe the combinatorial types of tropical planes using automorphisms of pseudotriangulations.

1. Cluster Algebras of type D_n

In this section, we present the cluster algebras of type D_n. Different models exist for these cluster algebras: in terms of centrally symmetric triangulations of a $2n$-gon with bicolored long diagonals [**43**, section 3.5][**42**, section 12.4], in terms of tagged triangulations of a punctured n-gon [**40**], or in terms of pseudotriangulations of a $2n$-gon with a small disk in the center [**22**]. We adopt the last model mentioned to deal with clusters combinatorially. The automorphisms of pseudotriangulations allow us to define the combinatorial type of a cluster. In this paper, we classify and compare clusters up these combinatorial types. We refer to the original paper [**22**] for a more detailed study of cluster algebras of type D_n in terms of pseudotriangulations, and briefly describe here their model.

Consider a regular convex $2n$-gon together with a disk D placed at the center, whose radius is small enough such that D only intersects the long diagonals of the $2n$-gon. We denote by $\mathbf{D}_n$ the resulting configuration. The vertices of $\mathbf{D}_n$ are labeled by $0, 1, \ldots, n-1, \overline{0}, \overline{1}, \ldots, \overline{n-1}$ in counterclockwise direction, such that two vertices p and $\overline{p}$ are symmetric with respect to the center of the polygon. The *chords* of $\mathbf{D}_n$ are all the diagonals of the $2n$-gon, except the long ones, and all the segments tangent to the disk D and with one endpoint among the vertices of the $2n$-gon; see Figure 2.
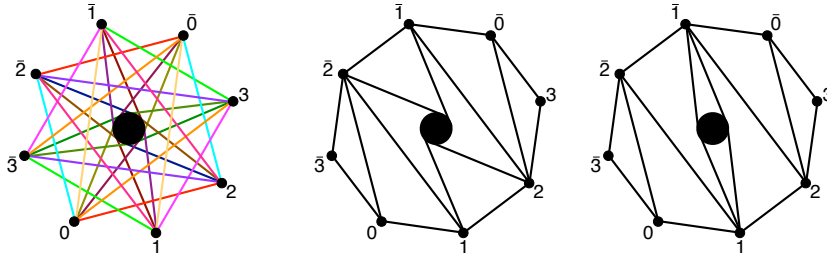
FIGURE 2. The configuration $\mathbf{D}_4$ has 16 centrally symmetric pairs of chords (left). A centrally symmetric pseudotriangulation T of $\mathbf{D}_4$ (middle). The centrally symmetric pseudotriangulation of $\mathbf{D}_4$ obtained from T by flipping the centrally symmetric pair of chords $\{2^{\mathrm{L}}, \overline{2}^{\mathrm{L}}\}$ (right).

Each vertex p is incident to two such chords; we denote by p^{L} (resp. by p^{R}) the chord emanating from p and tangent on the left (resp. right) to the disk D. We call these chords *central*.

Cluster variables, clusters, cluster mutations and exchange relations in the cluster algebra of type D_n can be interpreted geometrically as follows:

(1) Cluster variables correspond to *centrally symmetric pairs of (internal) chords* of the geometric configuration $\mathbf{D}_n$, as shown in Figure 2 (left). To simplify notations, we identify a chord δ, its centrally symmetric copy $\overline{\delta}$, and the pair $\{\delta, \overline{\delta}\}$.

(2) Clusters correspond to *centrally symmetric pseudotriangulations* of $\mathbf{D}_n$ (*i.e.* maximal centrally symmetric crossing-free sets of chords of $\mathbf{D}_n$). Each pseudotriangulation of $\mathbf{D}_n$ contains exactly $2n$ chords, and partitions $\mathrm{conv}(\mathbf{D}_n) \smallsetminus D$ into *pseudotriangles* (*i.e.* interiors of simple closed curves with three convex corners related by three concave chains); see Figure 2.

(3) Cluster mutations correspond to *flips* of centrally symmetric pairs of chords between centrally symmetric pseudotriangulations of $\mathbf{D}_n$. A flip in a pseudotriangulation T replaces an internal chord e by the unique other internal chord f such that $(T \smallsetminus e) \cup f$ is again a pseudotriangulation of T. More precisely, deleting e in T merges the two pseudotriangles of T incident to e into a pseudoquadrangle $\bowtie$ (*i.e.* the interior of a simple closed curve with four convex corners related by four concave chains), and adding f splits the pseudoquadrangle $\bowtie$ into two new pseudotriangles. The chords e and f are the two unique chords which lie both in the interior of $\bowtie$ and on a geodesic between two opposite corners of $\bowtie$.

(4) As in type A, the exchange relations between cluster variables during a cluster mutation can be understood in the geometric picture. This is illustrated for all different kinds of flips in Figure 3.
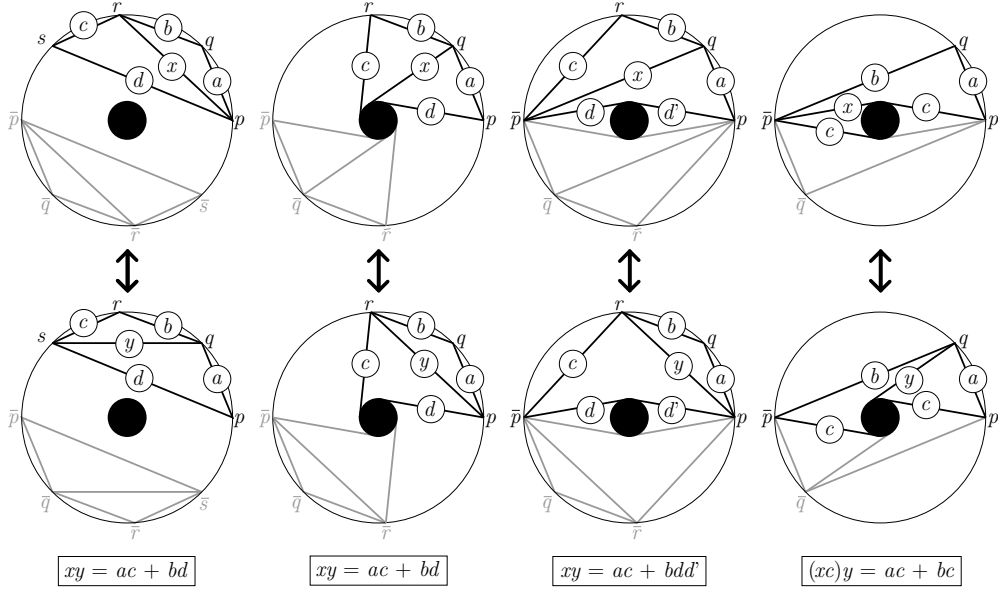
FIGURE 3. Different kinds of flips and exchange relations in type D_n

1.1. The Cluster Complex of Type D_4. The cluster complex of type D_n can also be described from the geometric model presented in [**22**]. We recall this description in the particular case of cluster algebras of type D_4. Let $\{\tau_1, \tau_2, \tau_3, \tau_4\}$ be the set of simple generators of the Coxeter group of type D_4 according to the labeling of the Dynkin diagram in Figure 4, and let $\Delta = \{\alpha_1, \alpha_2, \alpha_3, \alpha_4\}$ be the set of simple roots of the corresponding root system. We denote by $\Phi = \Phi^+ \sqcup \Phi^-$ the set of roots partitioned into positive and negative roots, and by $\Phi_{\geq -1} = -\Delta \sqcup \Phi^+$ the set of almost positive roots.
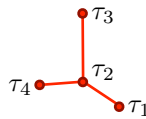
FIGURE 4. The Dynkin diagram of type D_4
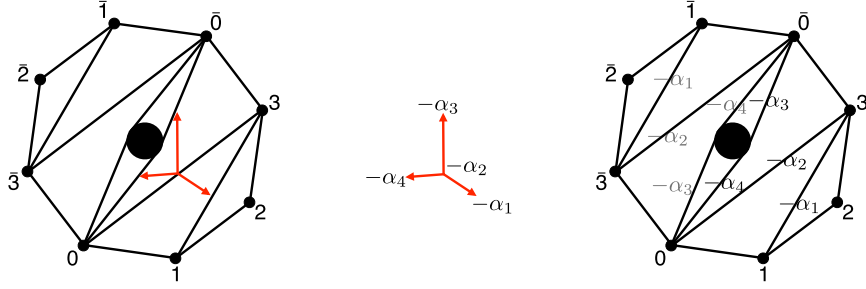
FIGURE 5. The snake pseudotriangulation T_0 (left), its corresponding quiver of type D_4 (middle), and the snake chords labeled with the negative simple roots (right)

Let $T_0 = \{0^{\mathrm{L}}, 0^{\mathrm{R}}, 03, 13\}$ be the "snake pseudotriangulation" illustrated in Figure 5. We label its centrally symmetric pairs of chords with the negative simple roots $\{-\alpha_1, -\alpha_2, -\alpha_3, -\alpha_4\}$ as shown, and identify any other chord δ with the positive root obtained by adding the simple roots associated to the chords of T_0 crossed by δ. This determines a bijection between the set of almost positive roots and the set of chords in the geometric configuration. The cluster complex is the simplicial complex whose maximal simplices are the sets of almost positive roots corresponding to pseudotriangulations.

EXAMPLE 1.1. For instance, the chord $\overline{12}$ corresponds to the positive root $\alpha_1 + 2\alpha_2 + \alpha_3 + \alpha_4$ since it crosses two chords of T_0 with label α_2 and one chord for each label α_1, α_3 and α_4. The cluster associated to the pseudotriangulation $T = \{1^{\mathrm{L}}, 2^{\mathrm{L}}, \overline{02}, \overline{12}\}$ is $\{\alpha_2 + \alpha_4, \alpha_1 + \alpha_2 + \alpha_4, \alpha_1 + \alpha_2, \alpha_1 + 2\alpha_2 + \alpha_3 + \alpha_4\}$. To lighten the notation, sometimes we write α_I for the positive root $\alpha_I = \sum_{i \in I} \alpha_i$ where I is a multi-set with possible repeated subindices. With this notation, the cluster corresponding to T is $\{\alpha_{24}, \alpha_{124}, \alpha_{12}, \alpha_{12234}\}$. The correspondence between all chords and the positive roots is illustrated in Figure 8 (right) on page 38, and explicitly presented in Figure 10 on page 40.

1.2. Combinatorial Types of Clusters of Type D_4. The cluster algebra of type D_n induces a natural *rotation* operation, denoted by τ, on clusters, see *e.g.* [**21**, section 2.2]. In the pseudotriangulation model, the action of τ corresponds to counterclockwise rotation by π/n, and exchanging p^{L} with p^{R}, see [**22**]. For instance, the chord 03 in Figure 5 is rotated to $1\overline{0}$, while 0^{R} is rotated to 1^{L}.

DEFINITION 1.2. *We say that two pseudotriangulations T_1 and T_2 are* combinatorially equivalent *modulo reflections and τ-rotations if there exists a sequence of reflections of the $2n$-gon and τ-rotations transforming T_1 into T_2. Further, we say that two clusters of type D_n are* combinatorially equivalent *if their corresponding pseudotriangulations are combinatorially equivalent modulo reflections and τ-rotations.*

PROPOSITION 1.3. *There are exactly 7 combinatorial types of clusters of type D_4 modulo reflections and τ-rotations.*

PROOF. The type-D_4 rotation τ exchanges p^{L} and p^{R} after usual rotation by $\frac{\pi}{4}$. Applying two reflections we also obtain a usual rotation by $\pi/4$ without this special rule. Combining D_4-rotations and reflections we can then obtain an operation that preserves the non-central chords and exchanges p^{L} and p^{R}. After an analysis of the 50 pseudotriangulations modulo these four operations (D_4-rotation, usual rotation, reflection, and exchange of central chords) we classify them into 7 combinatorial classes in Figure 5.   □

Using the fact that there are 7 combinatorial types of tropical planes in $\mathbb{TP}^5$ [**101**] we obtain:
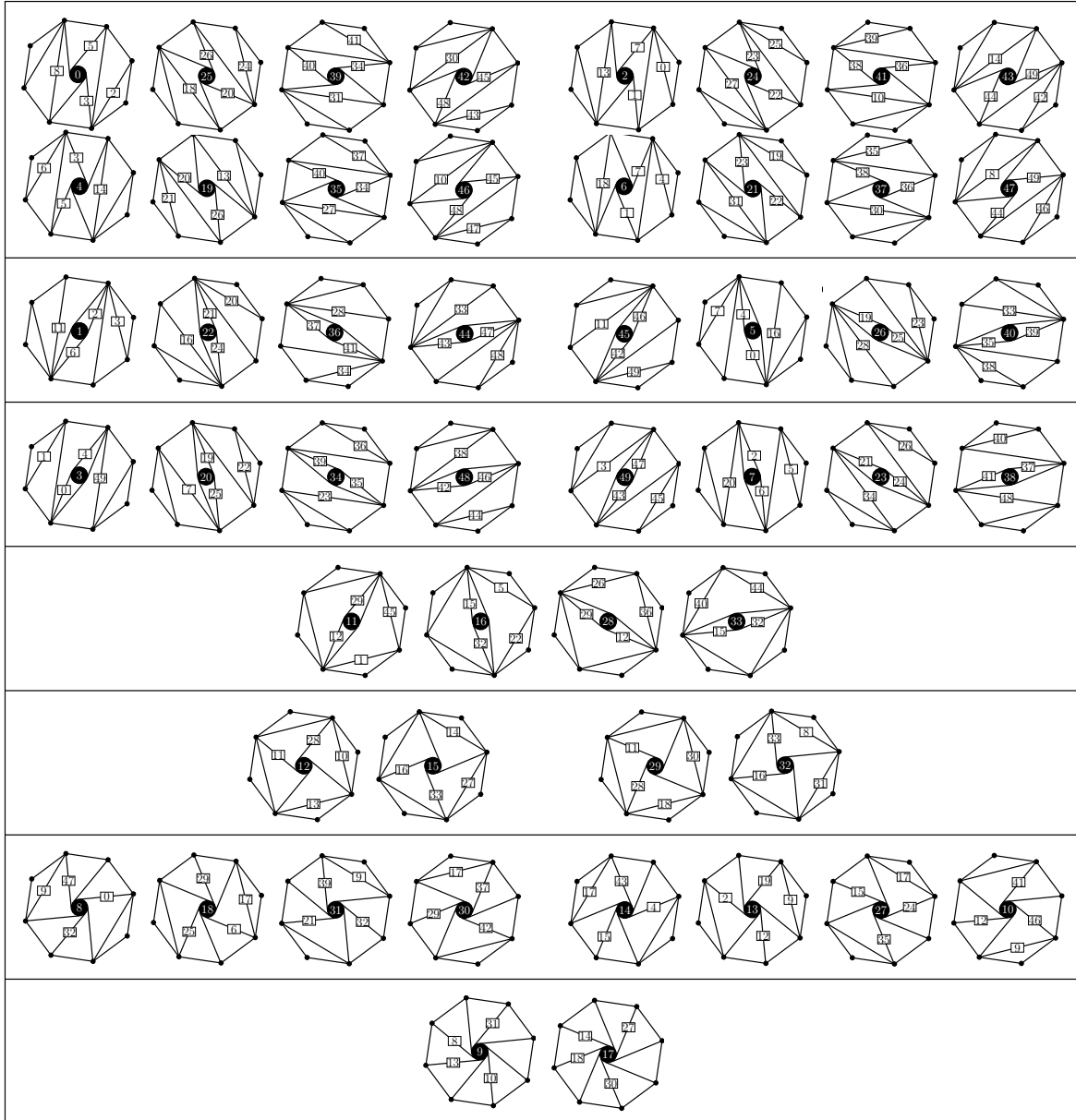
FIGURE 6. The seven combinatorial types of pseudotriangulations (or clusters) of type D_4 modulo reflections and τ rotation. The 50 pseudotriangulations are labeled with the numbers from 0 to 49 at the center of the disk. Each pair of chords in a pseudotriangulation is labeled with the pseudotriangulation obtained when flipping it.

COROLLARY 1.4. *The number of combinatorial types of clusters of type D_4 is equal to the number of combinatorial types of tropical planes in $\mathbb{TP}^5$.*

We emphasize this as a corollary as it is our main motivation for establishing a relationship between tropical planes in $\mathbb{TP}^5$ and clusters of type D_4. Before making a precise connection between clusters of type D_4 and tropical planes in $\mathbb{TP}^5$, we recall some preliminaries in tropical geometry.

2. Tropical Varieties and Their Positive Part

The min-plus, or *tropical*, semiring $\mathbb{T} := (\mathbb{R} \cup \{\infty\}, \oplus, \odot)$ is defined with the following operations:

$$x \oplus y = \min\{x, y\} \ \text{ and } \ x \odot y = x + y,$$

where the zero element is ∞ and the one element is 0. A *tropical monomial* is an expression of the form $c \odot x_1^{\odot a_1} \odot \cdots \odot x_n^{\odot a_n}$ and a *tropical polynomial* is a finite tropical sum of tropical monomials. Equivalently, a tropical polynomial is a piecewise linear concave function given as the minimum of finitely many linear functions of the form

$$(x_1, ..., x_n) \mapsto a_1 x_1 + ... + a_n x_n + c.$$

A *tropical hypersurface* is the set of all points $\bar{x} = (x_1, ..., x_n)$ in $\mathbb{R}^n$ such that its defining tropical polynomial is not linear at $\bar{x}$.

The tropical objects defined above are inherently tropical, in the sense that they are defined over $\mathbb{T}$. It is also possible to consider "classical" algebraic objects over a fixed field $\mathbb{K}$ and construct their tropical analogues via a nonarchimedean valuation.

Let us consider the field

$$\mathbb{K} := \mathbb{C}\{\{t\}\} = \{\sum \alpha_r t^{r/n} : \alpha_r \in \mathbb{C}, r \in \mathbb{Z}, n \in \mathbb{Z}_+\}$$

of *Puiseux series* over $\mathbb{C}$. This field is of characteristic 0, is algebraically closed, and has a natural nonarchimedean valuation $\mathrm{val} : \mathbb{K} \to \mathbb{T}$ sending 0 to ∞ and, for $a(t) \neq 0$, sending $a(t) \mapsto \min\{\frac{r}{n} : \alpha_r \neq 0\}$. Note that this valuation extends naturally to a valuation $\mathrm{Val} : \mathbb{K}^n \to \mathbb{T}^n$ on $\mathbb{K}^n$ via coordinatewise evaluation: $(a_1(t), ..., a_n(t)) \mapsto (\mathrm{val}(a_1(t)), ..., \mathrm{val}(a_n(t))$. Let us consider the polynomial

$$f = \sum_{i=1}^{k} a_i(t) x_1^{b_1^i} \cdots x_n^{b_n^i} \in \mathbb{K}[x_1, ..., x_n].$$

We then define the *tropicalization* of f, obtained by replacing $+$ with $\oplus$, $\cdot$ with $\odot$, and all coefficients with their valuation. There is also a notion of *tropical projective space*,

$$\mathbb{TP}^n := \mathbb{T}^{n+1} \backslash \{(\infty, ..., \infty)\},$$

which is defined by the equivalence relation $v \sim v + \lambda(1, ..., 1)$. We then have that the coordinate system $(x_1, ..., x_{n+1})$ on $\mathbb{T}^{n+1}$ induces a tropical homogeneous coordinate system $[x_1 : ... : x_{n+1}]$ on $\mathbb{TP}^n$ given by the natural embedding, $\mathbb{R}^n \to \mathbb{TP}^{n+1}$, $(x_1, ..., x_n) \mapsto [x_1 : ... : x_n : 0]$.

Picking a $w \in \mathbb{R}^n$, the *w-weight* of a term $a_i(t) x_1^{b_1^i} \cdots x_n^{b_n^i}$ of a polynomial f is equal to the dot product $\mathrm{val}(a_i(t)) + \langle w, \bar{b} \rangle$, where $\bar{b} = (b_1^i, ..., b_n^i)$. We then define $\mathrm{in}_w(f)$ to be the polynomial consisting of the sum of the terms of f with the smallest w-weight. A *tropical hypersurface* can then be defined as

$$\mathcal{T}(f) := \{w \in \mathbb{R}^n : \ \mathrm{in}_w(f) \text{ is not a monomial}\}.$$

It is straightforward to check that the "inherently tropical" definition of a tropical hypersurface given at the beginning of this section is equivalent to the one directly above. A *root of a tropical polynomial* f in n variables $x_1, ..., x_n$ is a point $(b_1, ..., b_n) \in \mathbb{R}^n$ such that the value $f(b_1, ..., b_n)$, is attained by at least two of the linear functions defining f.

A finite intersection of tropical hypersurfaces is called a *tropical prevariety*. Given an ideal $I \subseteq \mathbb{K}[x_1, ..., x_n]$ and $w \in \mathbb{R}^n$, we define the *tropical variety* $\mathcal{T}(I)$ to be the intersection of tropical hypersurfaces

$$\mathcal{T}(I) := \bigcap_{f \in I} \mathcal{T}(f)$$

along with a weight function $\Omega_w : \mathbb{K}[x_1, ...x_n] \to \mathbb{R}$, sending

$$a_i(t)x_1^{b_1^i} \cdots x_n^{b_n^i} \mapsto \text{val}(a_i(t)) + \langle w, \bar{b} \rangle$$

for each monomial of a polynomial $f = \sum_{i=1}^{k} a_i(t)x_1^{b_1^i} \cdots x_n^{b_n^i} \in I$, where $\bar{b} = (b_1^i, ..., b_n^i)$. Equivalently, the tropical variety $\mathcal{T}(I)$ can be defined as

$$\mathcal{T}(I) := \{w \in \mathbb{R}^n : \text{in}_w(I) \text{ has no monomials}\},$$

where $\text{in}_w(I)$ is the ideal generated by the set $\{\text{in}_w(f) : f \in I\}$. It is important for us to note that if we have a variety $V(I)$, we can consider the closure of the image of $V(I)$ under the map

$$\text{trop} : \mathbb{K}^n \to \mathbb{R}^n, x \mapsto \text{val}(x)$$

and that we get $\mathcal{T}(I) = \overline{\text{trop}(V(I))}$.

2.1. The Positive Part of a Tropical Variety. Now that we have some idea as to what a tropical variety is, we can define the positive part of a tropical variety. The *positive part* of a tropical variety $\mathcal{T}(I)$ is defined to be

$$\mathcal{T}^+(I) := \overline{trop(V(I) \cap (\mathbb{K}^+)^n)},$$

where

$$\mathbb{K}^+ := \{\alpha(t) \in \mathbb{K} : \text{coefficient of lowest term of } \alpha(t) \text{ is real and positive}\}.$$

The following theorems are useful for uncovering the positive part of a tropical variety:

THEOREM 2.1 (Speyer and Williams [**102**]). *A point $w = (w_1, ..., w_n)$ lies in $\mathcal{T}^+(I)$ if and only if $\text{in}_w(I)$ does not contain any nonzero polynomials in $\mathbb{K}^+[x_1, ..., x_n]$.*

THEOREM 2.2 (Speyer and Williams [**102**]). *An ideal I of $\mathbb{K}[x_1, ..., x_n]$ contains a nonzero element of $\mathbb{K}^+[x_1, ..., x_n]$ if and only if $(\mathbb{K}^+)^n \cap V(\text{in}_w(I)) = \emptyset$, for all $w \in \mathbb{K}^n$.*

In practice, the positive part of a tropical variety can be uncovered by identifying each domain of linearity with the sign of its defining monomial and taking the components of the tropical variety which separate regions of different signs to be the positive part. Let us see what this means through an example:

EXAMPLE 2.3. Let us consider the polynomial $1 - x - y + t^{-1}xy = 0$. Its tropicalization

$$f = \min\{0, x, y, x + y - 1\}$$

can be represented as a partition of the plane into polygonal regions, as illustrated in Figure 7. We want to find solutions in $\mathbb{K}^+$ to $1 - x - y + t^{-1}xy = 0$ and take the closure of the tropicalization of this to get the positive part. Say $(x, y) = (a_0 t^{b_0} + \cdots, c_0 t^{d_0} + \cdots)$ is such a solution, where a_0 and c_0 are the lowest terms. We then have that

$$1 - (a_0 t^{b_0} + \cdots) - (c_0 t^{d_0} + \cdots) + t^{-1}(a_0 t^{b_0} + \cdots)(c_0 t^{d_0} + \cdots) = 0,$$

and we can see that the only terms which have even the possibility of cancelling each other out are terms with different signs (as a_0 and c_0 are real and positive). So the positive part of our tropical variety is composed of the components of our tropical variety separating linear regions defined by monomials of different signs, as seen in Figure 7.

We can then see that finding the positive part of a tropical variety by identifying linear regions with the sign of their defining linear term works as a method for finding the positive part of a tropical variety in general, meaning that *the positive part of a tropical variety recaptures the sign of each monomial, which is initially lost through the tropicalization process.*

For this example specifically, we can identify the region in which f is equal to $x + y - 1$ with a "+" sign, since the sign of $t^{-1}xy$ is "+". Similarly, we identify the region in which f is equal to x and the region in which f is equal to y with "−" signs and the region in which f is 0 with a "+". The positive part is the subset of our tropical variety below defined by the components in bold as opposed to dashed.
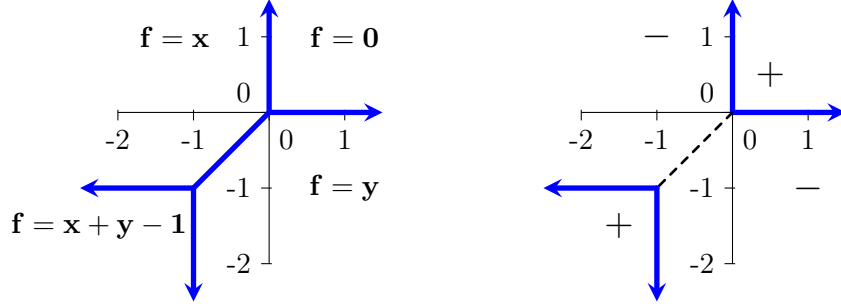
FIGURE 7. The tropical variety defined by $f = \min\{0, x, y, x + y - 1\}$ on the left, and its positive part on the right

2.2. The Dressian. As discussed in [**103**], a *tropical linear space* is a tropical variety $\mathcal{T}(I)$ given by an ideal of the form

$$I = \langle a_{i1}x_1 + a_{i2}x_2 + \cdots + a_{in}x_n : i = 1, 2, ..., n - d \rangle,$$

where the a_{ij} are the entries of any $(n-d) \times n$-matrix of rank $n-d$ with entries in $\mathbb{K}[x_1, ..., x_n]$. The ideal I can be rewritten in terms of a vector in $\mathbb{R}^{\binom{n}{d}}$ whose entries are the *Plücker coordinates*

$$p_{i_1 i_2 \cdots i_d} := (-1)^{i_1 + i_2 + \cdots + i_d} \cdot \det \begin{pmatrix} a_{1,j_1} & a_{1,j_2} & \cdots & a_{1,j_{n-d}} \\ a_{2,j_1} & a_{2,j_2} & \cdots & a_{2,j_{n-d}} \\ \vdots & \vdots & \ddots & \vdots \\ a_{n-d,j_1} & a_{n-d,j_2} & \cdots & a_{n-d,j_{n-d}} \end{pmatrix},$$

where $i_1 < \cdots < i_d, j_1 < \cdots < i_{n-d}$ and $\{i_1, ..., i_d, j_1, ..., j_{n-d}\} = \{1, ..., n\}$. Explicitly, we have

$$I = \langle \sum_{r=0}^{d} (-1)^r \cdot p_{i_0 i_1 \cdots \hat{i}_r \cdots i_d} \cdot x_{i_r} : \text{ for all } 1 \leq i_0 \leq i_1 < \cdots < i_r \leq n \rangle.$$

Speyer gives the details on how to derive I in terms of Plücker coordinates in [**103**]. The *Dressian* $\mathrm{Dr}(d, n)$ is the tropical prevariety which parametrizes $(d-1)$-dimensional tropical linear spaces, and is more explicitly the tropical prevariety consisting of the intersection of the tropical hypersurfaces given by all 3-term Plücker relations. The Dressian can also be defined as the polyhedral fan of those regular subdivisions of the *(d,n)-hypersimplex* which have the property that each cell is a *matroid polytope* [**56**]. More specifically, let $e_1, ..., e_n$ be the standard basis vectors for $\mathbb{R}^n$ and let $e_X := \sum_{i \in X} e_i$ for any subset $X \subseteq [n]$. Given a matroid $X \subseteq \binom{[n]}{d}$, we define its *matroid polytope* to be the polytope $P_X := \mathrm{conv}\{e_x : x \in X\}$. The *(d, n)-hypersimplex* $\triangle(d, n)$ in $\mathbb{R}^n$ is defined as $\triangle(d, n) := P_{\binom{[n]}{d}}$. A *matroid subdivision* of a polytope P is a polytopal subdivision of P such that each of its cells is a matroid polytope. A *weight vector* λ on a polytope P assigns a real number to each vertex of P. A given weight vector λ induces a polytopal subdivision of a polytope P by considering the set $\mathrm{conv}\{(v, \lambda(v)) : v \text{ vertex of } P\}$ in $\mathbb{R}^{n+1}$ and projecting the lower (or upper) envelope to the hyperplane $(\mathbb{R}^n, 0)$; a polytopal subdivision of this kind is called a *regular* polytopal subdivision. The Dressian is shown in [**56**] to be a subfan of the secondary fan of $\triangle(d, n)$:

PROPOSITION 2.4. (Herrmann, Jensen, Joswig, and Sturmfels [**55**, Proposition 3.1]) *A weight vector $\lambda \in \mathbb{R}^{\binom{[n]}{d}}$ lies in the Dressian $\mathrm{Dr}(d, n)$, seen as a fan, if and only if it induces a matroid subdivision of the hypersimplex $\triangle(d, n)$.*

It is pointed out in [**55**] that the three term Plücker relations define a natural Plücker fan structure on the Dressian: two weight vectors λ and λ' are in the same cone if they specify

the same initial form for each 3-term Plücker relation.

REMARK 2.5. Tropical Plücker vectors (i.e. vectors of tropicalizations of Plücker coordinates) can be viewed as valuated matroids [55, Remark 2.4]. A *valuated matroid* of rank d on a set $[n]$ is a map $\pi : [n]^d \to \mathbb{R} \cup \{\infty\}$ such that

   (1) $\pi(\omega)$ is independent of the ordering of the sequence vector ω,
   (2) $\pi(\omega) = \infty$ if an element occurs twice in ω,
   (3) for every $(d-1)$-subset σ and every $(d+1)$-subset $\tau = \{\tau_1, \tau_2, ..., \tau_{d+1}\}$ of $[n]$ the minimum of

$$\pi(\sigma \cup \{\tau_i\}) + \pi(\tau \backslash \{\tau_i\}) \text{ for } 1 \leq i \leq d+1$$

   is attained at least twice.

Tropical planes are dual to regular matroid subdivisions of the hypersimplex $\triangle(3, n)$, thus giving us another way to view $\mathrm{Dr}(3, n)$: The parameter space of tropical planes. A *tropical plane* L_p in $\mathbb{TP}^{n-1}$, for some $p \in \mathrm{Dr}(3, n)$, is the intersection of the tropical hyperplanes

$$\bigcap_{\{i,j,k,l\} \in \binom{[n]}{4}} \mathcal{T}(p_{ijk}x_l + p_{ijl}x_k + p_{ikl}x_j + p_{jkl}x_i),$$

where the Plücker coefficients appearing in $p_{ijk}x_l + p_{ijl}x_k + p_{ikl}x_j + p_{jkl}x_i$ are entries of p lexicographically indexed by the order $i < j < k < l$.

Just as planes in projective space $\mathbb{P}^{n-1}$ correspond to arrangements of n lines in $\mathbb{P}^2$, tropical planes in $\mathbb{TP}^{n-1}$ correspond to arrangements of n *tropical lines* in $\mathbb{TP}^2$. A *tropical line* in $\mathbb{TP}^{n-1}$ is an embedded metric tree which is balanced and has n unbounded edges pointing in the coordinate directions. Thus, we can use arrangements of trees to represent matroid subdivisions of $\triangle(3, n)$. We say trees, and not metric trees due to the following result:

PROPOSITION 2.6. (Herrmann, Jensen, Joswig, and Sturmfels [55, Proposition 4.1]) *Each metric tree arrangement gives rise to an abstract tree arrangement by ignoring the edge lengths.*

We then have that:

LEMMA 2.7. (Herrmann, Jensen, Joswig, and Sturmfels [55, Lemma 4.2]) *Each matroid subdivision Σ of $\triangle(3, n)$ defines an abstract arrangement $T(\Sigma)$ of n trees. Moreover, if Σ is regular then $T(\Sigma)$ supports a metric tree arrangement.*

For a definition of *abstract tree arrangement*, we refer the reader to [55, section 4]. The bijection between tropical planes and arrangements of metric trees is studied in great detail in [55], with their main theorem being:

THEOREM 2.8. (Herrmann, Jensen, Joswig, and Sturmfels [55, Theorem 4.4]) *The equivalence classes of arrangements of n metric trees are in bijection with regular matroid subdivision of the hypersimplex $\triangle(3, n)$. Moreover, the secondary fan structure on $\mathrm{Dr}(3, n)$ coincides with the Plücker fan structure.*

2.3. The Tropical Grassmannian and its Positive Part. The *tropical Grassmannian* $\mathrm{Gr}(d, n)$ is a tropical variety which is a subset of the Dressian $\mathrm{Dr}(d, n)$. As fans, the Grassmannian and the Dressian have the same n-dimensional lineality space and thus can be viewed as pointed fans in $\mathbb{R}^{\binom{n}{d}-n}$, one sitting inside of the other. Explicitly, the tropical Grassmannian is $\mathcal{T}(I_{d,n})$, where $I_{d,n}$ is the *Plücker ideal*; i.e. the ideal generated by the Plücker relations.

The tropical Grassmannian was first studied in Speyer and Sturmfels [101] and its positive part was then studied in Speyer and Williams [102]. Speyer and Williams lay out the first steps in studying the positive part of a tropical variety and explicitly outline a way of

parametrizing the positive part $\mathrm{Gr}^+(d, n)$ of $\mathrm{Gr}(d, n)$ using a particular kind of directed graph $\mathrm{Web}_{d,n}$, which is a special case of the ⌐-diagrams of Postnikov [**93**]. The short story of their parametrization is that they develop a bijection Φ_2 from $(\mathbb{R}^+)^{(d-1)(n-d-1)}$ to the real, positive points of the Grassmannian (modulo its lineality space) using $\mathrm{Web}_{d,n}$. They tropicalize this map to get a surjection from $\mathbb{R}^{(d-1)(n-d-1)}$ to the positive part of the tropical Grassmannian (modulo its lineality space). Then they define a complete fan $F_{d,n}$ in $\mathbb{R}^{(d-1)(n-d-1)}$ whose maximal cones are the domains of linearity of the tropicalization of Φ_2.

For $\mathrm{Gr}^+(2, n)$, Speyer and Williams [**102**] show that their fan $F_{2,n}$ is equal to the Stanley–Pitman fan F_{n-3} of [**105**], which is combinatorially isomorphic to the cluster complex of type A_{n-3}. They also show that the tropical Grassmannians $\mathrm{Gr}^+(3, 6)$ and $\mathrm{Gr}^+(3, 7)$ are closely related to the cluster complexes of type D_4 and E_6 respectively. The connection between $\mathrm{Gr}^+(3, 6)$ and the cluster complex of type D_4 will be made precise in section 3.

3. Connecting the Cluster Complex of Type D_4 to $\mathrm{Gr}^+(3, 6)$

In [**102**, Proposition 6.1], Speyer and Williams provide an explicit computation of the fan $F_{3,6}$ associated to the tropical Grassmannian $\mathrm{Gr}^+(3, 6)$, together with inequalities defining a polytope that $F_{3,6}$ is normal to. They computed the f-vector $(16, 66, 98, 48)$ of $F_{3,6}$ and noticed that it is very close to the f-vector $(16, 66, 100, 50)$ of the cluster complex of type D_4. They found that $F_{3,6}$ has two cones which are of the form of a cone over a bipyramid, and stated that when subdividing these two bipyramids into two tetrahedra each, one gets a fan that is combinatorially isomorphic to the cluster complex of type D_4.
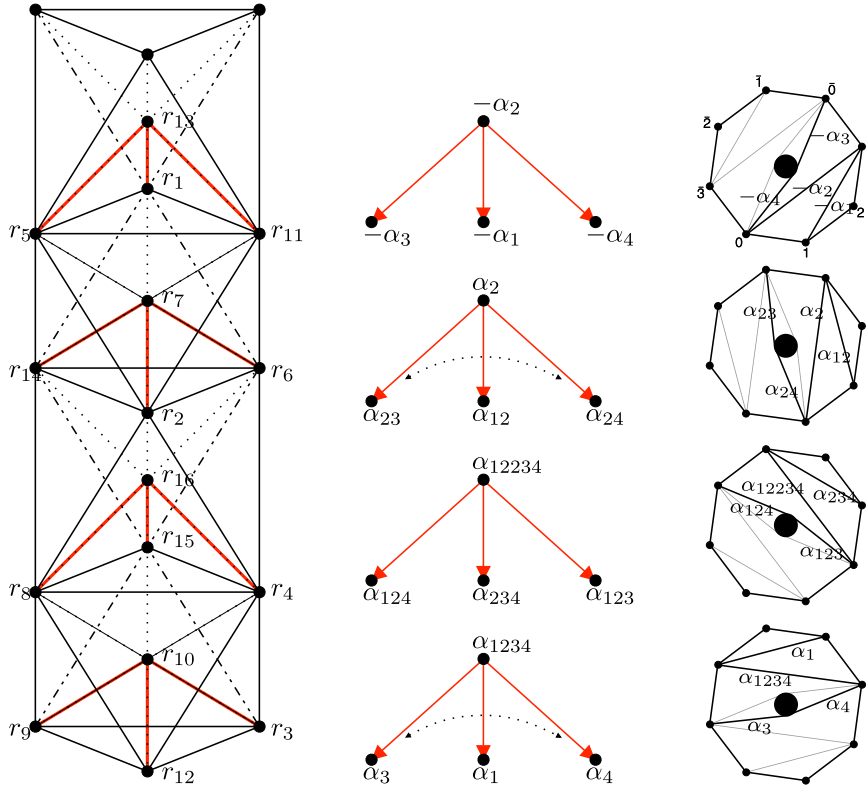
FIGURE 8. Speyer–Williams fan $F_{3,6}$ (part 1) and the bijection between its rays, almost positive roots, and centrally symmetric pairs of chords in the geometric model

In this section, we make this connection more precise by providing an explicit bijection between the rays of $F_{3,6}$ and the almost positive roots of type D_4. The cones of the fan
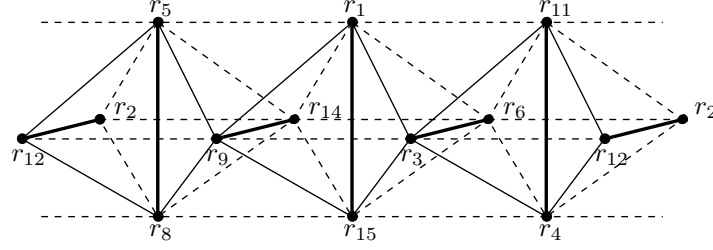
FIGURE 9. Speyer–Williams fan $F_{3,6}$ (part 2)

correspond to clusters, with the exception of the two cones over a bipyramid, which correspond to two clusters each, glued together on their common face.

The fan $F_{3,6}$ is a 4-dimensional fan whose intersection with a 3-sphere is illustrated in Figure 8 (left) and Figure 9. Each of the figures is a solid torus, and the two figures glue together to form a 3-sphere. The two bipyramids have vertices $\{r_1, r_5, r_7, r_{11}, r_{13}\}$ and $\{r_4, r_8, r_{10}, r_{15}, r_{16}\}$. These figures are reproduced from Speyer and Williams original figures [102, Figures 7 and 8]. In addition, we include part of the Auslander–Reiten quiver of type D_4, formed by repeating 4 copies of a bipartite quiver of type D_4. The 16 vertices of this "repetition quiver" are labelled by the 16 almost positive roots as shown in Figure 8 (middle). We also include the corresponding 16 pairs of chords in the geometric model in Figure 8 (right).

The labeling with almost positive roots in Figure 8 (middle) can be explained in two different ways. The first, and perhaps more intuitive one, assigns the negative simple roots to the vertices of the first copy of the D_4 quiver on the top, and the other labels are determined by rotation. Rotation sends a vertex in a copy of a D_4 quiver to the same vertex in the next copy directly below, if any. The last copy of the D_4 quiver in the bottom is rotated to the first copy on the top. The rotation on almost positive roots is the one induced by the τ rotation of chords in the geometric model. Recall that this is given by counterclockwise rotation by $\pi/4$ together with the special rule of exchanging central chords p^{R} and p^{L}. A chord δ not in the initial snake is labeled by the positive root obtained by adding the simple roots corresponding to the chords of the snake that are crossed by δ. Figure 8 (right) illustrates this rotation process together with the root labeling of the chords. Note that rotating one more time the chords in the bottom picture recovers back the initial snake pseudotriangulation. The second explanation of the labeling by almost positive roots can be done in terms of inversions of a word $P = \tau_2\tau_1\tau_3\tau_4|\tau_2\tau_1\tau_3\tau_4|\tau_2\tau_1\tau_3\tau_4$. The word P is a reduced expression for the longest element of the Coxeter group and its inversions give all positive roots. Moreover, it consists of three copies of $\tau_2\tau_1\tau_3\tau_4$, and its letters are in correspondence with the vertices of the last three copies of the bipartite quiver of type D_4 in Figure 8 (middle). The labeling assigns to the vertices of these last three copies the inversions of P, and to the vertices of the first copy of the D_4 quiver the negative simple roots. This second explanation is based in work on subword complexes in [20], we refer to [21, section 2.2] for a concise and more detailed presentation.

Let Ψ be the bijection from the rays of Speyer–Williams fan $F_{3,6}$ and almost positive roots given in Figure 10 (left and middle).

This bijection sends the vertices of the four bold D_4 quiver in Figure 8 (left) to the vertices of the four D_4 quivers in Figure 8 (middle), and exchanges the two external vertices of the second and fourth quiver as shown. Note that this special rule is similar to the rule of exchanging the corresponding central chords when rotating. The induced bijection between rays of the fan and centrally symmetric pairs of chords in the geometric model is illustrated in Figure 11.

Rays of $F_{3,6}$	$\longleftrightarrow$	$\Phi_{\geq -1}$ of type D_4	$\longleftrightarrow$	Chords	Rays of $F_{3,6}$	$\longleftrightarrow$	$\Phi_{\geq -1}$ of type D_4	$\longleftrightarrow$	Chords
$r_1 = (0,0,1,0)$	$\longleftrightarrow$	$-\alpha_1$	$\longleftrightarrow$	$1\bar{3}$	$r_9 = (0,0,1,-1)$	$\longleftrightarrow$	α_4	$\longleftrightarrow$	3^{L}
$r_2 = (0,0,-1,0)$	$\longleftrightarrow$	$\alpha_1 + \alpha_2$	$\longleftrightarrow$	$0\bar{2}$	$r_{10} = (1,0,0,-1)$	$\longleftrightarrow$	$\alpha_1 + \alpha_2 + \alpha_3 + \alpha_4$	$\longleftrightarrow$	$2\bar{3}$
$r_3 = (1,0,0,0)$	$\longleftrightarrow$	α_3	$\longleftrightarrow$	3^{R}	$r_{11} = (0,1,0,0)$	$\longleftrightarrow$	$-\alpha_4$	$\longleftrightarrow$	0^{R}
$r_4 = (1,0,-1,0)$	$\longleftrightarrow$	$\alpha_1 + \alpha_2 + \alpha_3$	$\longleftrightarrow$	2^{R}	$r_{12} = (0,1,0,-1)$	$\longleftrightarrow$	α_1	$\longleftrightarrow$	02
$r_5 = (-1,0,0,0)$	$\longleftrightarrow$	$-\alpha_3$	$\longleftrightarrow$	0^{L}	$r_{13} = (0,1,1,-1)$	$\longleftrightarrow$	$-\alpha_2$	$\longleftrightarrow$	03
$r_6 = (0,0,0,1)$	$\longleftrightarrow$	$\alpha_2 + \alpha_3$	$\longleftrightarrow$	1^{R}	$r_{14} = (0,-1,0,0)$	$\longleftrightarrow$	$\alpha_2 + \alpha_4$	$\longleftrightarrow$	1^{L}
$r_7 = (-1,0,0,1)$	$\longleftrightarrow$	α_2	$\longleftrightarrow$	$0\bar{1}$	$r_{15} = (1,-1,0,0)$	$\longleftrightarrow$	$\alpha_2 + \alpha_3 + \alpha_4$	$\longleftrightarrow$	13
$r_8 = (0,0,0,-1)$	$\longleftrightarrow$	$\alpha_1 + \alpha_2 + \alpha_4$	$\longleftrightarrow$	2^{L}	$r_{16} = (1,-1,-1,0)$	$\longleftrightarrow$	$\alpha_1 + 2\alpha_2 + \alpha_3 + \alpha_4$	$\longleftrightarrow$	$1\bar{2}$

FIGURE 10. A bijection from the rays of $F_{3,6}$ to the almost positive roots of type D_4 and to centrally symmetric pairs of chords in the geometric model
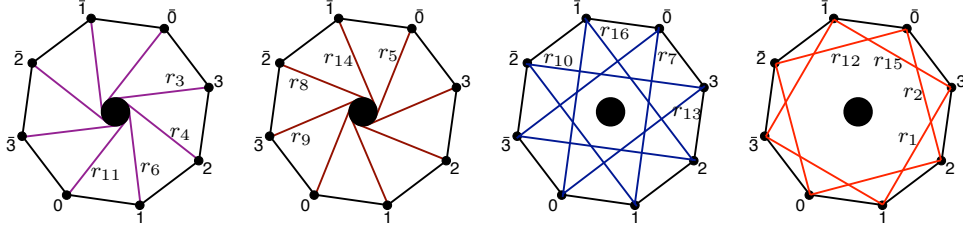
FIGURE 11. Bijection between rays of the fan F_{36} and centrally symmetric pairs of chords in geometric model

THEOREM 3.1. *Under the bijection Ψ, the cones of the fan $F_{3,6}$ correspond to clusters of type D_4, with the exception that the two cones over a bipyramid correspond to two clusters each, that are glued together on their common face:*

$$\{r_1, r_5, r_7, r_{11}, r_{13}\} \qquad\qquad \{r_4, r_8, r_{10}, r_{15}, r_{16}\}$$
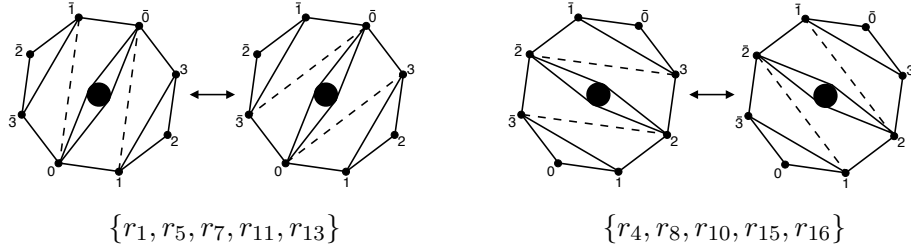
PROOF. The proof of this result uses the description of cluster complexes in terms of the compatibility degrees of Fomin and Zelevinsky in [**43**, section 3]. The compatibility degree is a map

$$\begin{aligned} \Phi_{\geq -1} \times \Phi_{\geq -1} &\longrightarrow & \mathbb{Z} \\ (\alpha, \beta) &\longmapsto & (\alpha \,||\, \beta) \end{aligned}$$

characterized by the two properties:

$$(-\alpha_i \,||\, \beta) = b_i, \qquad \text{for all } i \in [n] \text{ and } \beta = \sum b_i \alpha_i \in \Phi_{\geq -1}, \tag{II.1}$$

$$(\alpha \,||\, \beta) = (\tau\alpha \,||\, \tau\beta), \quad \text{for all } \alpha, \beta \in \Phi_{\geq -1}, \tag{II.2}$$

where τ is the rotation operation on almost positive roots defined in section 1.2. Two almost positive roots are said to be compatible if and only if their compatibility degree is zero. The cluster complex is the simplicial complex whose faces are sets of pairwise compatible roots. This complex is completely determined by its edges (1-dimensional simplices), and so it suffices to show that the edges in Figure 8 (left) and Figure 9 correspond exactly to the compatible pairs of almost positive roots under the map Ψ. This can be checked by inspection for the pairs involving a negative simple root, and by rotating the figures to obtain all other pairs. For instance, $-\alpha_1$ is compatible with $-\alpha_2, -\alpha_3, -\alpha_4, \alpha_2, \alpha_{23}, \alpha_{24}, \alpha_{234}, \alpha_3$, and α_4, while $r_1 = \Psi^{-1}(-\alpha_1)$ forms edges with the corresponding rays $r_{13}, r_5, r_{11}, r_7, r_6, r_{14}, r_{15}, r_3$,

and r_9. The pairs of compatible roots that do not appear as edges in Figure 8 (left) but do (in bold) in Figure 9 are:

$$\begin{array}{cccccc} (-\alpha_1, \alpha_{234}) & (-\alpha_3, \alpha_{124}) & (-\alpha_4, \alpha_{123}) & (\alpha_{12}, \alpha_1) & (\alpha_{23}, \alpha_3) & (\alpha_{24}, \alpha_4) \\ (r_1, r_{15}) & (r_5, r_8) & (r_{11}, r_4) & (r_2, r_{12}) & (r_6, r_3) & (r_{14}, r_9) \end{array}$$

Taking the clique complex of the compatibility relation finishes the proof. $\qquad\square$

4. Tropical Computations

In this section, we compute the fan $F_{3,6}$ of Speyer and Williams [102] and analyze which tropical planes in $\mathbb{TP}^5$ are realized by $\mathrm{Gr}^+(3,6)$. We follow suit and compute $F_{3,6}$ in the same fashion as Speyer and Williams would in [102]. First we draw the web diagram $\mathrm{Web}_{3,6}$ and label its interior regions as shown in Figure 12. This is the labeling implicitly used by Speyer and Williams in their computations.
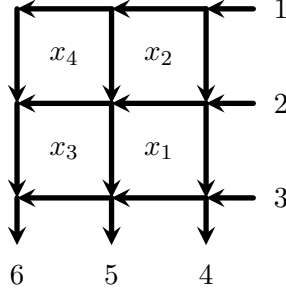
FIGURE 12. The labeling of the web diagram $\mathrm{Web}_{3,6}$

The fan $F_{3,6}$ is the complete fan in $\mathbb{R}^4$ whose maximal cones are the domains of linearity of the piecewise linear map

$$\mathrm{Trop}\,\Phi_2 : \mathbb{R}^4 \to \mathrm{Gr}^+(3,6)/(\mathrm{Trop}\,\phi)(\mathbb{R}^6),$$

where $\mathrm{Trop}\,\phi$ is the map sending $(a_1, ..., a_6)$ to the $\binom{6}{3}$-vector whose (i_1, i_2, i_3)-coordinate is $a_{i_1} + a_{i_2} + a_{i_3}$; its image is the common lineality space of all cones in $\mathrm{Gr}^+(3,6)$. The map $\mathrm{Trop}\,\Phi_2$ is defined by the tropicalization of the maximal minors of the 3×6 matrix $A_{3,6}$, whose entries are given by

$$a_{ij} = (-1)^{i+1} \sum_p \mathrm{Prod}_p,$$

where we are summing over all paths p from i to j in $\mathrm{Web}_{3,6}$, and Prod_p is the product of all the variables x_i appearing below a given path p. Specifically, the matrix we get is

$$A_{3,6} = \begin{bmatrix} 1 & 0 & 0 & 1 & x_1x_2 + x_1 + 1 & x_1x_2x_3x_4 + x_1x_2x_3 + x_1x_3 + x_1x_2 + x_1 + 1 \\ 0 & -1 & 0 & -1 & -(x_1 + 1) & -(x_1x_3 + x_1 + 1) \\ 0 & 0 & 1 & 1 & 1 & 1 \end{bmatrix}.$$

The tropicalization of the maximal minors P_{ijk} of $A_{3,6}$ are the following:

$P_{123} = 0$ $P_{234} = 0$

$P_{124} = 0$ $P_{235} = \min\{0, x_1, x_1 + x_2\}$

$P_{125} = 0$ $P_{236} = \min\{0, x_1, x_1 + x_2, x_1 + x_3, x_1 + x_2 + x_3, x_1 + x_2 + x_3 + x_4\}$

$P_{126} = 0$ $P_{245} = \min\{x_1, x_1 + x_2\}$

$P_{134} = 0$ $P_{246} = \min\{x_1, x_1 + x_2, x_1 + x_3, x_1 + x_2 + x_3, x_1 + x_2 + x_3 + x_4\}$

$P_{135} = \min\{0, x_1\}$ $P_{256} = \min\{x_1 + x_3, x_1 + x_2 + x_3, x_1 + x_2 + x_3 + x_4\}$

$P_{136} = \min\{0, x_1, x_1 + x_3\}$ $P_{345} = x_1 + x_2$

$P_{145} = x_1$ $P_{346} = \min\{x_1 + x_2, x_1 + x_2 + x_3, x_1 + x_2 + x_3 + x_4\}$

$P_{146} = \min\{x_1, x_1 + x_3\}$ $P_{356} = \min\{x_1 + x_2 + x_3, x_1 + x_2 + x_3 + x_4, 2x_1 + x_2 + x_3 + x_4\}$

$P_{156} = x_1 + x_3$ $P_{456} = 2x_1 + x_2 + x_3 + x_4$

We then have that each P_{ijk} gives rise to a fan $F(P_{ijk})$, and the simultaneous refinement of all of these fans is $F_{3,6}$. We compute this refinement using `Sage` [107] and get the rays:

$r_1 = (0, 0, 1, 0)$ $r_5 = (-1, 0, 0, 0)$ $r_9 = (0, 0, 1, -1)$ $r_{13} = (0, 1, 1, -1)$

$r_2 = (0, 0, -1, 0)$ $r_6 = (0, 0, 0, 1)$ $r_{10} = (1, 0, 0, -1)$ $r_{14} = (0, -1, 0, 0)$

$r_3 = (1, 0, 0, 0)$ $r_7 = (-1, 0, 0, 1)$ $r_{11} = (0, 1, 0, 0)$ $r_{15} = (1, -1, 0, 0)$

$r_4 = (1, 0, -1, 0)$ $r_8 = (0, 0, 0, -1)$ $r_{12} = (0, 1, 0, -1)$ $r_{16} = (1, -1, -1, 0)$

Now that we have $F_{3,6}$, we would like to see which combinatorial types of generic planes in $\mathbb{TP}^5$ are realized by $\mathrm{Gr}^+(3, 6)$. Speyer and Sturmfels [101] are the first to describe $\mathrm{Gr}(3, 6)$ as the parameter space for tropical planes in $\mathbb{TP}^5$ and a recipe for computing which planes in $\mathbb{TP}^5$ realized where in $\mathrm{Gr}(3, 6)$ is given by Herrmann, Jensen, Joswig, and Sturmfels in [55]. We follow this recipe to compute which planes in $\mathbb{TP}^5$ are realized by $\mathrm{Gr}^+(3, 6)$; for each maximal cone C of $F_{3,6}$, the recipe goes as follows:

  (1) Choose an interior point λ of C.
  (2) Compute its image $\mathrm{Trop}\,\Phi_2(\lambda)$.
  (3) By Proposition 2.4, we know $\mathrm{Trop}\,\Phi_2(\lambda)$ induces a matroid subdivision of the hypersimplex $\triangle(3, 6)$; Compute this subdivision using `Polymake` [48].
  (4) Compare the computed matroid subdivision with the matroid subdivisions given in [55] used to classify combinatorial types of generic tropical planes in $\mathbb{TP}^5$.

Step (4) of the recipe was done by computing the face lattices of each matroid polytope for the matroids and the dimension of the intersections in the computed subdivision. Comparing them to the face lattices of the matroid polytopes of the matroids in the subdivisions given in [55] classifies the combinatorial types of generic tropical planes in $\mathbb{TP}^5$. The graphical representation in Figure 1 of [55] shows the neighboring properties using edges and 2-cells. The difference between EEFFa and EEFFb is as follows: in Type EEFFa, there are two matroid polytopes that do not intersect, whereas in Type EEFFb, there are three 2-dimensional intersections between the matroid polytopes. These computations were all made using `Sage` [107]. As the combinatorial type of plane does not change within a maximal cone [55], by following the recipe above for each maximal cone of $F_{3,6}$, we get all planes realized by $\mathrm{Gr}^+(3, 6)$.

THEOREM 4.1. *Exactly six of the seven combinatorial types of tropical planes in $\mathbb{TP}^5$ are realized by $\mathrm{Gr}^+(3, 6)$. As named by Sturmfels and Speyer* [101], *the realizable combinatorial types are EEEG, EEFFa, EEFFb, EEFG, EFFG, and FFFGG.*

The partition into the combinatorial types is shown in Table 1.

5. Comparing Tropical Planes and Pseudotriangulations

Noting that $\mathrm{Dr}(3, 6)$ and $\mathrm{Gr}(3, 6)$ are equal as sets, Speyer and Sturmfels describe $\mathrm{Gr}(3, 6)$ as the parameter space for tropical planes in $\mathbb{TP}^5$. Using Theorem 4.1, we can deduce how the equivalence of tropical planes compares with equivalence of pseudotriangulations.

Type EEEG:	$\{r_3, r_9, r_{10}, r_{12}\}, \{r_2, r_6, r_{14}, r_{16}\}, \{r_3, r_9, r_{12}, r_{13}\}, \{r_2, r_6, r_7, r_{14}\}$
Type EEFFa:	$\{r_3, r_4, r_6, r_{15}\}, \{r_1, r_3, r_6, r_{11}\}, \{r_2, r_5, r_8, r_{12}\}, \{r_2, r_5, r_{11}, r_{12}\},$
	$\{r_1, r_3, r_6, r_{15}\}, \{r_1, r_5, r_9, r_{14}\}, \{r_2, r_4, r_8, r_{12}\}, \{r_3, r_4, r_6, r_{11}\},$
	$\{r_5, r_8, r_9, r_{14}\}, \{r_8, r_9, r_{14}, r_{15}\}, \{r_2, r_4, r_{11}, r_{12}\}, \{r_1, r_9, r_{14}, r_{15}\}$
Type EEFFb:	$\{r_2, r_5, r_8, r_{14}\}, \{r_1, r_3, r_9, r_{15}\}, \{r_2, r_4, r_6, r_{11}\}, \{r_5, r_8, r_9, r_{12}\},$
	$\{r_1, r_6, r_{14}, r_{15}\}, \{r_3, r_4, r_{11}, r_{12}\}$
Type EEFG:	$\{r_5, r_9, r_{12}, r_{13}\}, \{r_3, r_9, r_{10}, r_{15}\}, \{r_3, r_4, r_{10}, r_{12}\}, \{r_3, r_{11}, r_{12}, r_{13}\},$
	$\{r_1, r_3, r_9, r_{13}\}, \{r_6, r_{14}, r_{15}, r_{16}\}, \{r_1, r_6, r_7, r_{14}\}, \{r_2, r_8, r_{14}, r_{16}\},$
	$\{r_2, r_5, r_7, r_{14}\}, \{r_8, r_9, r_{10}, r_{12}\}, \{r_2, r_4, r_6, r_{16}\}, \{r_2, r_6, r_7, r_{11}\}$
Type EFFG:	$\{r_8, r_9, r_{10}, r_{15}\}, \{r_1, r_5, r_9, r_{13}\}, \{r_1, r_5, r_7, r_{14}\}, \{r_2, r_4, r_8, r_{16}\},$
	$\{r_1, r_3, r_{11}, r_{13}\}, \{r_2, r_5, r_7, r_{11}\}, \{r_8, r_{14}, r_{15}, r_{16}\}, \{r_3, r_4, r_{10}, r_{15}\},$
	$\{r_4, r_6, r_{15}, r_{16}\}, \{r_5, r_{11}, r_{12}, r_{13}\}, \{r_1, r_6, r_7, r_{11}\}, \{r_4, r_8, r_{10}, r_{12}\}$
Type FFFGG:	$\{r_4, r_8, \underline{r_{10}}, r_{15}, \underline{r_{16}}\}, \{r_1, r_5, \underline{r_7}, r_{11}, \underline{r_{13}}\}$

TABLE 1. The partition of the cone of the positive tropical Grassmannian into the corresponding combinatorial type of plane. In type FFFGG, the underlined rays represent the apexes of the splitted bipyramid to get the cluster complex.

THEOREM 5.1. *The combinatorial types of tropical planes in $\mathbb{TP}^5$ and the combinatorial types of pseudotriangulations of $\mathbf{D}_4$ intersect transversally as illustrated in Table 2.*

Interestingly, although the equivalence relations are transversal, they intersect in a way that respects the reflection and swapping equivalence of the pseudotriangulations. Using the table, we prove the next theorem giving a sufficient condition for two positive tropical planes to be combinatorially equivalent.

THEOREM 5.2. *If two pseudotriangulations of $\mathbf{D}_4$ are related by a sequence of reflections of the octagon preserving the parity of the vertices (when labeled cyclically from 1 up to 8), and possibly followed by a global exchange of central chords, then their corresponding tropical planes in $\mathbb{TP}^5$ are combinatorially equivalent.*

It turns out that this condition is necessary for types $EEEG$ and $FFFGG$. The four other positive types are obtained by taking unions of the classes generated by this finer equivalence on pseudotriangulations.

REMARK 5.3. It is possible to translate this finer equivalence of pseudotriangulations in the language of subword complexes, see [20]. It would also be interesting to know if this sufficient condition extends to tropical planes in $\mathbb{TP}^6$ when looking at the cluster complex of type E_6 as a subword complex.

TABLE 2. The combinatorial types of pseudotriangulations splitted into the combinatorial types of tropical planes.

Moduli of Tropical Plane Curves

Before introducing this chapter, it is important to note that this chapter is based on published work; the final publication is available at Springer via http://dx.doi.org/10.1186/s40687-014-0018-1. Tropical plane curves C are dual to regular subdivisions of their Newton polygon P. The tropical curve C is *smooth* if that subdivision is a unimodular triangulation Δ, i.e. it consists of triangles whose only lattice points are its three vertices. The *genus* $g = g(C)$ is the number of interior lattice points of P. Each bounded edge of C has a well-defined lattice length. The curve C contains a subdivision of a metric graph of genus g with vertices of valency ≥ 3 as in [**7**], and this subdivision is unique for $g \geq 2$. The underlying graph G is planar and has g distinguished cycles, one for each interior lattice point of P. We call G the *skeleton* of C. It is the smallest subspace of C to which C admits a deformation retract. While the metric on G depends on C, the graph is determined by Δ. For an illustration see Figure 13. The triangulation Δ on the left defines a family of smooth tropical plane curves of degree four. Such a curve has genus $g = 3$. Its skeleton G is shown on the right.
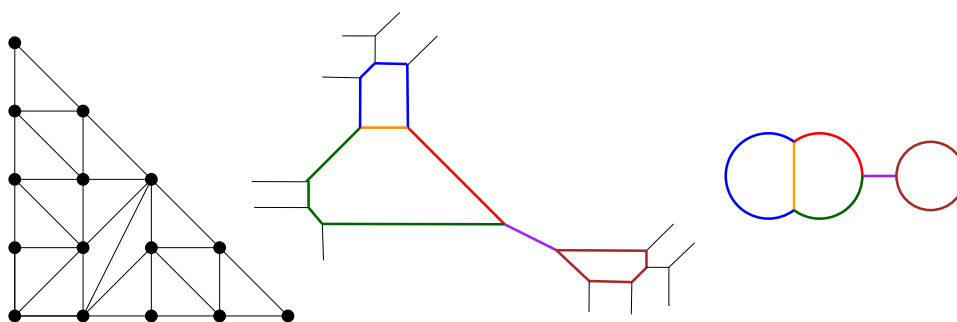
FIGURE 13. Unimodular triangulation, tropical quartic, and skeleton

For basics on tropical geometry and further references the reader is referred to [**61**, **80**]. Let $\mathbb{M}_g$ denote the *moduli space of metric graphs* of genus g. The moduli space $\mathbb{M}_g$ is obtained by gluing together finitely many orthants $\mathbb{R}^m_{\geq 0}$, $m \leq 3g-3$, one for each combinatorial type of graph, modulo the identifications corresponding to graph automorphisms. These automorphisms endow the moduli space $\mathbb{M}_g$ with the structure of a *stacky fan*. We refer to [**12**, **23**] for the definition of $\mathbb{M}_g$, combinatorial details, and applications in algebraic geometry. The maximal cones of $\mathbb{M}_g$ correspond to trivalent graphs of genus g. These have $2g - 2$ vertices and $3g - 3$ edges, so $\mathbb{M}_g$ is pure of dimension $3g - 3$. The number of trivalent graphs for $g = 2, 3, \ldots, 10$ is $2, 5, 17, 71, 388, 2592, 21096, 204638, 2317172$; see [**8**] and [**23**, Prop. 2.1].

Fix a (convex) lattice polygon P with $g = \#(\text{int}(P) \cap \mathbb{Z}^2)$. Let $\mathbb{M}_P$ be the closure in $\mathbb{M}_g$ of the set of metric graphs that are realized by smooth tropical plane curves with Newton polygon P. For a fixed regular unimodular triangulation Δ of P, let $\mathbb{M}_\Delta$ be the closure of the cone of metric graphs from tropical curves dual to Δ. These curves all have the same skeleton G, and $\mathbb{M}_\Delta$ is a convex polyhedral cone in the orthant $\mathbb{R}^{3g-3}_{\geq 0}$ of metrics on G. Working modulo automorphisms of G, we identify $\mathbb{M}_\Delta$ with its image in the stacky fan $\mathbb{M}_g$.

Now fix the skeleton G but vary the triangulation. The resulting subset of $\mathbb{R}^{3g-3}_{\geq 0}$ is a finite union of closed convex polyhedral cones, so it can be given the structure of a polyhedral fan. Moreover, by appropriate subdivisions, we can choose a fan structure that is invariant

under the symmetries of G, and hence the image in the moduli space $\mathbb{M}_g$ is a stacky fan:

$$\mathbb{M}_{P,G} \quad := \bigcup_{\substack{\Delta \text{ triangulation of P} \\ \text{with skeleton } G}} \mathbb{M}_\Delta. \tag{III.1}$$

We note that $\mathbb{M}_P$ is represented inside $\mathbb{M}_g$ by finite unions of convex polyhedral cones:

$$\mathbb{M}_P \quad = \bigcup_{\substack{G \text{ trivalent graph} \\ \text{of genus } g}} M_{P,G} \quad = \bigcup_{\substack{\Delta \text{ regular unimodular} \\ \text{triangulation of } P}} \mathbb{M}_\Delta. \tag{III.2}$$

The *moduli space of tropical plane curves of genus g* is the following stacky fan inside $\mathbb{M}_g$:

$$\mathbb{M}_g^{\text{planar}} \quad := \bigcup_P \mathbb{M}_P. \tag{III.3}$$

Here P runs over isomorphism classes of lattice polygons with g interior lattice points. The number of such classes is finite by Proposition 1.3.

This paper presents a computational study of the moduli spaces $\mathbb{M}_g^{\text{planar}}$. We construct the decompositions in (III.2) and (III.3) explicitly. Our first result reveals the dimensions:

THEOREM 0.1. *For all $g \geq 2$ there exists a lattice polygon P with g interior lattice points such that $\mathbb{M}_P$ has the dimension expected from classical algebraic geometry, namely,*

$$\dim(\mathbb{M}_g^{\text{planar}}) \quad = \quad \dim(\mathbb{M}_P) \quad = \quad \begin{cases} 3 & if \quad g = 2, \\ 6 & if \quad g = 3, \\ 16 & if \quad g = 7, \\ 2g + 1 & otherwise. \end{cases} \tag{III.4}$$

In each case, the cone $\mathbb{M}_\Delta$ of honeycomb curves supported on P attains this dimension.

Honeycomb curves are introduced in section 3. That section furnishes the proof of Theorem 0.1. The connection between tropical and classical curves will be explained in section 2. The number $2g + 1$ in (III.4) is the dimension of the classical moduli space of *trigonal curves of genus g*, whose tropicalization is related to our stacky fan $\mathbb{M}_g^{\text{planar}}$. Our primary source for the relevant material from algebraic geometry is the article [16] by Castryck and Voight. Our paper can be seen as a refined combinatorial extension of theirs. For related recent work that incorporates also immersions of tropical curves see Cartwright et al. [15].

We begin in section 1 with an introduction to the relevant background from geometric combinatorics. The objects in (III.1)–(III.3) are carefully defined, and we explain our algorithms for computing these explicitly, using the software packages TOPCOM [94] and polymake [4, 49].

Our main results in this chapter are Theorems 4.1, 5.3, 6.1, and 7.5. These concern $g = 3, 4, 5$ and they are presented in sections 4 through 7. The proofs of these theorems rely on the computer calculations that are described in section 1. In section 4 we study plane quartics as in Figure 13. Their Newton polygon is the size four triangle T_4. This models non-hyperelliptic genus 3 curves in their canonical embedding. We compute the space $\mathbb{M}_{T_4}$. Four of the five trivalent graphs of genus 3 are realized by smooth tropical plane curves.

Section 5 is devoted to hyperelliptic curves. We show that all metric graphs arising from hyperelliptic polygons of given genus arise from a single polygon, namely, the hyperelliptic triangle. We determine the space $\mathbb{M}_{3,\text{hyp}}^{\text{planar}}$, which together with $\mathbb{M}_{T_4}$ gives $\mathbb{M}_3^{\text{planar}}$. Section 6 deals with curves of genus $g = 4$. Here (III.3) is a union over four polygons, and precisely 13 of the 17 trivalent graphs G are realized in (III.2). The dimensions of the cones $\mathbb{M}_{P,G}$ range between 4 and 9. In Section 7 we study curves of genus $g = 5$. Here 38 of the 71 trivalent graphs are realizable. Some others are ruled out by the sprawling condition in Proposition 7.3. We end with a brief discussion of $g \geq 6$.

1. Combinatorics and Computations

The methodology of this chapter is computations in geometric combinatorics. In this section we fix notation, supply definitions, present algorithms, and give some core results. For additional background, the reader is referred to the book by De Loera, Rambau, and Santos [**31**].

Let P be a lattice polygon, and let $A = P \cap \mathbb{Z}^2$ be the set of lattice points in P. Any function $h : A \to \mathbb{R}$ is identified with a tropical polynomial with Newton polygon P, namely,

$$H(x,y) \;\; = \;\; \bigoplus_{(i,j) \in A} h(i,j) \odot x^i \odot y^j.$$

The tropical curve C defined by this min-plus polynomial consists of all points $(x,y) \in \mathbb{R}^2$ for which the minimum among the quantities $i \cdot x + j \cdot y + h(i,j)$ is attained at least twice as (i,j) runs over A. The curve C is dual to the *regular subdivision* Δ of A defined by h. To construct Δ, we lift each lattice point $a \in A$ to the height $h(a)$, then take the lower convex hull of the lifted points in $\mathbb{R}^3$. Finally, we project back to $\mathbb{R}^2$ by omitting the height. The *maximal cells* are the images of the facets of the lower convex hull under the projection. The set of all height functions h which induce the same subdivision Δ is a relatively open polyhedral cone in $\mathbb{R}^A$. This is called the *secondary cone* and is denoted $\Sigma(\Delta)$. The collection of all secondary cones $\Sigma(\Delta)$ is a complete polyhedral fan in $\mathbb{R}^A$, the *secondary fan* of A.

A subdivision Δ is a *triangulation* if all maximal cells are triangles. The maximal cones in the secondary fan $\Sigma(\Delta)$ correspond to the regular triangulations Δ of A. Such a cone is the product of a pointed cone of dimension $\#A - 3$ and a 3-dimensional subspace of $\mathbb{R}^A$.

We are interested in regular triangulations Δ of P that are *unimodular*. This means that each triangle in Δ has area $1/2$, or, equivalently, that every point in $A = P \cap \mathbb{Z}^2$ is a vertex of Δ. We derive an inequality representation for the secondary cone $\Sigma(\Delta)$ as follows. Consider any four points $a = (a_1, a_2)$, $b = (b_1, b_2)$, $c = (c_1, c_2)$ and $d = (d_1, d_2)$ in A such that the triples (c, b, a) and (b, c, d) are clockwise oriented triangles of Δ. Then we require

$$\det \begin{pmatrix} 1 & 1 & 1 & 1 \\ a_1 & b_1 & c_1 & d_1 \\ a_2 & b_2 & c_2 & d_2 \\ h(a) & h(b) & h(c) & h(d) \end{pmatrix} \;\geq\; 0. \tag{III.5}$$

This is a linear inequality for $h \in \mathbb{R}^A$. It can be viewed as a "flip condition", determining which of the two diagonals of a quadrilateral are in the subdivision. We have one such inequality for each interior edge bc of Δ. The set of solutions to these linear inequalities is the secondary cone $\Sigma(\Delta)$. From this it follows that the linearity space $\Sigma(\Delta) \cap -\Sigma(\Delta)$ of the secondary cone is 3-dimensional. It is the space $\mathrm{Lin}(A)$ of functions $h \in \mathbb{R}^A$ that are restrictions of affine-linear functions on $\mathbb{R}^2$. We usually identify $\Sigma(A)$ with its image in $\mathbb{R}^A/\mathrm{Lin}(A)$, which is a pointed cone of dimension $\#A - 3$. That pointed cone has finitely many rays and we represent these by vectors in $\mathbb{R}^A$.

Suppose that Δ has E interior edges and g interior vertices. We consider two linear maps

$$\mathbb{R}^A \;\xrightarrow{\;\lambda\;}\; \mathbb{R}^E \;\xrightarrow{\;\kappa\;}\; \mathbb{R}^{3g-3}. \tag{III.6}$$

The map λ takes h and outputs the vector whose bc-coordinate equals (III.5). This determinant is nonnegative: it is precisely the length of the edge of the tropical curve C that is dual to bc. Hence $\kappa(\lambda(h))$ is the vector whose $3g - 3$ coordinates are the lengths of the bounded edges of C.

REMARK 1.1. The (lattice) length of an edge of C with slope p/q, where p, q are relatively prime integers, is the Euclidean length of the edge divided by $\sqrt{p^2 + q^2}$. This lets one quickly read off the lengths from a picture of C without having to compute the determinant (III.5).

Each edge e of the skeleton G is a concatenation of edges of C. The second map κ adds up the corresponding lengths. Thus the composition (III.6) is the linear map with e^{th} coordinate

$$(\kappa \circ \lambda)(h)_e \;\; = \sum_{\substack{bc \,:\, \text{the dual of } bc \\ \text{contributes to } e}} \lambda(h)_{bc} \qquad \text{for all edges } e \text{ of } G.$$

By definition, the secondary cone is mapped into the nonnegative orthant under λ. Hence

$$\Sigma(\Delta) \;\; \xrightarrow{\;\lambda\;} \;\; \mathbb{R}^E_{\geq 0} \;\; \xrightarrow{\;\kappa\;} \;\; \mathbb{R}^{3g-3}_{\geq 0}. \tag{III.7}$$

Our discussion implies the following result on the cone of metric graphs arising from Δ:

PROPOSITION 1.2. *The cone $\mathbb{M}_\Delta$ is the image of the secondary cone $\Sigma(\Delta)$ under $\kappa \circ \lambda$.*

Given any lattice polygon P, we seek to compute the moduli space $\mathbb{M}_P$ via the decompositions in (III.2). Our line of attack towards that goal can now be summarized as follows:
  (1) compute all regular unimodular triangulations of $A = P \cap \mathbb{Z}^2$ up to symmetry;
  (2) sort the triangulations into buckets, one for each trivalent graph G of genus g;
  (3) for each triangulation Δ with skeleton G, compute its secondary cone $\Sigma(\Delta) \subset \mathbb{R}^A$;
  (4) for each secondary cone $\Sigma(\Delta)$, compute its image $\mathbb{M}_\Delta$ in the moduli space $\mathbb{M}_g$ via (III.7);
  (5) merge the results to get the fans $\mathbb{M}_{P,G} \subset \mathbb{R}^{3g-3}$ in (III.1) and the moduli space $\mathbb{M}_P$ in (III.2).

Step 1 is based on computing the secondary fan of A. There are two different approaches to doing this. The first, more direct, method is implemented in `Gfan` [**63**]. It starts out with one regular triangulation of Δ, e.g. a placing triangulation arising from a fixed ordering of A. This comes with an inequality description for $\Sigma(\Delta)$, as in (III.5). From this, `Gfan` computes the rays and the facets of $\Sigma(\Delta)$. Then `Gfan` proceeds to an adjacent secondary cone $\Sigma(\Delta')$ by producing a new height function from traversing a facet of $\Sigma(\Delta)$. Iterating this process results in a breadth-first-search through the edge graph of the *secondary polytope* of A.

The second method starts out the same. But it passes from Δ to a neighboring triangulation Δ' that need not be regular. It simply performs a purely combinatorial restructuring known as a *bistellar flip*. The resulting breadth-first search is implemented in `TOPCOM` [**94**].

Neither algorithm is generally superior to the other, and sometimes it is difficult to predict which one will perform better. The flip-algorithm may suffer from wasting time by also computing non-regular triangulations, while the polyhedral algorithm is genuinely costly since it employs exact rational arithmetic. The flip-algorithm also uses exact coordinates, but only in a preprocessing step which encodes the point configuration as an oriented matroid. Both algorithms can be modified to enumerate all regular *unimodular* triangulations up to symmetry only. For our particular planar instances, we found `TOPCOM` to be more powerful.

We start Step 2 by computing the dual graph of a given Δ. The nodes are the triangles and the edges record incidence. Hence each node has degree 1, 2 or 3. We then recursively delete the nodes of degree 1. Next, we recursively contract edges which are incident with a node of degree 2. The resulting trivalent graph G is the skeleton of Δ. It often has loops and multiple edges. In this process we keep track of the history of all deletions and contractions.

Steps 3 and 4 are carried out using `polymake` [**49**]. Here the buckets or even the individual triangulations can be treated in parallel. The secondary cone $\Sigma(\Delta)$ is defined in $\mathbb{R}^A$ by the linear inequalities $\lambda(h) \geq 0$ in (III.5). From this we compute the facets and rays of $\Sigma(\Delta)$. This is essentially a convex hull computation. In order to get unique rays modulo $\text{Lin}(A)$, we fix $h = 0$ on the three vertices of one particular triangle. Since the cones are rather small the choice of the convex hull algorithm does not matter much. For details on state-of-the-art convex hull computations and an up-to-date description of the `polymake` system see [**4**].

For Step 4, we apply the linear map $\kappa \circ \lambda$ to all rays of the secondary cone $\Sigma(\Delta)$. Their images are vectors in $\mathbb{R}^{3g-3}$ that span the moduli cone $\mathbb{M}_\Delta = (\kappa \circ \lambda)(\Sigma(\Delta))$. Via a convex hull computation as above, we compute all the rays and facets of $\mathbb{M}_\Delta$.

The cones $\mathbb{M}_\Delta$ are generally not full-dimensional in $\mathbb{R}^{3g-3}$. The points in the relative interior are images of interior points of $\Sigma(\Delta)$. Only these represent smooth tropical curves. However, it can happen that another cone $\mathbb{M}_{\Delta'}$ is a face of $\mathbb{M}_\Delta$. In that case, the metric graphs in the relative interior of that face are also realizable by smooth tropical curves.

Step 5 has not been fully automatized yet, but we carry it out in a case-by-case manner. This will be described in detail for curves of genus $g = 3$ in sections 4 and 5.

We now come to the question of what lattice polygons P should be the input for Step 1. Our point of departure towards answering that question is the following finiteness result.

PROPOSITION 1.3. *For every fixed genus $g \geq 1$, there are only finitely many lattice polygons P with g interior lattice points, up to integer affine isomorphisms in $\mathbb{Z}^2$.*

PROOF AND DISCUSSION. Scott [100] proved that $\#(\partial P \cap \mathbb{Z}^2) \leq 2g + 7$, and this bound is sharp. This means that the number of interior lattice points yields a bound on the total number of lattice points in P. This result was generalized to arbitrary dimensions by Hensley [53]. Lagarias and Ziegler [62] improved Hensley's bound and further observed that there are only finitely many lattice polytopes with a given total number of lattice points, up to unimodular equivalence [62, Theorem 2]. Castryck [17] gave an algorithm for finding all lattice polygons of a given genus, along with the number of lattice polygons for each genus up to 30. We remark that the assumption $g \geq 1$ is essential, as there are lattice triangles of arbitrarily large area and without any interior lattice point. $\square$

Proposition 1.3 ensures that the union in (III.3) is finite. However, from the full list of polygons P with g interior lattice points, only very few will be needed to construct $\mathbb{M}_g^{\text{planar}}$. To show this, and to illustrate the concepts seen so far, we now discuss our spaces for $g \leq 2$.

EXAMPLE 1.4. For $g = 1$, only one polygon P is needed in (III.3), and only one triangulation Δ is needed in (III.2). We take $P = \text{conv}\{(0,0), (0,3), (3,0)\}$, since every smooth genus 1 curve is a plane cubic, and we let Δ be the honeycomb triangulation from section 3. The skeleton G is a cycle whose length is the tropical j-invariant [7, §7.1]. We can summarize this as follows:

$$\mathbb{M}_\Delta \ = \ \mathbb{M}_{P,G} \ = \ \mathbb{M}_P \ = \ \mathbb{M}_1^{\text{planar}} \ = \ \mathbb{M}_1 \ = \ \mathbb{R}_{\geq 0}. \tag{III.8}$$

All inclusions in (III.12) are equalities for this particular choice of (P, Δ).
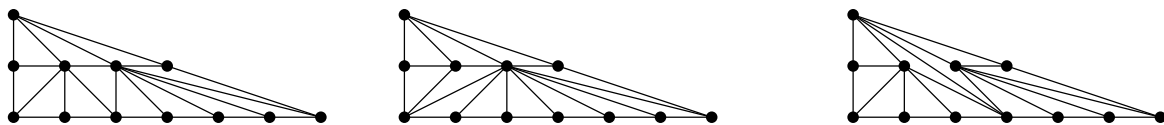
FIGURE 14. The triangulations Δ_1, Δ_1', and Δ_2

EXAMPLE 1.5. In classical algebraic geometry, all smooth curves of genus $g = 2$ are hyperelliptic, and they can be realized with the Newton polygon $P = \text{conv}\{(0,0), (0,2), (6,0)\}$. There are two trivalent graphs of genus 2, namely, the *theta graph* $G_1 = \ominus$ and the *dumbbell graph* $G_2 = \circ\!\!-\!\!\circ$. The moduli space $\mathbb{M}_2$ consists of two quotients of the orthant $\mathbb{R}_{\geq 0}^3$, one for each graph, glued together. For nice drawings see Figures 3 and 4 in [23]. Figure 14 shows three unimodular triangulations Δ_1, Δ_1', and Δ_2 of P such that almost all metric graphs in $\mathbb{M}_2$ are realized by a smooth tropical curve C dual to Δ_1, Δ_1', or Δ_2. We say "almost all" because here the three edges of G_1 cannot have all the same length [15, Proposition 4.7]. The triangulations Δ_1 and Δ_1' both give G_1 as a skeleton. If $a \geq b \geq c$ denote the edge lengths on G_1, then the curves dual to Δ_1 realize all metrics with $a \geq b > c$, and the curves dual to Δ_1' realize all metrics with $a > b = c$. The triangulation Δ_2 gives G_2 as a skeleton, and

the curves dual to it achieve all possible metrics. Since our 3-dimensional cones are closed by definition,

$$\left(\mathbb{M}_{\Delta_1} \cup \mathbb{M}_{\Delta_1'}\right) \cup \mathbb{M}_{\Delta_2} \;=\; \mathbb{M}_{P,G_1} \cup \mathbb{M}_{P,G_2}$$
$$=\; \mathbb{M}_P \;=\; \mathbb{M}_2^{\text{planar}} \;=\; \mathbb{M}_2 \;=\; [\mathbf{23}, \text{Figure 3}]. \tag{III.9}$$

In section 5 we extend this analysis to hyperelliptic curves of $g \geq 3$. The graphs G_1 and G_2 represent the *chains* for $g = 2$. For more information on hyperelliptic metric graphs see [**24**].

With $g = 1, 2$ out of the way, we now assume $g \geq 3$. We follow the approach of Castryck and Voight [**16**] in constructing polygons P that suffice for the union (III.3). We write P_{int} for the convex hull of the g interior lattice points of P. This is the *interior hull* of P. The relationship between the polygons P and P_{int} is studied in polyhedral adjunction theory [**34**].

LEMMA 1.6. *Let $P \subseteq Q$ be lattice polygons with $P_{\text{int}} = Q_{\text{int}}$. Then $\mathbb{M}_P$ is contained in $\mathbb{M}_Q$.*

PROOF. Every regular unimodular triangulation Δ of P can be extended to a regular unimodular triangulation Δ' of Q. (This is a special property of planar triangulations: it does not hold in higher dimensions.) This means that every tropical curve C dual to Δ is contained in a curve C' dual to Δ', except for unbounded edges of C. The skeleton and its possible metrics remain unchanged, since $P_{\text{int}} = Q_{\text{int}}$. We conclude that $\mathbb{M}_\Delta = \mathbb{M}_{\Delta'}$. The unions for P and Q in (III.2) show that $\mathbb{M}_P \subseteq \mathbb{M}_Q$. $\qquad\square$

This lemma shows that we only need to consider *maximal polygons*, i.e. those P that are maximal with respect to inclusion for fixed P_{int}. If P_{int} is 2-dimensional then this determines P uniquely. Namely, suppose that $P_{\text{int}} = \{(x,y) \in \mathbb{R}^2 \;:\; a_i x + b_i y \leq c_i \text{ for } i = 1, 2, \ldots, s\}$, where $\gcd(a_i, b_i, c_i) = 1$ for all i. Then P is the polygon $\{(x,y) \in \mathbb{R}^2 \;:\; a_i x + b_i y \leq c_i + 1 \text{ for } i = 1, 2, \ldots, s\}$. If P is a lattice polygon then it is a maximal lattice polygon. However, it can happen that P has non-integral vertices. In that case, the given P_{int} is not the interior of any lattice polygon.

The maximal polygon P is not uniquely determined by P_{int} when P_{int} is a line segment. For each $g \geq 2$ there are $g+2$ distinct *hyperelliptic trapezoids* to be considered. We shall see in Theorem 5.1 that for our purposes it suffices to use the triangle $\text{conv}\{(0,0), (0,2), (2g+2,0)\}$.

Here is the list of all maximal polygons we use as input for the pipeline described above.

PROPOSITION 1.7. *Up to isomorphism there are precisely* 12 *maximal polygons P such that P_{int} is 2-dimensional and $3 \leq g = \#(P_{\text{int}} \cap \mathbb{Z}^2) \leq 6$. For $g = 3$, there is a unique type, namely, $T_4 = \text{conv}\{(0,0), (0,4), (4,0)\}$. For $g = 4$ there are three types:*

$$Q_1^{(4)} = R_{3,3} \;=\; \text{conv}\{(0,0), (0,3), (3,0), (3,3)\}, \qquad Q_2^{(4)} \;=\; \text{conv}\{(0,0), (0,3), (6,0)\},$$
$$Q_3^{(4)} \;=\; \text{conv}\{(0,2), (2,4), (4,0)\}.$$

For $g = 5$ there are four types of maximal polygons:

$$Q_1^{(5)} \;=\; \text{conv}\{(0,0), (0,4), (4,2)\}, \qquad Q_2^{(5)} \;=\; \text{conv}\{(2,0), (5,0), (0,5), (0,2)\},$$
$$Q_3^{(5)} \;=\; \text{conv}\{(2,0), (4,2), (2,4), (0,2)\}, \qquad Q_4^{(5)} \;=\; \text{conv}\{(0,0), (0,2), (2,0), (4,4)\}.$$

For $g = 6$ there are four types of maximal polygons:

$$Q_1^{(6)} = T_5 \;=\; \text{conv}\{(0,0), (0,5), (5,0)\}, \qquad Q_2^{(6)} \;=\; \text{conv}\{(0,0), (0,7), (3,0), (3,1)\},$$
$$Q_3^{(6)} = R_{3,4} \;=\; \text{conv}\{(0,0), (0,4), (3,0), (3,4)\}, \qquad Q_4^{(6)} \;=\; \text{conv}\{(0,0), (0,4), (2,0), (4,2)\}.$$

The notation we use for polygons is as follows. We write $Q_i^{(g)}$ for maximal polygons of genus g, but we also use a systematic notation for families of polygons, including the *triangles* $T_d = \text{conv}\{(0,0), (0,d), (d,0)\}$ and the *rectangles* $R_{d,e} = \text{conv}\{(0,0), (d,0), (0,e), (d,e)\}$.

Proposition 1.7 is found by exhaustive search, using Castryck's method in [**17**]. We started by classifying all types of lattice polygons with precisely g lattice points. These are

our candidates for P_{int}. For instance, for $g = 5$, there are six such polygons. Four of them are the interior hulls of the polygons $Q_i^{(5)}$ with $i = 1, 2, 3, 4$. The other two are the triangles

$$\text{conv}\{(1,1),(1,4),(2,1)\} \qquad \text{and} \qquad \text{conv}\{(1,1),(2,4),(3,2)\}.$$

However, neither of these two triangles arises as P_{int} for any lattice polygon P.

For each genus g, we construct the stacky fans $\mathbb{M}_g^{\text{planar}}$ by computing each of the spaces $\mathbb{M}_{Q_i^{(g)}}$ and then subdividing their union appropriately. This is then augmented in section 5 by the spaces $\mathbb{M}_P$ where P_{int} is not two-dimensional, but is instead a line segment.

2. Algebraic Geometry

In this section we discuss the context from algebraic geometry that lies behind our computations and combinatorial analyses. Let K be an algebraically closed field that is complete with respect to a surjective non-archimedean valuation $\text{val} : K^* \to \mathbb{R}$. Every smooth complete curve $\mathcal{C}$ over K defines a metric graph G. This is the *Berkovich skeleton* of the analytification of $\mathcal{C}$ as in [7]. By our hypotheses, every metric graph G of genus g arises from some curve $\mathcal{C}$ over K. This defines a surjective tropicalization map from (the K-valued points in) the moduli space of smooth curves of genus g to the moduli space of metric graphs of genus g:

$$\text{trop} : \mathcal{M}_g \to \mathbb{M}_g. \tag{III.10}$$

Both spaces have dimension $3g - 3$ for $g \geq 2$. The map (III.10) is referred to as "naive set-theoretic tropicalization" by Abramovich, Caporaso, and Payne [1]. We point to that article and its bibliography for the proper moduli-theoretic settings for our combinatorial objects.

Consider plane curves defined by a Laurent polynomial

$$f = \sum_{(i,j) \in \mathbb{Z}^2} c_{ij} x^i y^j \in K[x^{\pm}, y^{\pm}]$$

with Newton polygon P. For τ a face of P we let $f|_\tau = \sum_{(i,j) \in \tau} c_{ij} x^i y^j$, and say that f is *non-degenerate* if for all faces τ of P, $f|_\tau$ has no singularities in $(K^*)^2$. Non-degenerate polynomials are useful for studying many subjects in algebraic geometry, including singularity theory [74], the theory of sparse resultants [50],and real algebraic curves in maximal condition [83].

Let P be any lattice polygon in $\mathbb{R}^2$ with g interior lattice points. We write $\mathcal{M}_P$ for the Zariski closure (inside the non-compact moduli space $\mathcal{M}_g$) of the set of curves that appear as non-degenerate plane curves over K with Newton polygon P. This space was introduced by Koelman [71]. analogy to (III.3), we consider the union over all relevant polygons:

$$\mathcal{M}_g^{\text{planar}} := \bigcup_P \mathcal{M}_P. \tag{III.11}$$

This moduli space was introduced and studied by Castryck and Voight in [16]. That article was a primary source of inspiration for our study. In particular, [16, Theorem 2.1] determined the dimensions of the spaces $\mathcal{M}_g^{\text{planar}}$ for all g. Whenever we speak about the "dimension expected from classical algebraic geometry", as we do in Theorem 0.1, this refers to the formulas for $\dim(\mathcal{M}_P)$ and $\dim(\mathcal{M}_g^{\text{planar}})$ that were derived by Castryck and Voight.

By the Structure Theorem for Tropical Varieties [80, §3.3], these dimensions are preserved under the tropicalization map (III.10). The images $\text{trop}(\mathcal{M}_P)$ and $\text{trop}(\mathcal{M}_g^{\text{planar}})$ are stacky fans that live inside $\mathbb{M}_g = \text{trop}(\mathcal{M}_g)$ and have the expected dimension. Furthermore, all maximal cones in $\text{trop}(\mathcal{M}_P)$ have the same dimension since $\mathcal{M}_P$ is irreducible (in fact, unirational).

We summarize the objects discussed so far in a diagram of surjections and inclusions:

$$
\begin{array}{ccccc}
\mathcal{M}_P & \subseteq & \mathcal{M}_g^{\mathrm{planar}} & \subseteq & \mathcal{M}_g \\
\downarrow & & \downarrow & & \downarrow \\
\mathrm{trop}(\mathcal{M}_P) & \subseteq & \mathrm{trop}(\mathcal{M}_g^{\mathrm{planar}}) & \subseteq & \mathrm{trop}(\mathcal{M}_g) \\
\cup| & & \cup| & & \| \\
\mathbb{M}_\Delta \subseteq \mathbb{M}_{P,G} \subseteq \mathbb{M}_P & \subseteq & \mathbb{M}_g^{\mathrm{planar}} & \subseteq & \mathbb{M}_g
\end{array}
\qquad \text{(III.12)}
$$

For $g \geq 3$, the inclusions between the second row and the third row are strict, by a wide margin. This is the distinction between tropicalizations of plane curves and tropical plane curves. One main objective of this paper is to understand how the latter sit inside the former.

For example, consider $g = 3$ and $T_4 = \mathrm{conv}\{(0,0),(0,4),(4,0)\}$. Disregarding the hyperelliptic locus, equality holds in the second row:

$$
\mathrm{trop}(\mathcal{M}_{T_4}) \;=\; \mathrm{trop}(\mathcal{M}_3^{\mathrm{planar}}) \;=\; \mathrm{trop}(\mathcal{M}_3) \;=\; \mathbb{M}_3. \qquad \text{(III.13)}
$$

This is the stacky fan in [**23**, Figure 1]. The space $\mathbb{M}_{T_4} = \mathbb{M}_{3,\mathrm{nonhyp}}^{\mathrm{planar}}$ of tropical plane quartics is also six-dimensional, but it is smaller. It fills up less than 30% of the curves in $\mathbb{M}_3$; see Corollary 4.2. Most metric graphs of genus 3 do **not** come from plane quartics.

For $g = 4$, the canonical curve is a complete intersection of a quadric surface with a cubic surface. If the quadric is smooth then we get a curve of bidegree $(3,3)$ in $\mathbb{P}^1 \times \mathbb{P}^1$. This leads to the Newton polygon

$$
R_{3,3} = \mathrm{conv}\{(0,0),(3,0),(0,3),(3,3)\}.
$$

Singular surfaces lead to families of genus 4 curves of codimension 1 and 2 that are supported on two other polygons [**16**, §6]. As we shall see in Theorem 6.1, $\mathbb{M}_P$ has the expected dimension for each of the three polygons P. Furthermore, $\mathbb{M}_4^{\mathrm{planar}}$ is strictly contained in $\mathrm{trop}(\mathcal{M}_4^{\mathrm{planar}})$. Detailed computations that reveal our spaces for $g = 3, 4, 5$ are presented in sections 4, 5, 6, and 7.

We close this section by returning once more to classical algebraic geometry. Let $\mathcal{T}_g$ denote the *trigonal locus* in the moduli space $\mathcal{M}_g$. It is well known that $\mathcal{T}_g$ is an irreducible subvariety of dimension $2g + 1$ when $g \geq 5$. For a proof see [**46**, Proposition 2.3]. A recent theorem of Ma [**77**] states that $\mathcal{T}_g$ is a rational variety for all g.

We note that Ma's work, as well as the classical approaches to trigonal curves, are based on the fact that canonical trigonal curves of genus g are realized by a certain special polygon P. This is either the rectangle in (III.16) or the trapezoid in (III.17). These polygons appear in [**16**, section 12], where they are used to argue that $\mathcal{T}_g$ defines one of the irreducible components of $\mathcal{M}_g^{\mathrm{planar}}$, namely, $\mathcal{M}_P$. The same P appear in the next section, where they serve to prove one inequality on the dimension in Theorem 0.1. The combinatorial moduli space $\mathbb{M}_P$ is full-dimensional in the tropicalization of the trigonal locus. The latter space, denoted $\mathrm{trop}(\mathcal{T}_g)$, is contained in the space of trigonal metric graphs, by Baker's Specialization Lemma [**5**, §2].

In general, $\mathcal{M}_g^{\mathrm{planar}}$ has many irreducible components other than the trigonal locus $\mathcal{T}_g$. As a consequence, there are many skeleta in $\mathbb{M}_g^{\mathrm{planar}}$ that are not trigonal in the sense of metric graph theory. This is seen clearly in the top dimension for $g = 7$, where $\dim(\mathcal{T}_7) = 15$ but $\dim(\mathcal{M}_7^{\mathrm{planar}}) = 16$. The number 16 comes from the family of trinodal sextics in [**16**, §12].

3. Honeycombs

We now prove Theorem 0.1. This will be done using the special family of *honeycomb curves*. The material in this section is purely combinatorial. No algebraic geometry will be required.

We begin by defining the polygons that admit a honeycomb triangulation. These polygons depend on four integer parameters a, b, c and d that satisfy the constraints

$$0 \leq c \leq a, b \leq d \leq a + b. \tag{III.14}$$

To such a quadruple (a, b, c, d), we associate the polygon

$$H_{a,b,c,d} \quad = \quad \{(x, y) \in \mathbb{R}^2 : 0 \leq x \leq a \text{ and } 0 \leq y \leq b \text{ and } c \leq x + y \leq d\}.$$

If all six inequalities in (III.14) are non-redundant then $H_{a,b,c,d}$ is a hexagon. Otherwise it can be a pentagon, quadrangle, triangle, segment, or just a point. The number of lattice points is

$$\#(H_{a,b,c,d} \cap \mathbb{Z}^2) \quad = \quad ad + bd - \frac{1}{2}(a^2 + b^2 + c^2 + d^2) + \frac{1}{2}(a + b - c + d) + 1,$$

and, by Pick's Theorem, the number of interior lattice points is

$$g \;=\; \#((H_{a,b,c,d})_{\text{int}} \cap \mathbb{Z}^2) \;=\; ad + bd - \frac{1}{2}(a^2 + b^2 + c^2 + d^2) - \frac{1}{2}(a + b - c + d) + 1.$$

The *honeycomb triangulation* Δ subdivides $H_{a,b,c,d}$ into $2ad + 2bd - (a^2 + b^2 + c^2 + d^2)$ unit triangles. It is obtained by slicing $H_{a,b,c,d}$ with the vertical lines $\{x = i\}$ for $0 < i < a$, the horizontal lines $\{y = j\}$ for $0 < j < b$, and the diagonal lines $\{x + y = k\}$ for $c < k < d$. The tropical curves dual to Δ look like honeycombs, as in Figure 15. The corresponding skeleta G are called *honeycomb graphs*.
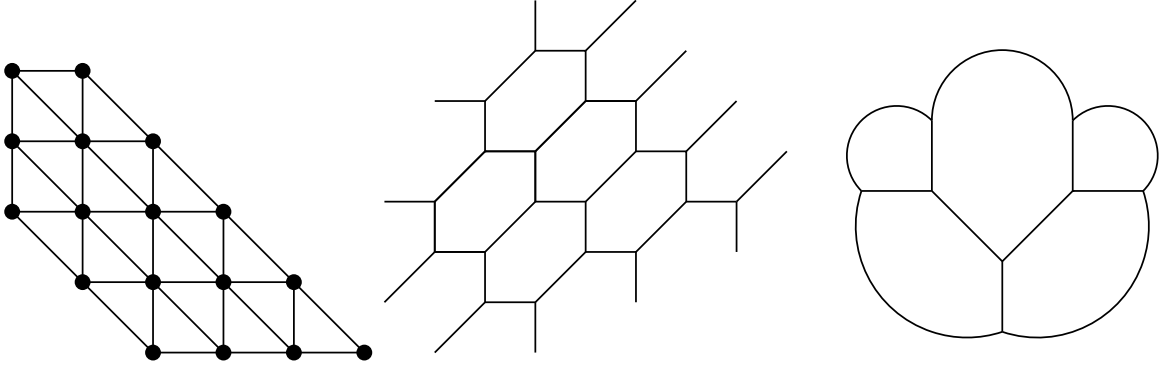
FIGURE 15. The honeycomb triangulation of $H_{5,4,2,5}$, the tropical curve, and its skeleton

If $P = H_{a,b,c,d}$ then its interior P_{int} is a honeycomb polygon as well. Indeed, a translate of P_{int} can be obtained from P by decreasing the values of a, b, c, d by an appropriate amount. For instance, if $P = H_{5,4,2,5}$ is the polygon in Figure 15 then its interior is $P_{\text{int}} = H_{3,3,1,2} + (1, 1)$.

LEMMA 3.1. *Let Δ be the honeycomb triangulation of $P = H_{a,b,c,d}$. Then*

$$\dim(\mathbb{M}_\Delta) \;=\; \#(P_{\text{int}} \cap \mathbb{Z}^2) \;+\; \#(\partial P_{\text{int}} \cap \mathbb{Z}^2) \;+\; \#\text{vertices}(P_{\text{int}}) \;-\; 3.$$

PROOF. The honeycomb graph G consists of $g = \#(P_{\text{int}} \cap \mathbb{Z}^2)$ hexagons. The hexagons associated with lattice points on the boundary of P_{int} have vertices that are 2-valent in G. Such 2-valent vertices get removed, so these boundary hexagons become cycles with fewer than six edges. In the orthant $\mathbb{R}_{\geq 0}^{3g-3}$ of all metrics on G, we consider the subcone of metrics that arise from P. In addition to the nonnegativity constraints, this convex cone is defined by

(a) one linear inequality for each vertex of P_{int};
(b) one linear equation for each lattice point in the relative interior of an edge of P_{int};
(c) two linear equations for each lattice point in the interior of P_{int}.

These inequalities and equations can be seen as follows. Let $\ell_1, \ell_2, \ell_3, \ell_4, \ell_5, \ell_6$ denote the lengths of the edges (labeled cyclically) of a hexagon in a honeycomb curve. Then

$$\ell_1 + \ell_2 = \ell_4 + \ell_5, \quad \ell_2 + \ell_3 = \ell_5 + \ell_6, \quad \text{and} \quad \ell_3 + \ell_4 = \ell_6 + \ell_1.$$

These three equations are linearly dependent, and they give rise to the inequalities in (a) and to the equations in (b) and (c). The linear equations (b) and (c), when taken over all hexagons, have a triangular structure. These linear equations are thus linearly independent. This implies that the codimension of the cone $\mathbb{M}_\Delta$ inside the orthant $\mathbb{R}_{\geq 0}^{3g-3}$ equals

$$\begin{aligned}
\operatorname{codim}(\mathbb{M}_\Delta) \;=\; & \big(\#(\partial P_{\text{int}} \cap \mathbb{Z}^2) - \#\operatorname{vertices}(P_{\text{int}})\big) \\
& + 2 \cdot \#(\operatorname{int}(P_{\text{int}}) \cap \mathbb{Z}^2).
\end{aligned} \tag{III.15}$$

This expression can be rewritten as

$$g \;+\; \#(\operatorname{int}(P_{\text{int}}) \cap \mathbb{Z}^2) \;-\; \#\operatorname{vertices}(P_{\text{int}}) = 2g \;-\; \#(\partial P_{\text{int}} \cap \mathbb{Z}^2) \;-\; \#\operatorname{vertices}(P_{\text{int}}).$$

Subtracting this codimension from $3g - 3$, we obtain the desired formula. $\qquad\square$

PROOF OF THEOREM 0.1. For the classical moduli space $\mathcal{M}_g^{\text{planar}}$, formula (III.4) was proved in [16]. That dimension is preserved under tropicalization. The inclusion $\mathbb{M}_g^{\text{planar}} \subseteq \operatorname{trop}(\mathcal{M}_g^{\text{planar}})$ in (III.12) shows that the right-hand side in (III.4) is an upper bound on $\dim(\mathbb{M}_g^{\text{planar}})$.

To prove the lower bound, we choose P to be a specific honeycomb polygon with honeycomb triangulation Δ. Our choice depends on the parity of the genus g. If $g = 2h$ is even then we take the rectangle

$$R_{3,h+1} \;=\; H_{3,h+1,0,h+4} \;=\; \operatorname{conv}\{(0,0), (0, h+1), (3,0), (3, h+1)\}. \tag{III.16}$$

The interior hull of $R_{3,h+1}$ is the rectangle

$$(R_{3,h+1})_{\text{int}} \;=\; \operatorname{conv}\{(1,1), (1,h), (2,1), (2,h)\} \;\cong\; R_{1,h-1}.$$

All $g = 2h$ lattice points of this polygon lie on the boundary. From Lemma 3.1, we see that $\dim(\mathbb{M}_\Delta) = g + g + 4 - 3 = 2g + 1$. If $g = 2h + 1$ is odd then we take the trapezoid

$$H_{3,h+3,0,h+3} \;=\; \operatorname{conv}\{(0,0), (0, h+3), (3,0), (3, h)\}. \tag{III.17}$$

The convex hull of the interior lattice points in $H_{3,h+3,0,h+3}$ is the trapezoid

$$(H_{3,h+3,0,h+3})_{\text{int}} \;=\; \operatorname{conv}\{(1,1), (1, h+1), (2,1), (2,h)\}.$$

All $g = 2h+1$ lattice points of this polygon lie on its boundary, and again $\dim(\mathbb{M}_\Delta) = 2g+1$.

For all $g \geq 4$ with $g \neq 7$, this matches the upper bound obtained from [16]. We conclude that $\dim(\mathbb{M}_P) = \dim(\mathbb{M}_g) = 2g + 1$ holds in all of these cases. For $g = 7$ we take $P = H_{4,4,2,6}$. Then P_{int} is a hexagon with $g = 7$ lattice points. From Lemma 3.1, we find $\dim(M_\Delta) = 7 + 6 + 6 - 3 = 16$, so this matches the upper bound. Finally, for $g = 3$, we will see $\dim(M_{T_4}) = 6$ in section 4. The case $g = 2$ follows from the discussion in Example 1.5. $\qquad\square$

There are two special families of honeycomb curves: those arising from the triangles T_d for $d \geq 4$ and rectangles $R_{d,e}$ for $d, e \geq 3$. The triangle T_d corresponds to curves of degree d in the projective plane $\mathbb{P}^2$. Their genus is $g = (d-1)(d-2)/2$. The case $d = 4, g = 3$ will be our topic in section 4. The rectangle $R_{d,e}$ corresponds to curves of bidegree (d, e) in $\mathbb{P}^1 \times \mathbb{P}^1$. Their genus is $g = (d-1)(e-1)$. The case $d = e = 3, g = 4$ appears in section 6.

PROPOSITION 3.2. *Let P be the triangle T_d with $d \geq 4$ or the rectangle $R_{d,e}$ with $d, e \geq 3$. The moduli space $\mathbb{M}_P$ of tropical plane curves has the expected dimension inside $\mathbb{M}_g$, namely,*

$$\dim(\mathbb{M}_{T_d}) = \frac{1}{2}d^2 + \frac{3}{2}d - 8 \quad \text{and} \quad \operatorname{codim}(\mathbb{M}_{T_d}) = (d-2)(d-4), \text{ whereas}$$

$$\dim(\mathbb{M}_{R_{d,e}}) = de + d + e - 6 \quad \text{and} \quad \operatorname{codim}(\mathbb{M}_{R_{d,e}}) = 2(de - 2d - 2e + 3).$$

In particular, the honeycomb triangulation defines a cone $\mathbb{M}_\Delta$ of this maximal dimension.

PROOF. For our standard triangles and rectangles, the formula (III.15) implies

$$\begin{aligned} \text{codim}(\mathbb{M}_{T_d}) &= 3(d-3) - 3 + 2 \cdot \tfrac{1}{2}(d-4)(d-5), \\ \text{codim}(\mathbb{M}_{R_{d,e}}) &= 2((d-2)+(e-2)) - 4 + 2 \cdot (d-3)(e-3). \end{aligned}$$

Subtracting from $3g - 3 = \dim(\mathbb{M}_g)$, we get the desired formulas for $\dim(\mathbb{M}_P)$. $\square$

The above dimensions are those expected from algebraic geometry. Plane curves with Newton polygon T_d form a projective space of dimension $\frac{1}{2}(d+2)(d+1) - 1$ on which the 8-dimensional group $\text{PGL}(3)$ acts effectively, while those with $R_{d,e}$ form a space of dimension $(d+1)(e+1) - 1$ on which the 6-dimensional group $\text{PGL}(2)^2$ acts effectively. In each case, $\dim(\mathcal{M}_P)$ equals the dimension of the family of all curves minus the dimension of the group.

4. Genus Three

In classical algebraic geometry, all non-hyperelliptic smooth curves of genus 3 are plane quartics. Their Newton polygon $T_4 = \text{conv}\{(0,0),(0,4),(4,0)\}$ is the unique maximal polygon with $g = 3$ in Proposition 1.7. In this section, we compute the moduli space $\mathbb{M}_{T_4}$, and we characterize the dense subset of metric graphs that are realized by smooth tropical quartics. In the next section, we study the hyperelliptic locus $\mathbb{M}_{g,\text{hyp}}^{\text{planar}}$ for arbitrary g, and we compute it explicitly for $g = 3$. The full moduli space is then obtained as

$$\mathbb{M}_3^{\text{planar}} = \mathbb{M}_{T_4} \cup \mathbb{M}_{3,\text{hyp}}^{\text{planar}}. \tag{III.18}$$

Just like in classical algebraic geometry, $\dim(\mathbb{M}_{T_4}) = 6$ and $\dim(\mathbb{M}_{3,\text{hyp}}^{\text{planar}}) = 5$.
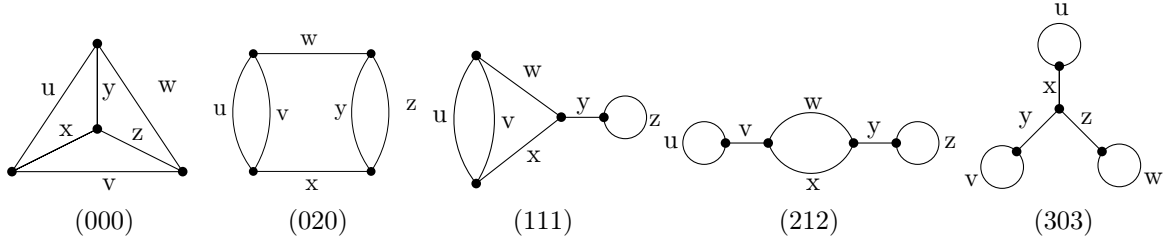
FIGURE 16. The five trivalent graphs of genus 3, with letters labeling each graph's six edges

The stacky fan $\mathbb{M}_3$ of all metric graphs has five maximal cones, as shown in [**23**, Figure 4]. These correspond to the five (leafless) trivalent graphs of genus 3, pictured in Figure 16. Each graph is labeled by the triple (ℓbc), where ℓ is the number of loops, b is the number of bi-edges, and c is the number of cut edges. Here, ℓ, b, and c are single digit numbers, so there is no ambiguity to this notation. Our labeling and ordering is largely consistent with [**8**].

Although $\mathbb{M}_{T_4}$ has dimension 6, it is not pure due to the realizable metrics on (111). It also misses one of the five cones in $\mathbb{M}_3$: the graph (303) cannot be realized in $\mathbb{R}^2$ by Proposition 7.3. The restriction of $\mathbb{M}_{T_4}$ to each of the other cones is given by a finite union of convex polyhedral subcones, characterized by the following piecewise-linear formulas:

THEOREM 4.1. *A graph in $\mathbb{M}_3$ arises from a smooth tropical quartic if and only if it is one of the first four graphs in Figure* 16*, with edge lengths satisfying the following, up to symmetry:*

  ▷ (000) *is realizable if and only if* $\max\{x,y\}\leq u$, $\max\{x,z\}\leq v$ *and* $\max\{y,z\}\leq w$, *where*
    ⋆ *at most two of the inequalities can be equalities, and*
    ⋆ *if two are equalities, then either x,y,z are distinct and the edge (among u,v,w) that connects the shortest two of x,y,z attains equality, or $\max\{x,y,z\}$ is attained exactly twice, and the edge connecting those two longest does not attain equality.*

▷ (020) *is realizable if and only if* $v \le u$, $y \le z$, *and* $w + \max\{v, y\} \le x$, *and if the last inequality is an equality, then:* $v = u$ *implies* $v < y < z$, *and* $y = z$ *implies* $y < v < u$.

▷ (111) *is realizable if and only if* $w < x$ *and*

$$(v + w = x \text{ and } v < u) \text{ or } (v + w < x \le v + 3w \text{ and } v \le u) \text{ or }$$
$$(v + 3w < x \le v + 4w \text{ and } v \le u \le 3v/2) \text{ or } \qquad \text{(III.19)}$$
$$(v + 3w < x \le v + 4w \text{ and } 2v = u) \text{ or } (v + 4w < x \le v + 5w \text{ and } v = u).$$

▷ (212) *is realizable if and only if* $w < x \le 2w$.

To understand the qualifier "up to symmetry" in Theorem 4.1, it is worthwhile to read off the automorphisms from the graphs in Figure 16. The graph (000) is the complete graph on four nodes. Its automorphism group is the symmetric group of order 24. The automorphism group of the graph (020) is generated by the three transpositions $(u\ v)$, $(y\ z)$, $(w\ x)$ and the double transposition $(u\ y)(v\ z)$. Its order is 16. The automorphism group of the graph (111) has order 4, and it is generated by $(u\ v)$ and $(w\ x)$. The automorphism group of the graph (212) is generated by $(u\ z)(v\ y)$ and $(w\ x)$, and has order 4. The automorphism group of the graph (303) is the symmetric group of order 6. Each of the five graphs contributes an orthant $\mathbb{R}^6_{\ge 0}$ modulo the action of that symmetry group to the stacky fan $\mathbb{M}_3$.

TABLE 1. Dimensions of the 1278 moduli cones $\mathbb{M}_\Delta$ within $\mathbb{M}_{T_4}$

$G \setminus \dim$	3	4	5	6	#Δ's
(000)	18	142	269	144	573
(020)		59	216	175	450
(111)		10	120	95	225
(212)			15	15	30
total	18	211	620	429	1278

PROOF OF THEOREM 4.1. This is based on explicit computations as in Section 1. The symmetric group S_3 acts on the triangle T_4. We enumerated all unimodular triangulations of T_4 up to that symmetry. There are 1279 (classes of) such triangulations, and of these precisely 1278 are regular. The unique non-regular triangulation is a refinement of [**80**, Figure 2.3.9]. For each regular triangulation we computed the graph G and the polyhedral cone $\mathbb{M}_\Delta$. Each $\mathbb{M}_\Delta$ is the image of the 12-dimensional secondary cone of Δ. We found that $\mathbb{M}_\Delta$ has dimension 3, 4, 5 or 6, depending on the structure of the triangulation Δ. A census is given by Table 1. For instance, 450 of the 1278 triangulations Δ have the skeleton $G = (020)$. Among these 450, we found that 59 have $\dim(\mathbb{M}_\Delta) = 4$, 216 have $\dim(\mathbb{M}_\Delta) = 5$, and 175 have $\dim(\mathbb{M}_\Delta) = 6$.

For each of the 1278 regular triangulations Δ we checked that the inequalities stated in Theorem 4.1 are valid on the cone $\mathbb{M}_\Delta = (\kappa \circ \lambda)(\Sigma(\Delta))$. This proves that the dense realizable part of $\mathbb{M}_{T_4}$ is contained in the polyhedral space described by our constraints.

For the converse direction, we need to go through the four cases and construct a planar tropical realization of each metric graph that satisfies our constraints. We shall now do this.

All realizable graphs of **type (000)**, except for lower-dimensional families, arise from a single triangulation Δ, shown in Figure 17 with its skeleton. The cone $\mathbb{M}_\Delta$ is six-dimensional. Its interior is defined by $x < \min\{u, v\}$, $y < \min\{u, w\}$, and $z < \min\{v, w\}$. Indeed, the parallel segments in the outer edges can be arbitrarily long, and each outer edge be as close as desired to the maximum of the two adjacent inner edges. This is accomplished by putting as much length as possible into a particular edge and pulling extraneous parts back.

There are several lower dimensional collections of graphs we must show are achievable:

(i) $y < x = u$, $\max\{x, z\} < v$, $\max\{y, z\} < w$; $\qquad\qquad\qquad$ (dim = 5)
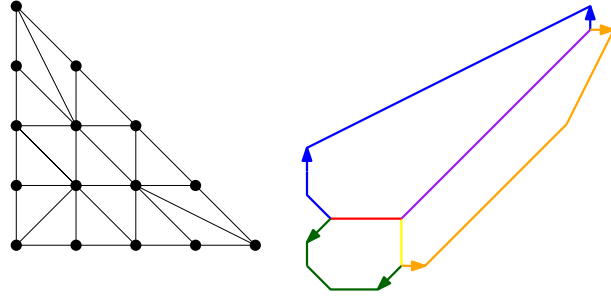
FIGURE 17. A triangulation that realizes almost all realizable graphs of type (000)
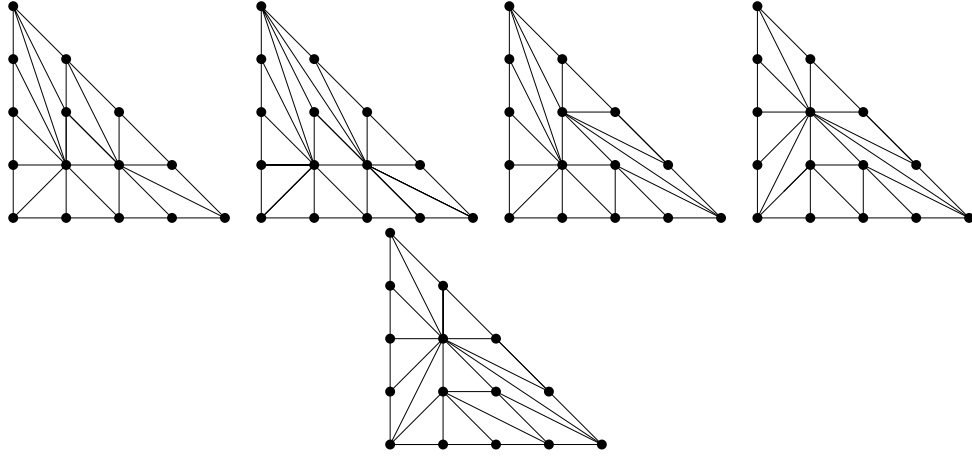
FIGURE 18. Triangulations giving all metrics in the cases (i) through (v) for the graph (000)

(ii) $y = x = u$, $\max\{x, z\} < v$, $\max\{y, z\} < w$;	(dim = 4)
(iii) $z < y < x < v$, $u = x$, $w = y$;	(dim = 4)
(iv) $z < y < x < u$, $v = x$, $w = y$;	(dim = 4)
(v) $z < y = x = v = w < u$.	(dim = 3)

In Figure 18 we show triangulations realizing these five special families. Dual edges are labeled

$$(1,1) \overset{x}{-} (1,2) \overset{y}{-} (2,1) \overset{z}{-} (1,1).$$
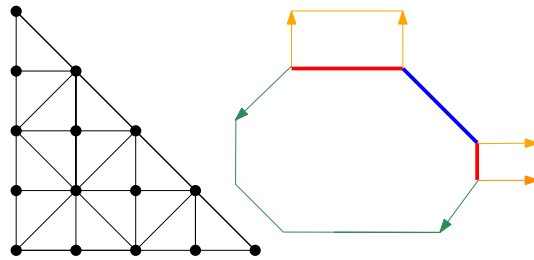
FIGURE 19. A triangulation that realizes almost all realizable graphs of type (020)

Next, we consider **type (020)**. Again, except for some lower-dimensional cases, all graphs arise from single triangulation, pictured in Figure 19. The interior of $\mathbb{M}_\Delta$ is given by $v < u$, $y < z$, and $w + \max\{v, y\} < x$. There are several remaining boundary cases, all of whose graphs are realized by the triangulations in Figure 20:

(i) $v < u$, $y < z$, $w + \max\{v, y\} = x$;	(dim = 5)
(ii) $u = v$, $y < z$, $w + \max\{v, y\} < x$;	(dim = 5)

(iii) $u = v$, $y = z$, $w + \max\{v, y\} < x$;　　　　　　　　　　　　　　　(dim = 4)
(iv) $u = v$, $v < y < z$, $w + \max\{v, y\} = x$.　　　　　　　　　　　　(dim = 4)
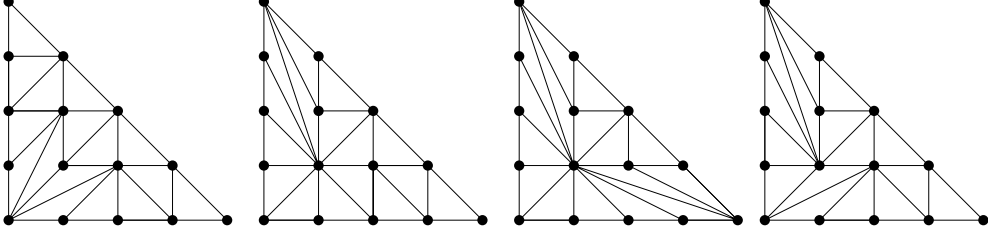
FIGURE 20. Triangulations giving all metrics in the cases (i) through (iv) for the graph (020)

Type (111) is the most complicated. We begin by realizing the metric graphs that lie in $\mathrm{int}(\mathbb{M}_{T_4,(111)})$. These arise from the second and third cases in the disjunction (III.19).

We assume $w < x$. The triangulation to the left in Figure 21 realizes all metrics on (111) satisfying $v + w < x < v + 3w$ and $v < u$. The dilation freedom of u, y, and z is clear. To see that the edge x can have length arbitrarily close to $v + 3w$, simply dilate the double-arrowed segment to be as long as possible, with some very small length given to the next two segments counterclockwise. Shrinking the double-arrowed segment as well as the vertical segment of x brings the length close to $v + w$. The triangulation to the right in Figure 21 realizes all metrics satisfying $v + 3w < x < v + 4w$ and $v < u < 3v/2$. Dilation of x is more free due to the double-arrowed segment of slope $1/2$, while dilation of u is more restricted.
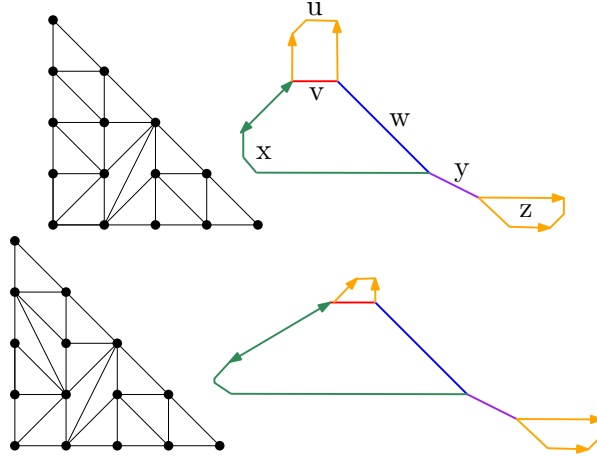
FIGURE 21. Triangulations of type (111) realizing $v + w < x < v + 2x$ and $v < u$ (on the left) and $v + 3w < x < v + 4w$ and $v < u < 3v/2$ (on the right)

Many triangulations are needed in order to deal with low-dimensional case. In Figure 22 we show triangulations that realize each of the following families of type (111) graphs:

(i) $v + w < x < v + 5w$, $v = u$;　　　　　　　　　　　　　　　　　(dim = 5)
(ii) $v + w < x < v + 4w$, $2v = u$;　　　　　　　　　　　　　　　(dim = 5)
(iii) $v + w = x$, $v < u$;　　　　　　　　　　　　　　　　　　　　(dim = 5)
(iv) $x = v + 3w$, $v < u$;　　　　　　　　　　　　　　　　　　　(dim = 5)
(v) $x = v + 4w$, $v < u \leq 3v/2$;　　　　　　　　　　　　　　　(dim = 5)
(vi) $x = v + 5w$, $v = u$;　　　　　　　　　　　　　　　　　　　(dim = 4)
(vii) $x = v + 4w$, $2v = u$.　　　　　　　　　　　　　　　　　　(dim = 4)

All graphs of **type (212)** can be achieved with the two triangulations in Figure 23. The left gives all possibilities with $w < x < 2w$, and the right realizes $x = 2w$. The edges u, v, y, z are completely free to dilate. This completes the proof of Theorem 4.1. □
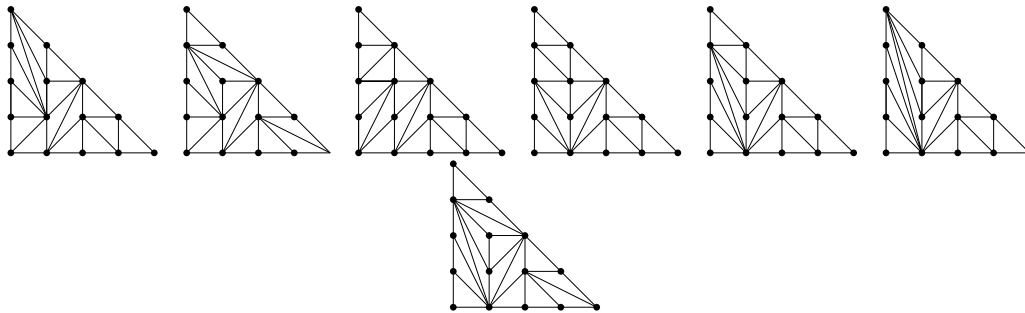
FIGURE 22. Triangulations of type (111) that realize the boundary cases (i) through (vii)
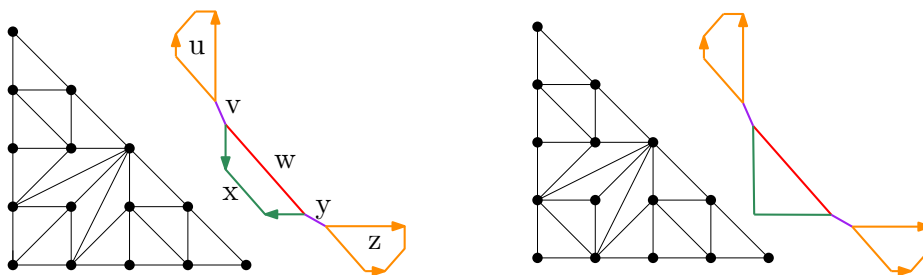
FIGURE 23. Triangulations giving graphs of type (212) giving $w < x < 2w$ and $x = 2w$

The space $\mathbb{M}_{T_4}$ is not pure-dimensional because of the graphs (111) with $u = v$ and $v + 4w < x < v + 5w$. These appear in the five-dimensional $\mathbb{M}_\Delta$ where Δ is the leftmost triangulation in Figure 22, but $\mathbb{M}_\Delta$ is not contained in the boundary of any six-dimensional $\mathbb{M}_{\Delta'}$.

We close this section by suggesting an answer to the following question: *What is the probability that a random metric graph of genus 3 can be realized by a tropical plane quartic?*

To examine this question, we need to endow the moduli space $\mathbb{M}_3$ with a probability measure. Here we fix this measure as follows. We assume that the five trivalent graphs G are equally likely, and all non-trivalent graphs have probability 0. The lengths on each trivalent graph G specify an orthant $\mathbb{R}^6_{\geq 0}$. We fix a probability measure on $\mathbb{R}^6_{\geq 0}$ by normalizing so that $u + v + w + x + y + z = 1$, and we take the uniform distribution on the resulting 5-simplex. With this probability measure on the moduli space $\mathbb{M}_3$ we are asking for the ratio of volumes

$$\mathrm{vol}(\mathbb{M}_3^{\mathrm{planar}}) / \mathrm{vol}(\mathbb{M}_3). \tag{III.20}$$

This ratio is a rational number, which we computed from our data in Theorem 4.1.

COROLLARY 4.2. *The rational number in (*III.20*) is* 31/105. *This means that, in the measure specified above, about* 29.5% *of all metric graphs of genus 3 come from tropical plane quartics.*

PROOF AND EXPLANATION. The graph (303) is not realizable, since none of the 1278 regular unimodular triangulations of the triangle T_4 has this type. So, its probability is zero. For the other four trivalent graphs in Figure 16 we compute the volume of the realizable edge lengths, using the inequalities in Theorem 4.1. The result of our computations is the table

Graph	(000)	(020)	(111)	(212)	(303)
Probability	4/15	8/15	12/35	1/3	0

A non-trivial point in verifying these numbers is that Theorem 4.1 gives the constraints only up to symmetry. We must apply the automorphism group of each graph in order to obtain

the realizable region in its 5-simplex $\{(u, v, w, x, y, z) \in \mathbb{R}_{\geq 0}^6 : u + v + w + x + y + z = 1\}$. Since we are measuring volumes, we are here allowed to replace the regions described in Theorem 4.1 by their closures. For instance, consider type (020). After taking the closure, and after applying the automorphism group of order 16, the realizability condition becomes

$$\max\big(\min(u, v), \min(y, z)\big) \;\leq\; |x - w|. \tag{III.21}$$

The probability that a uniformly sampled random point in the 5-simplex satisfies (III.21) is equal to 8/15. The desired probability (III.20) is the average of the five numbers in the table. $\qquad\square$

Notice that asking for those probabilities only makes sense since the dimension of the moduli space agrees with the number of skeleton edges. In view of (III.4) this occurs for the three genera $g = 2, 3, 4$. For $g \geq 5$ the number of skeleton edges exceeds the dimension of the moduli space. Hence, in this case, the probability that a random metric graph can be realized by a tropical plane curve vanishes a priori. For $g = 2$ that probability is one; see Example 1.5. For $g = 4$ that probability is less than 0.5% by Corollary 6.2 below.

5. Hyperelliptic Curves

A polygon P of genus g is *hyperelliptic* if P_{int} is a line segment of length $g - 1$. We define the moduli space of hyperelliptic tropical plane curves of genus g to be

$$\mathbb{M}_{g,\text{hyp}}^{\text{planar}} \;:=\; \bigcup_P \mathbb{M}_P,$$

where the union is over all hyperelliptic polygons P of genus g. Unlike when the interior hull P_{int} is two-dimensional, there does not exist a unique maximal hyperelliptic polygon P with given P_{int}. However, are only finitely many such polygons up to isomorphism. These are

$$E_k^{(g)} \;:=\; \text{conv}\{(0, 0), (0, 2), (g + k, 0), (g + 2 - k, 2)\} \qquad \text{for } 1 \leq k \leq g + 2.$$

These hyperelliptic polygons interpolate between the rectangle $E_1^{(g)} = R_{g+1,2}$ and the triangle $E_{g+2}^{(g)}$. The five maximal hyperelliptic polygons for genus $g = 3$ are pictured in Figure 24.
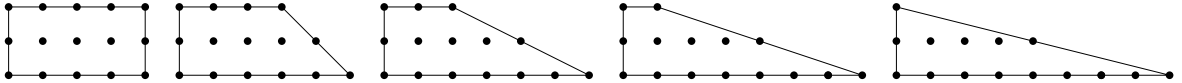
FIGURE 24. The five maximal hyperelliptic polygons of genus 3

This finiteness property makes a computation of $\mathbb{M}_{g,\text{hyp}}^{\text{planar}}$ feasible: compute $\mathbb{M}_{E_k^{(g)}}$ for all k, and take the union. By [**66**, Proposition 3.4], all triangulations of hyperelliptic polygons are regular, so we need not worry about non-regular triangulations arising in the TOPCOM computations described in section 1. We next show that it suffices to consider the triangle:

THEOREM 5.1. *For each genus $g \geq 2$, the hyperelliptic triangle $E_{g+2}^{(g)}$ satisfies*

$$\mathbb{M}_{E_{g+2}^{(g)}} \;=\; \mathbb{M}_{g,\text{hyp}}^{\text{planar}} \;\subseteq\; \mathbb{M}_g^{\text{chain}} \cap \mathbb{M}_g^{\text{planar}}. \tag{III.22}$$

The equality holds even before taking closures of the spaces of realizable graphs. The spaces on the left-hand side and right-hand side of the inclusion in (III.22) both have dimension $2g - 1$.

Before proving our theorem, we define $\mathbb{M}_g^{\text{chain}}$. This space contains all metric graphs that arise from triangulating hyperelliptic polygons. Start with a line segment on $g - 1$ nodes where the $g - 2$ edges have arbitrary non-negative lengths. Double each edge so that the resulting parallel edges have the same length, and attach two loops of arbitrary lengths at the endpoints. Now, each of the $g - 1$ nodes is 4-valent. There are two possible ways to split each node into two nodes connected by an edge of arbitrary length. Any metric graph arising

from this procedure is called a *chain of genus g*. Although there are 2^{g-1} possible choices in this procedure, some give isomorphic graphs. There are $2^{g-2} + 2^{\lfloor (g-2)/2 \rfloor}$ combinatorial types of chains of genus g. In genus 3 the chains are (020), (111), and (212) in Figure 16, and in genus 4 they are (020), (021), (111), (122), (202), and (223) in Figure 33.

By construction, there are $2g - 1$ degrees of freedom for the edge lengths in a chain of genus g, so each such chain defines an orthant $\mathbb{R}_{\geq 0}^{2g-1}$. We write $\mathbb{M}_g^{\text{chain}}$ for the stacky subfan of $\mathbb{M}_g$ consisting of all chains. Note that $\mathbb{M}_g^{\text{chain}}$ is strictly contained in the space $\mathbb{M}_g^{\text{hyp}}$ of all hyperelliptic metric graphs, seen in [**24**]. Hyperelliptic graphs arise by the same construction from any tree with $g - 1$ nodes, whereas for chains that tree must be a line segment.

The main claim in Theorem 5.1 is that any metric graph arising from a maximal hyperelliptic polygon $E_k^{(g)}$ also arises from the hyperelliptic triangle $E_{g+2}^{(g)}$. Given a triangulation Δ of $E_k^{(g)}$, our proof constructs a triangulation Δ' of $E_{g+2}^{(g)}$ that gives rise to the same collection of metric graphs, so that $\mathbb{M}_\Delta = \mathbb{M}_{\Delta'}$, with equality holding even before taking closures. Before our proof, we illustrate this construction with the following example.

EXAMPLE 5.2. Let Δ be the triangulation of $R_{4,2}$ pictured on the left in Figure 25 along with a metric graph Γ arising from it. The possible metrics on Γ are determined by the slopes of the edges emanating from the vertical edges. For instance, consider the constraints on v and y imposed by the width w (which equals x). If most of the w and x edges are made up of the segments emanating from v, we find y close to $v + 2w$. If instead most of the w and x edges are made up of the segments emanating from y, we find y close to $v - 2w$. Interpolating gives graphs achieving $v - 2w < y < v + 2w$. This only depends on the *difference* of the slopes emanating either left or right from the edges v and y: the same constraints would be imposed if the slopes emanating from v to the right were 2 and 0 rather than 1 and -1. Boundary behavior determines constraints on u and z, namely $v < u$ and $y < z$.
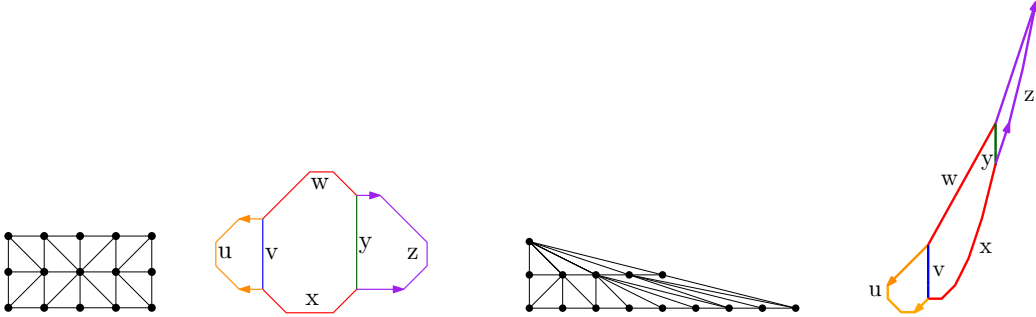
FIGURE 25. Triangulations of $R_{4,2}$ and $E_5^{(3)}$, giving rise to skeletons with the same possible metrics.

Also pictured in Figure 25 is a triangulation Δ' of $E_5^{(3)}$. The skeleton Γ' arising from Δ' has the same combinatorial type as Γ, and the slopes emanating from the vertical edges have the same differences as in Γ. Combined with similar boundary behavior, this shows that Γ and Γ' have the exact same achievable metrics. In other words, $\mathbb{M}_\Delta = \mathbb{M}_{\Delta'}$, with equality even before taking closures of the realizable graphs.

We now explain how to construct Δ' from Δ, an algorithm spelled out explicitly in the proof of Theorem 5.1. We start by adding edges from $(0, 2)$ to the interior lattice points (since any unimodular triangulation of $E_5^{(3)}$ must include these edges), and then add additional edges based on the combinatorial type of Δ, as pictured in Figure 26.

Next we add edges connecting the interior lattice points to the lower edge of the triangle. We will ensure that the outgoing slopes from the vertical edges in the Γ' have the same difference as in Γ. For $i = 1, 2, 3$, we will connect $(i, 1)$ to all points between $(2i + a_i, 0)$ and $(2i + b_i, 0)$ where a_i is the difference between the reciprocals of the slopes of the leftmost edges from $(i, 1)$ to the upper and lower edges of $R_{4,2}$ in Δ, and b_i is defined similarly but
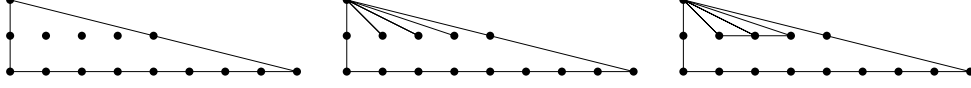
FIGURE 26. The start of Δ'.

with the rightmost edges. Here we take the reciprocal of ∞ to be 0. In the dual tropical curve, this translates to slopes emanating from vertical edges in the tropical curve having the same difference as from Δ.
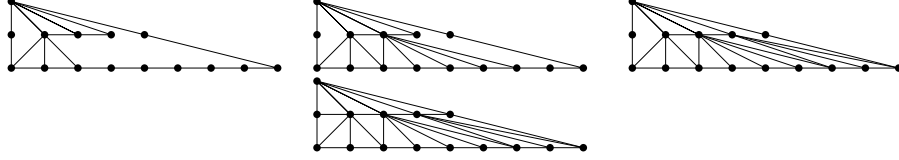
FIGURE 27. Several steps leading up to Δ', on the right.

We compute $a_1 = \frac{1}{-1} - \frac{1}{1} = -2$ and $b_1 = \frac{1}{\infty} - \frac{1}{\infty} = 0$. Since $2 \cdot 1 + a_1 = 0$ and $2 \cdot 1 + b_1 = 2$, we add edges from $(1,1)$ to $(0,0)$, to $(0,2)$, and to all points in between, in this case just $(0,1)$. We do similarly for the other two interior lattice points, as pictured in the first three triangles in Figure 28. The fourth triangle includes the edges $(0,1) - (1,1)$ and $(3,1) - (4,1)$, which ensures the same constraints as from Δ on the first and third loops of the corresponding metric graph.
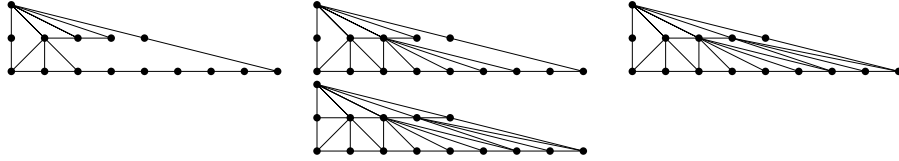
FIGURE 28. Several steps leading up to Δ', on the right.

PROOF OF THEOREM 5.1. The inclusion $\mathbb{M}^{\mathrm{planar}}_{g,\mathrm{hyp}} \subseteq \mathbb{M}^{\mathrm{chain}}_g$ holds because every unimodular triangulation of a hyperelliptic polygon is dual to a chain graph. Such a chain has $2g - 1$ edges, and hence $\dim(\mathbb{M}^{\mathrm{chain}}_g) = 2g - 1$. We also have $\dim(\mathbb{M}^{\mathrm{planar}}_{g,\mathrm{hyp}}) \geq 2g - 1$ because Lemma 3.1 implies $\dim(\mathbb{M}_{R_{g+1,2}}) = 2g - 1$. Hence the inclusion implies the dimension statement.

It remains to prove the equality $\mathbb{M}_{E^{(g)}_{g+2}} = \mathbb{M}^{\mathrm{planar}}_{g,\mathrm{hyp}}$. Given any triangulation Δ of a hyperelliptic polygon $E^{(g)}_k$, we shall construct a triangulation Δ' of $E^{(g)}_{g+2}$ such that $\mathbb{M}_\Delta = \mathbb{M}_{\Delta'}$. Our construction will show that the equality even holds at the level of smooth tropical curves.

We start constructing Δ' by drawing g edges from $(0,2)$ to the interior lattice points. The next $g - 1$ edges of Δ' are those that give it the same skeleton as Δ. This means that Δ' has the edge $(i,1) - (i+1,1)$ whenever that edge is in Δ, and Δ' has the edge $(0,2) - (2i+1,0)$ whenever $(i,1) - (i+1,1)$ is not an edge in Δ. Here $i = 1, \ldots, g-1$.

Next we will include edges in Δ' that give the same constraints on vertical edge lengths as Δ. This is accomplished by connecting the point $(i,1)$ to $(2i+a_i,0)$, to $(2i+b_i,0)$, and to all points in between, where a_i and b_i are defined as follows. Let a_i be the difference between the reciprocals of the slopes of the leftmost edges from $(i,1)$ to the upper and lower edges of $E^{(g)}_k$ in Δ. Here we take the reciprocal of ∞ to be 0. Let b_i be defined similarly, but with the rightmost edges. These new edges in Δ' do not cross due to constraints on the slopes in Δ. Loop widths and differences in extremal slopes determine upper and lower bounds on the lengths of vertical edges. These constraints on the $g - 2$ interior loops mostly guarantee

$\mathbb{M}_\Delta = \mathbb{M}_{\Delta'}$. To take care of the 1st and g^{th} loops, we must complete the definition of Δ'. Let $(n, 0)$ be the leftmost point of the bottom edge of $E_{g+2}^{(g)}$ connected to $(1, 1)$ so far in Δ'.

(i) If $n = 0$ then Δ' includes the edge $(0, 1) - (1, 1)$.

(ii) If $n \geq 2$ then Δ' includes $(0, 1) - (1, 1)$ and all edges $(0, 1) - (0, m)$ with $0 \leq m \leq n$.

(iii) If $n = 1$ and $(0, 1) - (1, 1)$ is an edge of Δ then Δ' includes $(0, 1) - (1, 1)$ and $(0, 1) - (1, 0)$.

(iv) If $n = 1$ and $(0, 1) - (1, 1)$ is not an edge Δ then Δ' includes $(0, 2) - (1, 0)$ and $(0, 1) - (1, 0)$.

Perform a symmetric construction around $(g, 1)$. These edge choices will give the same constraints on the 1st and g^{th} loops as those imposed by Δ. This completes the proof. $\square$

We now return to genus $g = 3$, our topic in section 4, and we complete the computation of $\mathbb{M}_3^{\text{planar}}$. By (III.18) and Theorem 5.1, it suffices to compute the 5-dimensional space $\mathbb{M}_{E_{g+2}^{(g)}}$. An explicit computation as in section 1 reveals that the rectangle $E_1^{(3)} = R_{4,2}$ realizes precisely the same metric graphs as the triangle $E_5^{(3)}$. With this, Theorem 5.1 implies $\mathbb{M}_{3,\text{hyp}}^{\text{planar}} = \mathbb{M}_{R_{4,2}}$. To complete the computation in section 4, it thus suffices to analyze the rectangle $R_{4,2}$.

TABLE 2. Dimensions of the moduli cones $\mathbb{M}_\Delta$ for $R_{4,2}$ and $E_5^{(3)}$

	$R_{4,2}$				$E_5^{(3)}$			
$G \setminus$ dim	3	4	5	#Δ's	3	4	5	#Δ's
(020)	42	734	1296	2072	42	352	369	763
(111)		211	695	906		90	170	260
(212)			127	127			25	25
total	42	945	2118	3105	42	442	564	1048

It was proved in [**6**] that $\mathbb{M}_{R_{4,2}}$ and $\mathbb{M}_{T_4}$ have disjoint interiors. Moreover, $\mathbb{M}_{R_{4,2}}$ is not contained in $\mathbb{M}_{T_4}$. This highlights a crucial difference between (III.13) and (III.18). The former concerns the tropicalization of classical moduli spaces, so the hyperelliptic locus lies in the closure of the non-hyperelliptic locus. The analogous statement is false for tropical plane curves. To see that $\mathbb{M}_{T_4}$ does not contain $\mathbb{M}_{R_{4,2}}$ consider the (020) graph with all edge lengths equal to 1. By Theorems 4.1 and 5.3, this metric graph is in $\mathbb{M}_{R_{4,2}}$ but not in $\mathbb{M}_{T_4}$. What follows is the hyperelliptic analogue to the non-hyperelliptic Theorem 4.1.

THEOREM 5.3. *A graph in $\mathbb{M}_3$ arises from $R_{4,2}$ if and only if it is one of the graphs (020), (111), or (212) in Figure 16, with edge lengths satisfying the following, up to symmetry:*

▷ (020) *is realizable if and only if $w = x$, $v \leq u$, $v \leq y \leq z$, and*
$$(y < v + 2w) \quad or \quad (y = v + 2w \text{ and } y < z)$$
$$or$$
$$(y < v + 3w \text{ and } u \leq 2v) \quad or \quad (y = v + 3w \text{ and } u \leq 2v \text{ and } y < z) \qquad \text{(III.23)}$$
$$or$$
$$(y < v + 4w \text{ and } u = v) \quad or \quad (y = v + 4w \text{ and } u = v \text{ and } y < z).$$

▷ (111) *is realizable if and only if $w = x$ and $\min\{u, v\} \leq w$.*

▷ (212) *is realizable if and only if $w = x$.*

PROOF. This is based on an explicit computation as described in section 1. The hyperelliptic rectangle $R_{4,2}$ has 3105 unimodular triangulations up to symmetry. All triangulations are regular. For each such triangulation we computed the graph G and the polyhedral cone $\mathbb{M}_\Delta$. Each $\mathbb{M}_\Delta$ has dimension 3, 4, or 5, with census given on the left in Table 2. For each cone $\mathbb{M}_\Delta$ we then checked that the inequalities stated in Theorem 5.3 are satisfied. This proves that the dense realizable part of $\mathbb{M}_{R_{4,2}}$ is contained in the polyhedral space described by our constraints.

For the converse direction, we construct a planar tropical realization of each metric graph that satisfies our constraints. For the graph **(020)**, we consider eleven cases:

(i) $y < v + 2w$, $u \neq v$, $y \neq z$;   (dim = 5)

(ii) $y = v + 2w$, $u \neq v$, $y \neq z$;   (dim = 5)

(iii) ($y < v + 3w$, $v < u < 2v$, $y \neq z$) or ($y < v + 2w$, $u \neq v$, $y < z < 2y$);   (dim = 5)

(iv) ($y < v + 3w$, $u = 2v$, $y \neq z$) or ($y < v + 2w$, $u \neq v$, $z = 2y$);   (dim = 4)

(v) ($y < v + 3w$, $v < u < 2v$, $y = z$) or ($y < v + 4w$, $u = v$, $y < z < 2z$);   (dim = 4)

(vi) ($y < v + 3w$, $u = 2v$, $y = z$) or ($y < v + 4w$, $u = v$, $z = 2y$);   (dim = 3)

(vii) $y = v + 3w$, $v < u < 2v$, $y \neq z$;   (dim = 4)

(viii) $y = v + 3w$, $u = 2v$, $y \neq z$;   (dim = 3)

(ix) ($y < v + 4w$, $u = v$, $y \neq z$) or ($y < v + 2w$, $y = z$, $u \neq v$);   (dim = 3)

(x) $y < v + 4w$, $u = v$, $y = z$;   (dim = 3)

(xi) $y = v + 4w$, $u = v$, $y \neq z$.   (dim = 3)

The disjunction of (i),(ii),...,(xi) is equivalent to (III.23). Triangulations giving all metric graphs satisfying each case are pictured in Figure 29. Next to the first triangulation is a metric graph arising from it.
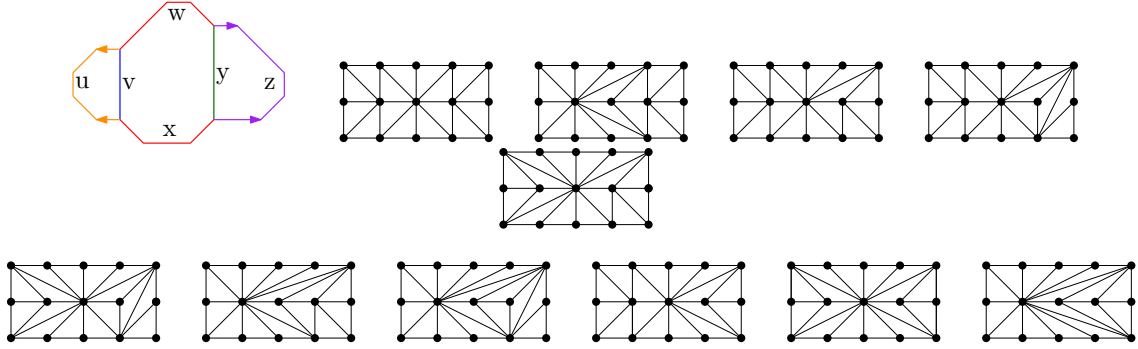
FIGURE 29. Triangulations giving all realizable hyperelliptic metrics for the graph (020)

Next we deal with graph **(111)**. Here we need two triangulations, one for $u \neq v$ and one for $u = v$. They are pictured in Figure 30. The left gives $u \neq v$, and the middle gives $u = v$.
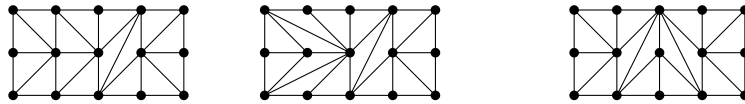
FIGURE 30. Triangulations realizing hyperelliptic metrics for the graphs (111) and (212)

Finally, for the graph **(212)**, the single triangulation on the right in Figure 30 suffices. □

6. Genus Four

In this section we compute the moduli space of tropical plane curves of genus 4. This is

$$\mathbb{M}_4^{\mathrm{planar}} = \mathbb{M}_{Q_1^{(4)}} \cup \mathbb{M}_{Q_2^{(4)}} \cup \mathbb{M}_{Q_3^{(4)}} \cup \mathbb{M}_{4,\mathrm{hyp}}^{\mathrm{planar}},$$

where $Q_i^{(4)}$ are the three genus 4 polygons in Proposition 1.7. They are shown in Figure 31.

There are 17 trivalent genus 4 graphs, of which 16 are planar. These were first enumerated in [**8**], and are shown in Figure 33. All have 6 vertices and 9 edges. The labels (ℓbc) are as in section 4: ℓ is the number of loops, b the number of bi-edges, and c the number of cut edges. This information is enough to uniquely determine the graph with the exception of
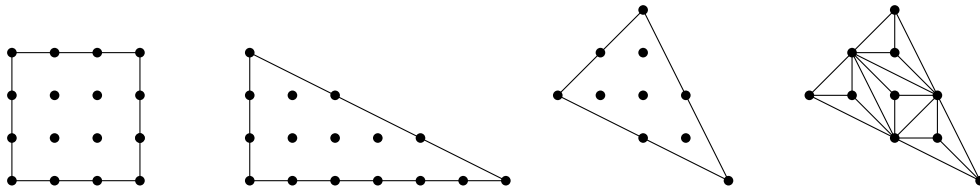
FIGURE 31. The three non-hyperelliptic genus 4 polygons and a triangulation

(000), where "A" indicates the honeycomb graph and "B" the complete bipartite graph $K_{3,3}$.

Up to their respective symmetries, the square $Q_1^{(4)} = R_{3,3}$ has 5941 unimodular triangulations, the triangle $Q_2^{(4)}$ has 1278 unimodular triangulations, and the triangle $Q_3^{(4)}$ has 20 unimodular triangulations. We computed the cone $\mathbb{M}_\Delta$ for each triangulation Δ, and we ran the pipeline of section 1. We summarize our findings as the main result of this section:

THEOREM 6.1. *Of the* 17 *trivalent graphs, precisely* 13 *are realizable by tropical plane curves. The moduli space* $\mathbb{M}_4^{\mathrm{planar}}$ *is 9-dimensional, but it is not pure: the left decomposition in* (III.2) *has components* (III.1) *of dimensions 7, 8 and 9. That decomposition is explained in Table* 3.

The four non-realizable graphs are (000)B, (213), (314) and (405). This is obvious for (000)B, because $K_{3,3}$ is not planar. The other three are similar to the genus 3 graph (303), and are ruled out by Proposition 7.3 below. The 13 realizable graphs G appear in the rows in Table 3. The first three columns correspond to the polygons $Q_1^{(4)}$, $Q_2^{(4)}$ and $Q_3^{(4)}$. Each entry is the number of regular unimodular triangulations Δ of $Q_i^{(4)}$ with skeleton G. The entry is blank if no such triangulation exists. Six of the graphs are realized by all three polygons, five are realized by two polygons, and two are realized by only one polygon. For instance, the graph (303) comes from a unique triangulation of the triangle $Q_3^{(4)}$, shown on the right in Figure 31. Neither $Q_1^{(4)}$ nor $Q_2^{(4)}$ can realize this graph.

Our moduli space $\mathbb{M}_4^{\mathrm{planar}}$ has dimension 9. We know this already from Proposition 3.2, where the square $Q_1^{(4)}$ appeared as $R_{3,3}$. In classical algebraic geometry, that square serves as the Newton polygon for canonical curves of genus 4 lying on a smooth quadric surface. In Table 3, we see that all realizable graphs except for (303) arise from triangulations of $R_{3,3}$. However, only five graphs allow for the maximal degree of freedom. Corresponding triangulations are depicted in Figure 32.

The last three columns in Table 3 list the dimensions of the moduli space $\mathbb{M}_{Q_i^{(4)},G}$, which is the maximal dimension of any cone $\mathbb{M}_\Delta$ where Δ triangulates $Q_i^{(4)}$ and has skeleton G. More detailed information is furnished in Table 4. The three subtables (one each for $i = 1, 2, 3$) explain the decomposition (III.1) of each stacky fan $\mathbb{M}_{Q_i^{(4)},G}$. The row sums in Table 4 are the first three columns in Table 3. For instance, the graph (030) arises in precisely 23 of the
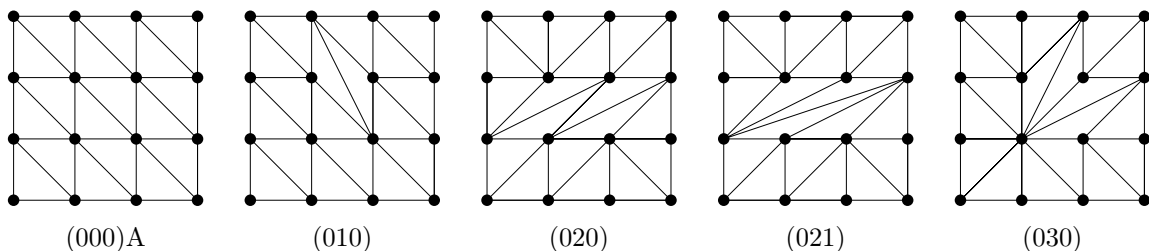
FIGURE 32. Triangulations Δ of $Q_1^{(4)}$ with $\dim(\mathbb{M}_\Delta) = 9$
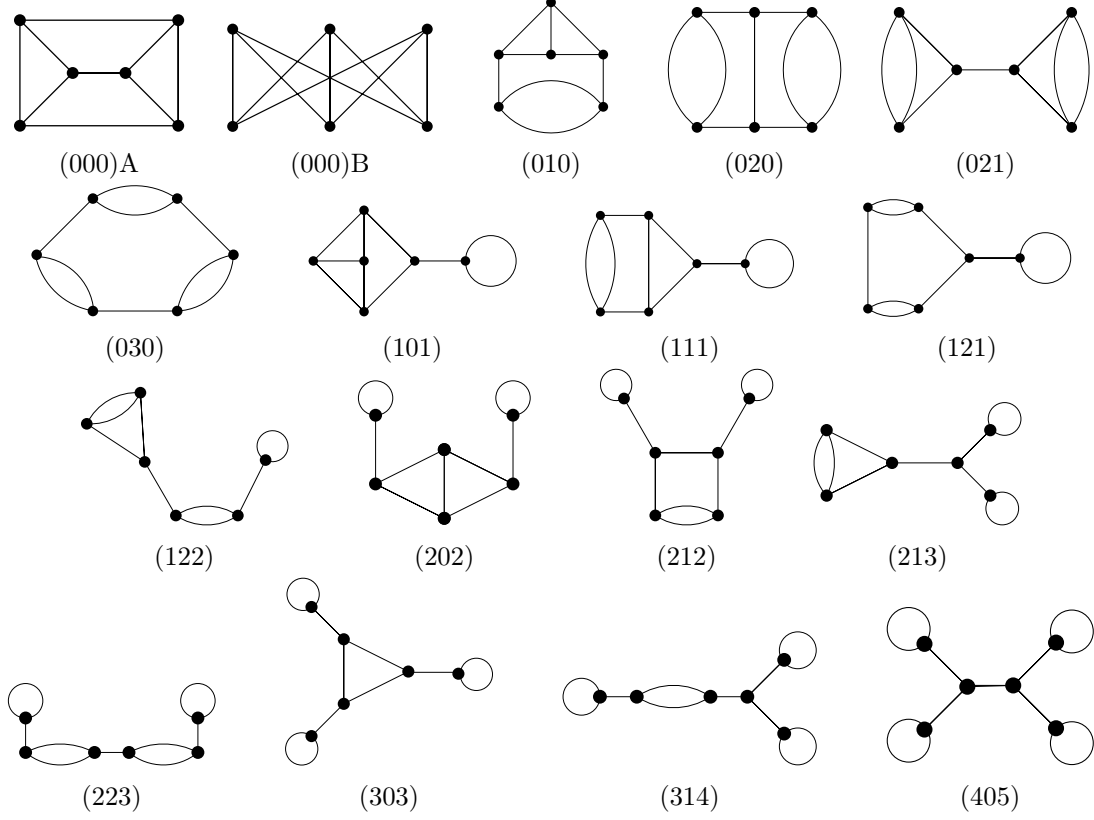
FIGURE 33. The 17 trivalent graphs of genus 4. All are planar except for (000)B.

TABLE 3. The number of triangulations for the graphs of genus 4 and their moduli dimensions

G	$\#\Delta_{Q_1^{(4)},G}$	$\#\Delta_{Q_2^{(4)},G}$	$\#\Delta_{Q_3^{(4)},G}$	$\dim(\mathbb{M}_{Q_1^{(4)},G})$	$\dim(\mathbb{M}_{Q_2^{(4)},G})$	$\dim(\mathbb{M}_{Q_3^{(4)},G})$
(000)A	1823	127	12	9	8	7
(010)	2192	329	2	9	8	7
(020)	351	194		9	8	
(021)	351	3		9	7	
(030)	334	23	1	9	8	7
(101)	440	299	2	8	8	7
(111)	130	221		8	8	
(121)	130	40	1	8	8	7
(122)	130	11		8	7	
(202)	15	25		7	7	
(212)	30	6	1	7	7	7
(223)	15			7		
(303)			1			7
total	5941	1278	20			

1278 triangulations Δ of the triangle $Q_2^{(4)}$. Among the corresponding cones $\mathbb{M}_\Delta$, three have dimension six, twelve have dimension seven, and eight have dimension eight.

Equipped with these data, we can now extend the probabilistic analysis of Corollary 4.2 from genus 3 to genus 4. As before, we assume that all 17 trivalent graphs are equally likely and we fix the uniform distribution on each 8-simplex that corresponds to one of the

TABLE 4. All cones $\mathbb{M}_\Delta$ from triangulations Δ of the three polygons in Figure 31

G\dim	$Q_1^{(4)}$					$Q_2^{(4)}$				$Q_3^{(4)}$			
	5	6	7	8	9	5	6	7	8	4	5	6	7
(000)	103	480	764	400	76	5	52	60	10	1	6	3	2
(010)	38	423	951	652	128	7	113	155	54			1	1
(020)	3	32	152	128	36		53	100	41				
(021)	3	32	152	128	36		1	2					
(030)		45	131	122	36		3	12	8				1
(101)	15	155	210	60		19	122	128	30			1	1
(111)		10	80	40			52	126	43				
(121)		35	65	30			8	20	12				1
(122)		10	80	40					1				
(202)			15					25					
(212)		15	15				4	2					1
(223)			15										
(303)													1

17 maximal cones in the 9-dimensional moduli space $\mathbb{M}_4$. The five graphs that occur with positive probability are those with $\dim(\mathbb{M}_{Q_1^{(4)},G}) = 9$. Full-dimensional realizations were seen in Figure 32. The result of our volume computations is the following table:

Graph	(000)A	(010)	(020)	(021)	(030)
Probability	0.0101	0.0129	0.0084	0.0164	0.0336

In contrast to the exact computation in Corollary 4.2, our probability computations for genus 4 rely on a Monte-Carlo simulation, with one million random samples for each graph.

COROLLARY 6.2. *Less than* 0.5% *of all metric graphs of genus 4 come from plane tropical curves. More precisely, the fraction is approximately* $\mathrm{vol}(\mathbb{M}_4^{\mathrm{planar}})/\mathrm{vol}(\mathbb{M}_4) = 0.004788$.

By Theorem 5.1, $\mathbb{M}_{4,\mathrm{hyp}}^{\mathrm{planar}} = \mathbb{M}_{E_{g+2}^{(g)}}$. This space is 7-dimensional, with 6 maximal cones corresponding to the chains (020), (021), (111), (122), (202), and (223). The graphs (213), (314), and (405) are hyperelliptic if given the right metric, but beyond not being chain graphs, these are not realizable in the plane even as combinatorial types by Proposition 7.3.

7. Genus Five and Beyond

The combinatorial complexity of trivalent graphs and of regular triangulations increases dramatically with g, and one has to be judicious in deciding what questions to ask and what computations to attempt. One way to start is to rule out families of trivalent graphs G that cannot possibly contribute to $\mathbb{M}_g^{\mathrm{planar}}$. Clearly, non-planar graphs G are ruled out. We begin this section by identifying another excluded class. Afterwards we examine our moduli space for $g = 5$, and we check which graphs arise from the polygons $Q_i^{(5)}$ in Proposition 1.7.

DEFINITION 7.1. *A connected, trivalent, leafless graph G is called* sprawling *if there exists a vertex s of G such that $G\backslash\{s\}$ consists of three distinct components.*

REMARK 7.2. Each component of $G\backslash\{s\}$ must have genus at least one; otherwise G would not have been leafless. The vertex s need not be unique. The genus 3 graph (303) in Figure 16 is sprawling, as are the genus 4 graphs (213), (314), and (405) in Figure 33.

PROPOSITION 7.3. *Sprawling graphs are never the skeletons of smooth tropical plane curves.*

This was originally proven in [15, Prop. 4.1]. We present our own proof for completeness.

PROOF. Suppose the skeleton of a smooth tropical plane curve C is a sprawling graph G with separating vertex s. After a change of coordinates, we may assume that the directions emanating from s are $(1,1)$, $(0,-1)$, and $(-1,0)$. The curve C is dual to a unimodular triangulation Δ of a polygon $P \subset \mathbb{R}^2$. Let $T \in \Delta$ be the triangle dual to s. We may take $T = \mathrm{conv}\{(0,0),(0,1),(1,0)\}$ after an appropriate translation of P. Let P_1, P_2, P_3 be the subpolygons of P corresponding to the components of $G \backslash \{s\}$. After relabeling, we have $P_1 \cap P_2 = \{(0,1)\}$, $P_1 \cap P_3 = \{(0,0)\}$, and $P_2 \cap P_3 = \{(1,0)\}$. Each P_i has at least one interior lattice point, since each component of $G \backslash \{s\}$ must have genus at least 1.
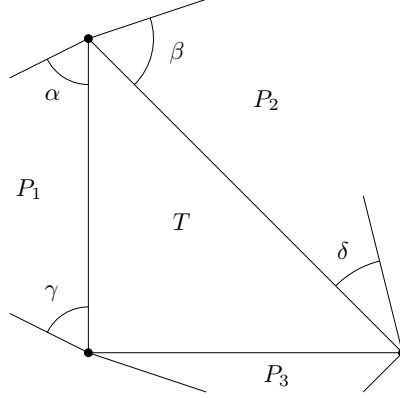
FIGURE 34. The triangle T with angles formed between it and the boundary edges of P

Let $\alpha, \beta, \gamma, \delta$ be angles between the triangle T and the boundary edges of P emanating from the vertices of T, as pictured in Figure 34. Since P is convex, we know $\alpha + \beta \leq 3\pi/4$, $\gamma < \pi/2$, and $\delta < 3\pi/4$. As P_1 contains at least one interior lattice point, and $\gamma < \pi/2$, we must also have that $\alpha > \pi/2$; otherwise $P_1 \subset (\infty, 0] \times [0, 1]$, which has no interior lattice points. Similarly, as P_2 has at least one interior lattice point and $\delta < 3\pi/4$, we must have that $\beta > \pi/4$. But we now have that $\alpha + \beta > \pi/2 + \pi/4 = 3\pi/4$, a contradiction. Thus, the skeleton of C cannot be a sprawling graph, as originally assumed. $\square$

REMARK 7.4. If G is sprawling then $\mathbb{M}_g^{\mathrm{planar}} \cap \mathbb{M}_G \neq \emptyset$ because edge lengths can become zero on the boundary. However, it is only in taking closures of spaces of realizable graphs that this intersection becomes nonempty.

We will now consider the moduli space of tropical plane curves of genus 5. That space is

$$\mathbb{M}_5^{\mathrm{planar}} \;=\; \mathbb{M}_{Q_1^{(5)}} \cup \mathbb{M}_{Q_2^{(5)}} \cup \mathbb{M}_{Q_3^{(5)}} \cup \mathbb{M}_{Q_4^{(5)}} \;\cup\; \mathbb{M}_{5,\mathrm{hyp}}^{\mathrm{planar}},$$

where $Q_1^{(5)}, Q_2^{(5)}, Q_3^{(5)}, Q_4^{(5)}$ are the four genus 5 polygons in Proposition 1.7. They are shown in Figure 35. Modulo their respective symmetries, the numbers of unimodular triangulations of these polygons are: 508 for $Q_1^{(5)}$, 147908 for $Q_2^{(5)}$, 162 for $Q_3^{(5)}$, and 968 for $Q_4^{(5)}$.
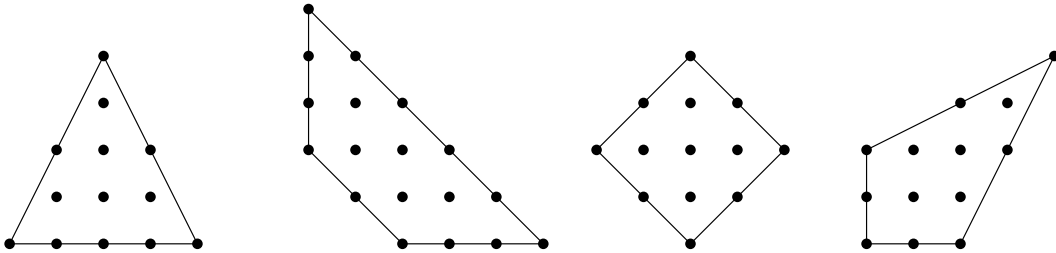
FIGURE 35. The genus 5 polygons $Q_1^{(5)}, Q_2^{(5)}, Q_3^{(5)}$ and $Q_4^{(5)}$

We applied the pipeline described in section 1 to all these triangulations. The outcome of our computations is the following result which is the genus 5 analogue to Theorem 6.1.

THEOREM 7.5. *Of the* 71 *trivalent graphs of genus* 5, *precisely* 38 *are realizable by smooth tropical plane curves. The four polygons satisfy* $\dim(\mathbb{M}_{Q_i^{(5)}}) = 9, 11, 10, 10$ *for* $i = 1, 2, 3, 4$.

All but one of the 38 realizable graphs arise from $Q_1^{(5)}$ or $Q_2^{(5)}$. The remaining graph, realized only by a single triangulation of $Q_4^{(5)}$, is illustrated in Figure 36. This is reminiscent of the genus 4 graph (303), which was realized only by the triangulation of $Q_3^{(4)}$ in Figure 31. The other 37 graphs are realized by at least two of the polygons $Q_1^{(5)}, \ldots, Q_4^{(5)}, E_7^{(5)}$.
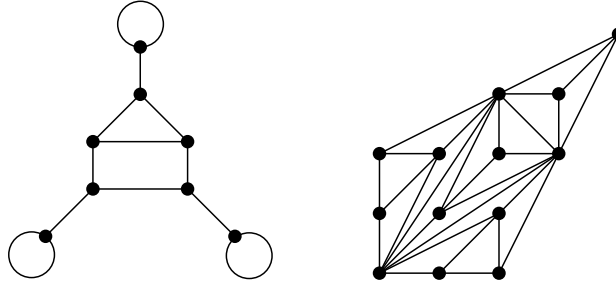
FIGURE 36. A genus 5 graph, and the unique triangulation that realizes it

Among the 71 trivalent graphs of genus 5, there are four non-planar graphs and 15 sprawling graphs, with none both non-planar and sprawling. This left us with 52 possible candidates for realizable graphs. We ruled out the remaining 14 by the explicit computations described in section 1. Three of these 14 graphs are shown in Figure 37. At present we do not know any general rule that discriminates between realizable and non-realizable graphs.
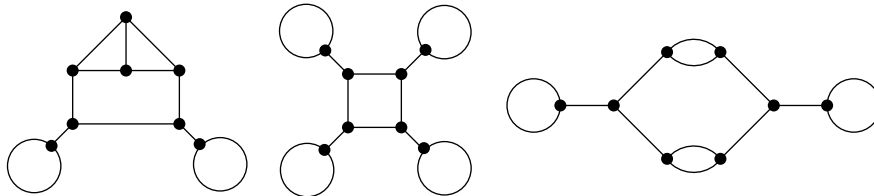
FIGURE 37. Some non-realizable graphs of genus 5

The process we have carried out for genus $g = 3$, 4, and 5 can be continued for $g \geq 6$. As the genus increases so does computing time, so it may be prudent to limit the computations to special cases of interest. For $g = 6$ we might focus on the triangle $Q_1^{(6)} = T_5$. This is of particular interest as it is the Newton polygon of a smooth plane quintic curve. This triangle has 561885 regular unimodular triangulations up to symmetry.

Although T_5 is interesting as the Newton polygon of plane quintics, it has the downside that $\mathbb{M}_{T_5}$ is not full-dimensional inside $\mathbb{M}_6^{\text{planar}}$. Proposition 3.2 implies that $\dim(\mathbb{M}_{T_5}) = 12$, while $\dim(\mathbb{M}_6^{\text{planar}}) = 13$, and this dimension is attained by the rectangle $R_{3,4}$ as in (III.16).

This might lead us to focus on *full-dimensional polygons* of genus g. By this we mean polygons P whose moduli space $\mathbb{M}_P$ has the dimension in (III.4). For each genus from 3 to 5, our results show that there is a unique full-dimensional polygon, namely, T_4, $R_{3,3}$, and $Q_2^{(5)}$. The proof of Theorem 0.1 furnishes an explicit example for each genus $g \geq 6$: take the rectangle in (III.16) or the trapezoid in (III.17) if $g \neq 7$, or the hexagon $H_{4,4,2,6}$ if $g = 7$. Preliminary calculations show that there are exactly two full-dimensional maximal polygons for $g = 6$, namely, $Q_3^{(6)} = R_{3,4}$ and $Q_4^{(}6)$ from Proposition 1.7.

We conclude with several open questions.

QUESTION 7.6. Let P be a maximal lattice polygon with at least 2 interior lattice points.

(1) What is the relationship between $\mathbb{M}_P$ and $\mathcal{M}_P$? In particular, does the equality $\dim(\mathbb{M}_P) = \dim(\mathcal{M}_P)$ hold for all P?

(2) How many P with g interior lattice points give a full dimensional $\mathbb{M}_P$ inside $\mathbb{M}_g^{\mathrm{planar}}$?

(3) Is there a more efficient way of determining if a combinatorial graph of genus g appears in $\mathbb{M}_g^{\mathrm{planar}}$ than running the pipeline in section 1?

Zonotopal Algebra

The theory of zonotopal algebras introduced by Holtz and Ron [**59**] gives a means of associating some of the most fundamental objects in combinatorics to solution sets of differential equations. Starting with a *box-spline*, the central Dahmen-Micchelli space can be constructed: a space of polynomials which satisfies the same differential equations as the polynomials locally describing the starting box-spline. The central Dahmen-Micchelli space is the Macaulay inverse system of an ideal generated by powers of linear forms; these linear forms are indexed by the cocircuits of the matroid whose ground set consists of the vectors defining the underlying zonotope of the starting box-spline. Holtz and Ron [**59**] also define a dual space to the central Dahmen-Micchelli space, the $\mathcal{P}$-central space, which has the same Hilbert polynomial as the central Dahmen-Micchelli space and can be associated to a hyperplane arrangement derived from a power ideal in which the $\mathcal{P}$-central space is the Macaulay inverse system of. There are also the internal and external Dahmen-Micchelli spaces and their duals as well, leaving us with many algebraic objects to play with.

Having this strong bridge between approximation theory (via the box-spline) and combinatorics is powerful. But the question still remains, where can this powerful bridge be applied? Here we link the machinery of zonotopal algebra with two particular polytopes, showing that the zonotopal spaces derived from two particular graphs capture the volumes of these polytopes, as well as the volumes of polytopes appearing in particular polyhedral subdivisions of these polytopes.

The first of the two is the Stanley-Pitman polytope. The Stanley-Pitman polytope, introduced by Stanley and Pitman [**106**], has a polyhedral subdivision whose chambers are indexed naturally by rooted binary trees, giving us a representation of the associahedra. For $t \in \mathbb{R}_+^n$, the Stanley-Pitman polytope is specifically the n-dimensional polytope $Q_n(t)$ defined by the equations

$$Q_n(t) := \{r \in \mathbb{R}_+^n : \sum_{i=j}^n r_i \leq \sum_{i=j}^n t_i, 1 \leq j \leq n\},$$

where we define $\mathbb{R}_+ := [0, \infty)$. Stanley and Pitman study the volume of $Q_n(t)$,

$$q_n(t) := \text{vol}(Q_n(t)),$$

and show in [**106**] that $q_n(t)$ is a polynomial which is the sum of exactly $C_n := \frac{\binom{2n}{n}}{n+1}$ normalized monomials.

PROPOSITION 0.1 (Pitman and Stanley, [**106**]). *For each $n \in \mathbb{N}\backslash\{0\}$, we have that*

$$q_n(t) = \sum_{k \in K_n} \prod_{i=1}^n \frac{t_i^{k_i}}{k_i!} = \frac{1}{n!} \sum_{k \in K_n} \binom{n}{k_1, ..., k_n} t_1^{k_1} \cdots t_n^{k_n},$$

where

$$K_n := \{k \in \mathbb{N}^n : \sum_{i=1}^j k_i \geq j \text{ for all } 1 \leq i \leq n-1 \text{ and } \sum_{i=1}^n k_i = n\}$$

with $\mathbb{N} := \{0, 1, 2, ...\}$.

The volume $q_n(t)$ of the Stanley-Pitman polytope $Q_n(t)$ can be captured via the zonotopal algebra of the *broken wheel graph BW_n*: a finite undirected graph with $n+1$ vertices and $2n$

edges, which defines the graphical matroid needed for our constructions. In section 1, we will rigorously define the broken wheel graph BW_n, define what it means to be a *parking function* of BW_n, and discuss some properties of such parking functions. We will then use these properties in section 2, where we will discuss the Tutte polynomial and Hilbert series of BW_n, as well as develop the zonotopal algebra of BW_n, after giving a review of the general theory of zonotopal algebra. Section 3 we will specifically address the Stanley-Pitman polytope and use the machinery developed to prove that the Stanley-Pitman volume polynomial $q_n(t)$ is the monic polynomial in the central Dahmen-Micchelli space of BW_n which corresponds to the parking function $(1, ..., 1) \in \mathbb{R}^n$, and that it is the unique internally monic polynomial of maximal degree in the internal Dahmen-Micchelli space of BW_n which corresponds to the unique internal parking function $(1, 1, ..., 1, 0) \in \mathbb{R}^{n+1}$. Using the following notation, we will also further characterize the volume polynomial $q_n(t)$ with the following two theorems: denote partial differentiation with respect to t_i by D_i; i.e with $p_i : \mathbb{R}^n \to \mathbb{R}^n, t \mapsto t_i$, we have $D_i := p_i(D)$, and $D_0 := 0$. We then have that:

THEOREM 0.2. *The polynomial $q_n(t)$ is the only polynomial (up to normalization) of degree n that is annihilated by each of the following differential operators*

$$D_i(D_i - D_{i-1}), \ i = 1, ..., n.$$

Moreover, let $\mathcal{P}_{n,j}$ be the subspace of homogeneous polynomials (in n indeterminates) of degree j that are annihilated by each of the above differential operators. Then:

(1) $\mathcal{P}_{n,j}$ lies in the span of the translates of $q_n(t)$.
(2) dim $\mathcal{P}_{n,j} = \binom{n}{j}$.

THEOREM 0.3. *The polynomial $q_n(t)$ is the only polynomial $q(t)$ (in n variables) that satisfies the following two properties:*

(1) With m the square-free monomial

$$m : t \mapsto \prod_{i=1}^{n} t_i,$$

the monomial support of $(q - m)(t)$ is disjoint of the monomial support of the polynomial

$$t \mapsto \prod_{i=1}^{n} (t_i + t_{i-1}), \ t_0 := 0.$$

(2) $q(t)$ is annihilated by each of the following differential operators:

$$(D_{j+1} - D_j)(\prod_{k=i}^{j} D_k)(D_i - D_{i-1}), \ 1 \le i \le j < n,$$

and

$$(\prod_{k=1}^{n} D_k)(D_i - D_{i-1}), \ 1 \le i \le n.$$

We will then review the polyhedral subdivision of $Q_n(t)$ given by Pitman and Stanley [**106**], whose set of interior faces, ordered by inclusion, is isomorphic to the face lattice of the dual associahedron, and note how the volume of each polytope in this subdivision is captured by the zonotopal algebra of the broken wheel graph. This observation is motivation for studying the volumes of polyhedral subdivisions in terms of zonotopal algebras and lead us to our study of the second polytope.

In section 4 we will introduce the second polytope: the regular simplex $\mathfrak{Sim}_n(t_1, ..., t_n)$ with parameters $t_1, ..., t_n \in \mathbb{R}_+^n$, defined by the inequalities

$$\sum_{i=1}^{n} r_i \le \sum_{i=1}^{n} t_i, \ r_i \in \mathbb{R}_+^n,$$

where the $(r_i)_{i \in [n]}$ are variables. For every rooted tree T with n vertices, we can construct 2^{n-1} directed graphs, which we will refer to as *generalized broken wheel graphs*. Each generalized broken wheel graph constructed from T will give us a polytope, its volume polynomial, and a *reference monomial*. The 2^{n-1} polytopes together give a polyhedral subdivision of $\mathfrak{Sim}_n(t_1, ..., t_n)$, their volume polynomials together give a basis for the subspace of homogeneous polynomials of degree n of the corresponding central Dahmen-Micchelli space, and their reference monomials together give a basis for its dual. And so, for each rooted tree with n vertices we have a polyhedral subdivision of $\mathfrak{Sim}_n(t_1, ..., t_n)$ completely characterized by the zonotopal algebra of the generalized broken wheel graphs constructed from T.

Our study provides intriguing and quite rich examples of zonotopal algebra, on the one hand, and sheds new light on how volumes of polytopes, and their polyhedral subdivisions, can be studied on the other. This paper is meant for both the eyes of those familiar and unfamiliar with the study of zonotopal algebras. For those familiar, we hope to provide you with an enriching application which will spark your further interest. For those unfamiliar, we hope to illustrate to you the potential of zonotopal algebras as a combinatorial way to connect to analytic tools.

1. The Broken Wheel Graph

Before we jump into the details of the broken wheel graph, let's define it precisely. The *broken wheel graph* BW_n is a finite undirected graph with $n + 1$ vertices $[0{:}n]$ and $2n$ edges. The root vertex 0 is connected twice to the vertex 1, and once to each other vertex. In addition, a single edge connects each consecutive pair i and $i + 1$, with $i = 1, ..., n - 1$.

A *wheel graph* W_n consists of the edges of a regular n-gon, together with all the radii that connect the vertices of the n-gon to its center. In algebraic graph theory, the n vertices of the n-gon are associated with the standard basis $(e_i)_{i=1}^n$ of $\mathbb{R}^n$, while the center is identified with $e_0 := 0$. The edge that connects the vertices i and j is realized by the vector $e_i - e_j$ (or $e_j - e_i$, as the sign will not matter for us). For certain purposes (such as the definition of the internal activity and the external activity of the forests of the graph) it is necessary to order the edges, viz. their vector realization. The order that serves our needs is as follows:

$$x_{2i-1} = e_i - e_{i-1}, x_{2i} = e_i, i = 1, 2, ..., n.$$

The vectors $X_n := (x_1, ..., x_{2n})$ correspond to the edges of the wheel W_n: odd numbered vectors corresponding to the edges of the n-gon and the even vectors corresponding to the radii. Note that we have written $x_1 = e_1 - e_0 = e_1$. This is because the broken wheel BW_n is obtained from the wheel W_n when replacing the n-gon edge $e_1 - e_n$ by the radius e_1. Thus, the edge e_1 is doubled in BW_n. We then use the following order on the edge set of BW_n:

$$BW_n := (x_1 \prec x_2 \prec \cdots \prec x_{2n}).$$
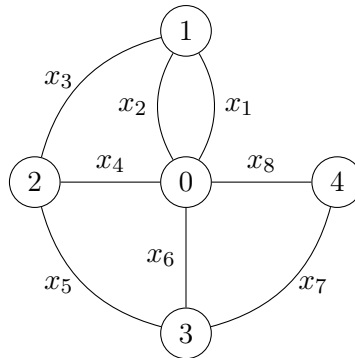
FIGURE 38. The broken wheel graph BW_4.

With this order, the edges of BW_n form the columns of an $n \times 2n$ matrix denoted X_n. For example, the matrix X_4 is

$$X_4 = \begin{bmatrix} 1 & 1 & -1 & 0 & 0 & 0 & 0 & 0 \\ 0 & 0 & 1 & 1 & -1 & 0 & 0 & 0 \\ 0 & 0 & 0 & 0 & 1 & 1 & -1 & 0 \\ 0 & 0 & 0 & 0 & 0 & 0 & 1 & 1 \end{bmatrix}.$$

With this identification, ordering of the edges of BW_n, and the matrix X_n we have enough to construct three pairs of polynomial spaces, which are examples of the fundamental pairs of polynomial spaces studied generally in the field zonotopal algebra. Before we do this (in section 2), we need to talk about the *parking functions* of BW_n, as they are key to discussing these pairs of spaces.

1.1. The Parking Functions of the Broken Wheel Graph. Given a subset of vertices $[i : j]$ of BW_n and a vertex $k \in [i : j]$, we denote by

$$d(i, k, j)$$

the *out-degree* of k, viz. the number of edges that connect k to vertices in the complement of $[i : j]$. Note that $d(i, k, j) \in \{1, 2, 3\}$, $0 < i \leq k \leq j \leq n$, for BW_n. Parking functions of graphs are studied in generality by Postnikov and Shapiro in [**92**]. Following their definition, a *parking function* of the graph is a function $s \in \mathbb{N}^n$, with $s(i)$ denoting the ith entry of s, which satisfies the following condition: given any $1 \leq i \leq j \leq n$, there exists a $k \in [i : j]$ such that $s(k) < d(i, k, j)$. This definition follows suit from the definition of parking functions given in [**106**]. A parking function s is called an *internal parking function* of a graph if for every $1 \leq i \leq j \leq n$, we either have a $k \in [i : j - 1]$ such that $s(k) < d(i, k, j)$ or $s(j) < d(i, j, j) - 1$. Let the set of parking functions of BW_n be denoted by

$$S(BW_n)$$

and the set of internal parking functions of BW_n by

$$S_-(BW_n).$$

LEMMA 1.1. *If s is a parking function of BW_n, then $\prod_{k=i}^{j} s(k) \leq 2$, while $\prod_{k=i}^{n} s(k) \leq 1$, for every $1 \leq i \leq j \leq n$.*

PROOF. Consider $s \in S(BW_n)$. If $i = j = n$, then the only k we can choose is $k = n$ and we must then have that $s(n) \leq 1$, as $d(n, n, n) = 2$ for BW_n. If we choose $i = j < n$, then the only k we can choose is $k = i = j < n$ and we must then have that $s(n) \leq 2$.

If we have that $s(i) = 2$, and we choose j to be n, then we can see that $d(i, i, n) = 2$ and, for $k > i$, $d(i, k, n) = 1$. We can then conclude from these two observations that $s(k) = 0$ for some $k > i$, as this is the only way we can find a $k \in [i{:}n]$ such that $s(k) < d(i, k, n)$.

Let's now assume a bit further that $s(i) = s(j) = 2$ for some $1 \leq i < j < n$. As $d(i, i, j) = d(i, j, j) = 2$, while $d(i, k, j) = 1$ for $i < k < j$, we can see that $s(k) = 0$ for some $i < k < j$.

From all of these observations, we can conclude that, in order for s to be a parking function of BW_n, we must have that $\prod_{k=i}^{j} s(k) \leq 2$, while $\prod_{k=i}^{n} s(k) \leq 1$, for every $1 \leq i \leq j \leq n$. $\square$

Let us now define a particular subset of $S(BW_n)$ which will be necessary for our studies. The set of *maximal parking functions* $S_{max}(BW_n)$ of BW_n is defined as

$$S_{max}(BW_n) := \{s \in S(BW_n) : |s| := \sum_{i=1}^{n} s(i) = n.$$

We can explicitly define the sets $S(BW_n), S_{max}(BW_n)$, and $S_-(BW_n)$ as the *support* of certain polynomials. For $s \in \mathbb{Z}_+^n$, let us define the monomial

$$m_s : t \mapsto t^s := \prod_{i=1}^n t_i^{s(i)}.$$

Then, given a polynomial $p \in \mathbb{K}[t_1, ..., t_n]$, where $\mathbb{K}$ is a field of characteristic 0, the *monomial support* supp $p(t)$ of $p(t)$ is the set of vectors $s \in \mathbb{Z}_+^n$ for which

$$m_s(D)p(t)|_{t=0} \neq 0.$$

EXAMPLE 1.2. For $q_2(t) = t_2^2/2 + t_1 t_2$, we have that supp $q_2(t) = \{(1,1), (0,2)\}$.

We now have the following two theorems which characterize the sets $S(BW_n), S_{max}(BW_n)$, and $S_-(BW_n)$ as the support of certain polynomials:

PROPOSITION 1.3. *For $a \in \{0, 1\}$, let*

$$p_{n,a}(t) := \prod_{i=1}^n (a + t_{i-1} + t_i), \ t_0 := 0.$$

Then

$$S_{max}(BW_n) = \text{supp } p_{n,0}(t) \text{ and } S(BW_n) = \text{supp } p_{n,1}(t),$$

and we have that

$$|S_{max}(BW_n)| = 2^{n-1} \text{ and } |S(BW_n)| \leq 2 \cdot 3^{n-1}.$$

PROOF. Consider the polynomial expansion of $p_{n,0}(t)$:

$$p_{n,0}(t) = \prod_{i=1}^n (t_{i-1} + t_i) = (t_1^2 + t_1 t_2) \prod_{i=3}^n (t_{i-1} + t_i). \tag{IV.1}$$

We can see that $p_{n,0}(t)$ is a polynomial with 2^{n-1} monomials, as it is a polynomial which can be factored into n binomials. Thus we have that $|\text{supp } p_{n,0}(t)| = 2^{n-1}$.

Let us prove the equality in question by induction on n. First, let us assume that $n = 1$. We then have that $p_{1,0}(t) = t_1$, giving us that supp $p_{1,0}(t) = \{(1)\}$. Corollary 2.5 of this note tells us that the set of maximal parking functions is exactly the subset of $\mathbb{N}^n$ of all sequences s that can be written as a sum

$$s = e_1 + \sum_{j=1}^{n-1} a_j,$$

with $(e_i)_{i=1}^n$ the standard basis for $\mathbb{N}^n$, and $a_j \in \{e_j, e_{j+1}\}$ for every j. Thus $S_{max}(BW_1) = \{(1)\}$ and we have equality for our base case.

Now, assuming that $S_{max}(BW_k) = \text{supp } p_{k,0}(t)$ for $k \leq n$, we have

$$p_{n+1,0}(t) = p_{n,0}(t)(t_n + t_{n+1}) = p_{n,0}(t)t_n + p_{n,0}(t)t_{n+1}.$$

First, let us consider any $s \in \text{supp } p_{n,0}(t)t_n$. We have that the first $n-1$ entries of s are going to satisfy the conditions of corollary 2.5, the nth entry of s is going to be either 1 or 2 (as the degree of t_n for any term of $p_{n,0}(t)$ is 0 or 1), and that the $(n+1)^{st}$ entry of s is 0. Thus, s is such a vector described in corollary 2.5, meaning that $s \in S_{max}(BW_{n+1})$ and supp $p_{n,0}(t)t_n \subseteq S_{max}(BW_{n+1})$. Similarly, let's consider any $s \in \text{supp } p_{n,0}(t)t_{n+1}$. We then have that the first $n-1$ entries of s satisfy the conditions of corollary 2.5, the nth entry of s is going to be either 0 or 1, and that the $(n+1)^{st}$ entry of s is 1. Thus, s is such a vector described in corollary 2.5, meaning that $s \in S_{max}(BW_{n+1})$ and supp $p_{n,0}(t)t_{n+1} \subseteq S_{max}(BW_{n+1})$. Thus, supp $p_{n+1,0}(t) = \text{supp } p_{n,0}(t)t_n \cup \text{supp } p_{n,0}(t)t_{n+1} \subseteq S_{max}(BW_{n+1})$. To show that our inclusion is actually an equality, let us assume our inclusion is strict and find a contradiction. If our inclusion is strict, then there exists an $s \in S_{max}(BW_{n+1})$ such that $s \notin \text{supp } p_{n+1,0}(t)$. We then have that

$$m_s(D)p_{n+1,0}(t) = m_s(D)[p_{n,0}(t)(t_n + t_{n+1})]|_{t=0} = 0.$$

Since we have that $m_s(D)p_{n,0}(t)|_{t=0} \neq 0$ by our induction hypothesis, we must have $s(n) = s(n+1) = 0$. This means, however, that when expressing s as stipulated in corollary 2.5,

$$s = e_1 + \sum_{j=1}^{n} a_j,$$

we cannot have $a_n \in \{e_n, e_{n+1}\}$ as required. Thus, we have our contradiction and the equality desired. And so, in particular, we have that $|S_{max}(BW_n)| = 2^{n-1}$.

Now, let us consider $p_{n,1}(t)$. We can see that $p_{n,1}(t)$ is a polynomial with $2 \cdot 3^{n-1}$ terms by noting that

$$p_{n,1} = (1 + t_1) \prod_{i=2}^{n} (1 + t_{i-1} + t_i).$$

For $n = 1$, we have that $p_{1,1} = 1 + t_1$ and thus that supp $p_{1,1}(t) = \{(0), (1)\}$. Checking the definition of a parking function against each element of the support of $p_{1,1}(t)$, we can see that our only choice for i and j is $i = j = 1$. We can then see that $0 < d(1, 1, 1) = 2$ and $1 < d(1, 1, 1) = 2$; this shows us that supp $p_{1,1} \subset S(BW_1)$. And as $|S(BW_1)| = 2$, as the number of spanning trees of SW_1 is 2, we have equality.

Now, assuming $S(BW_k) = $ supp $p_{k,1}(t)$ for $k \leq n$, let's consider

$$p_{n+1,1}(t) := p_{n,1}(t)(1 + t_n + t_{n+1}) = p_{n,1}(t) + t_n p_{n,1}(t) + t_{n+1} p_{n,1}(t),$$

a polynomial with at most $2 \cdot 3^{n-1}$ terms; thus $|\text{supp } p_{n+1,1}(t)| \leq 2 \cdot 3^{n-1}$. We have established in lemma 1.1 that if a vector s is a parking function of BW_{n+1} then $\prod_{k=i}^{j} s(k) \leq 2$ and $\prod_{k=1}^{n+1} s(k) \leq 1$ for every $1 \leq i \leq j \leq n + 1$. For supp $p_{n,1}(t)$, these conditions are met by our induction hypothesis.

For supp $t_n p_{n,1}(t)$, we also have that our conditions are met: $\prod_{k=1}^{n+1} s(k) = 1 \cdot \prod_{k=1}^{n} s(k) \leq 1$, and as $\prod_{k=i}^{n} s(k) \leq 1$ for every $1 \leq i \leq j \leq n$, we have that $\prod_{k=i}^{n} s(k) \leq 2$ for every $1 \leq i \leq j \leq n + 1$ via our extra factor of t_n in every monomial of $t_n p_{n,1}(t)$. For supp $t_{n+1} p_{n,1}(t)$, we also have that our conditions are met, as adding a 1 to either of the products in question will not change their numerical value. As supp $p_{n+1,1}(t) = $ supp $p_{n,1}(t) \cup $ supp $t_n p_{n,1}(t) \cup$ supp $t_{n+1} p_{n,1}(t)$, we thus have that supp $p_{n+1,1}(t) \subseteq S(BW_{n+1})$.

To prove that this inclusion is actually an equality, let us assume that the inclusion is strict and find a contradiction. If our inclusion is strict, then there exists an $s \in S(BW_{n+1})$ such that $s \notin$ supp $p_{n+1,1}$. We then have that

$$m_s(D)p_{n+1,1}|_{t=0} = m_s(D)[p_{n,1}(1 + t_n + t_{n+1})] = 0.$$

This would then imply that $m_s(D)p_{n,1} = 0$, a contradiction to our induction hypothesis. Thus, we must have the equality desired. And so, in particular, we have that $|S(BW_{n+1})| \leq 2 \cdot 3^{n-1}$. □

PROPOSITION 1.4. *Let*

$$p_{n,-}(t) := \prod_{i=1}^{n-1} (1 + t_i).$$

Then $S_-(BW_n) = $ supp $p_{n,-}(t)$ *and* $|S_-(BW_n)| = 2^{n-1}$.

PROOF. Let us consider the polynomial $p_{n,-}(t) := \prod_{i=1}^{n-1}(1+t_i)$ and prove our proposition by induction on n. As always, let's first consider our base case, $n = 1$. We then have that $p_{1,-}(t) = 1$. The support of this polynomial is supp $p_{1,-}(t) = \{(0)\}$. Following the definition of an internal parking function, as our only choice for i and j is $i = j = 1$, we have that $0 < d(1, 1, 1) - 1 = 2 - 1 = 1$. Thus, we have that (0) is in $S_-(BW_1)$ and that supp $p_{1,-}(t) = S_-(BW_1)$.

Now, let us assume that $S_-(BW_k) = $ supp $p_{k,-}(t)$ for $k \leq n$ and show that this equality is also true for $k = n + 1$. We have that $p_{n+1,-}(t) = \prod_{i=1}^{n}(1 + t_i) = p_{n,-}(t)(1 + t_n) =$

$p_{n,-}(t) + p_{n,-}(t)t_n$. Thus, supp $p_{n+1,-}(t) = $ supp $p_{n,-}(t) \cup $ supp $p_{n,-}(t)t_n$, where $p_{n,1}(t)$ is considered as a polynomial in n variables. If $s \in$ supp $p_{n,-}(t)$, then we know that for every $k \in [i : j-1]$, $1 \leq i \leq j \leq n$, we have that either $s(k) < d(i,k,j)$ or $s(j) < d(i,j,j) - 1$. We also know that $s(n) = 0$, meaning that these inequalities certainly still hold after we extend $1 \leq i \leq j \leq n$ to $1 \leq i \leq j \leq n+1$. Thus, we have that supp $p_{n,-}(t) \subseteq S(BW_{n+1})$. If $s \in$ supp $p_{n,-}(t)t_n$, then we know that $s(n) = 1$. As we know that for every $k \in [i : j-1]$, $1 \leq i \leq j \leq n$, we have that either $s(k) < d(i,k,j)$ or $s(j) < d(i,j,j) - 1$, we need to only check the cases when $i = j = n+1$ and when $j = n+1$ and $i < n+1$. For when $i = j = n+1$, we have that $s(n) = 1 < d(n,n,n) = 3$. For $i < n+1$, we have that $s(n) = 1 < 2 \leq d(i,n,n)$. Thus, our conditions are satisfied and that supp $p_{n,-}(t)t_n \subseteq S(BW_{n+1})$. We now have that supp $p_{n+1,-}(t) \subseteq S(BW_{n+1})$. To prove that this inclusion is actually an equality, let us assume that the inclusion is strict and find a contradiction. If our inclusion is strict, then there exists an $s \in S(BW_{n+1})$ which is not in supp $p_{n+1,-}(t)$. We then must have that

$$m_s(D)p_{n+1,-}(t)|_{t=0} = m_s(D)[p_{n,-}(t)(1+t_n)]|_{t=0} = 0.$$

This would then mean that $m_s(D)p_{n,-}(t)|_{t=0} = 0$, a contradiction to our induction hypothesis. Thus we must have equality. And in particular, we have $|S_-(BW_n)| = 2^{n-1}$. $\square$

Note that, while $q_n(t)$ and $p_{n,0}(t)$ are both homogeneous polynomials of degree n in n variables, their support is almost disjoint:

$$\text{supp } p_{n,0}(t) \cap \text{supp } q_n(t) = \{(1, ..., 1)\}.$$

This observation is key to the proof of theorem 0.3. As for the internal parking functions of BW_n, we have

$$|\{s \in S_-(BW_{n+1}) : |s| = j\}| = \binom{n-1}{j}, \ 0 \leq j \leq n-1.$$

This observation is key to the proof of theorem 0.2.

We will see that the zonotopal algebra of BW_n hinges on the parking functions of BW_n. The Hilbert series presented in the next section, the monomial bases for the $\mathcal{P}$-central and $\mathcal{P}$-internal spaces, and the results connecting to the Stanley-Pitman polytope are all framed in terms of the parking functions of BW_n.

2. The Zonotopal Algebra of the Broken Wheel Graph

The zonotopal algebra of a graph consists of three pairs of polynomial spaces: a central pair, an internal pair, and an external pair. We will discuss the central and internal pairs of spaces for the broken wheel graph, and not the external pair as it does not play a role in our study. We will discuss the central Dahmen-Micchelli space $\mathcal{D}(X_n)$ of BW_n and its dual, the $\mathcal{P}$-central space $\mathcal{P}(X_n)$. We will observe that $\mathcal{P}(X_n)$ is *monomial*; i.e. has a monomial basis. Postnikov and Shapiro [**92**] show that the monomial basis for $\mathcal{P}(X_n)$ must be given by the parking functions:

$$\{m_s : s \in S(X_n)\}.$$

We will show that the volume polynomial $q_n(t)$ of the the Stanley-Pitman polytope lies in $\mathcal{D}(X_n)$, and that $q_n(t)$ is precisely the polynomial in a particular basis of $\mathcal{D}(X_n)$ that corresponds to the monomial $t_1 t_2 \cdots t_n$ in the monomial basis of $\mathcal{P}(BW_n)$. Theorem 0.3 follows from this observation. We also show that once we reverse the order of the variables in $q_n(t)$, $\bar{q}_n(t_1, ..., t_n) := q_n(t_n, ..., t_1)$, the polynomial $\bar{q}_n(t)$ lies in the internal zonotopal space $\mathcal{D}_-(X_{n+1})$. At the same time, the internal zonotopal space $\mathcal{P}_-(X_{n+1})$ is monomial, with its monomial basis necessarily determined by the internal parking functions

$$\{m_s : s \in S_-(X_{n+1})\}.$$

Theorem 0.2 follows from this observation. But in order to define and discuss these spaces in detail, we must first discuss the Tutte polynomial and Hilbert series of the broken wheel graph.

2.1. The Tutte Polynomial and Hilbert Series of the Broken Wheel Graph.
Let X be the corresponding matrix of a graph. Recall that the collection of its spanning trees
$\mathbb{B}(X)$ correspond to the $n \times n$ invertible submatrices of X. We now define two valuations on
the set $\mathbb{B}(X)$ that are the reversal of the external activity and internal activity as defined by
Tutte.

Both valuations require an ordering on X, we use the above-defined order $\prec$: $x_i \prec x_j$ if
and only if $i < j$. Given $B \in \mathbb{B}(X)$, its *valuation* is defined by

$$val(B) := |\{x \in (X \backslash B) : \{x\} \cup \{b \in B : b \prec x\} \text{ is independent (in } \mathbb{R}^n)\}| \, .$$

Its *dual valuation* is then defined as

$$val^*(B) := |\{b \in B : \{B \backslash b\} \cup \{x \in X \backslash B : b \prec x\} \text{ spans } \mathbb{R}^n\}| \, .$$

The *Tutte polynomial* is defined as the following bivariate polynomial, in the variables s and
t:

$$T_X(s,t) := \sum_{B \in \mathbb{B}(X)} s^{n-val(B)} t^{n-val^*(B)}.$$

PROPOSITION 2.1. *The Tutte polynomial $T_{X_n}(s,t)$ of the broken wheel graph BW_n is
symmetric:*

$$T_{X_n}(s,t) = T_{X_n}(t,s).$$

PROOF. Let A be the $2n \times \mathbb{Z}$ matrix whose first row has entries

$$a(1,j) := \begin{cases} 1 & j = 1, 2 \\ -1 & j = 3 \\ 0 & \text{otherwise} \end{cases}$$

and whose entries are $a(i,j) := a(1, i + j - 1)$ everywhere else. Note that each even row of
this matrix is orthogonal to all the odd rows. We can see that X_n is the submatrix of A
that corresponds to the rows indexed by $1, 3, ..., 2n - 1$ and columns $1, ..., 2n$. Let Y_n be the
matrix that has the same columns as X_n, but the complementary set of rows. The rows of
Y_n are still orthogonal to entries of X_n. Moreover, the matrix Y_n is obtained from X_n by
performing the following operations:

(i): Multiply by -1 each odd column x_{2i-1},
(ii): Reverse the order of the columns.

Thus Y_n represents the same graph as X_n, with respect to a reverse order of the edges. Since
the Tutte polynomial is invariant to the ordering of the edges, $T_{X_n}(s,t) = T_{Y_n}(s,t)$. On the
other hand, since the row span of Y_n is orthogonal to the row span of X_n, Y_n is isomorphic
to the dual matroid of X_n. It is further known that for every matroid X with dual $\hat{X}$,
$T_X(s,t) = T_{\hat{X}}(t,s)$. And so we have

$$Y_{X_n}(s,t) = T_{Y_n}(s,t) = T_{\hat{X}_n}(s,t) = T_{X_n}(t,s).$$

$\square$

A spanning tree $B \in \mathbb{B}(X)$ is called *internal* if $val^*(B) = n$ and *maximal* if $val(B) = n$.
Note that the number of internal trees of a graph X equals $T_X(1,0)$, while the number of
maximal trees equals $T_X(0,1)$.

PROPOSITION 2.2. *The Tutte polynomial of the broken wheel BW_n satisfies*

$$T_{X_n}(1,0) = T_{X_n}(0,1) = 2^{n-1}.$$

PROOF. Let's consider first the set $\mathbb{B}_{max}(X_n)$ of maximal trees. For every $B \in \mathbb{B}_{max}(X_n)$,
it follows directly from the definition that $x_1 \notin B$, while $x_{2n} \in B$. After removing x_{2n} from
each maximal basis, we obtain a modified set $\mathbb{B}'_{max}(X_n)$. It is impossible that $\{x_{2i}, x_{2i+1}\} \subset B$
for some $1 \le i < n$, since $x_{2i} + x_{2i+1} = x_{2i+2}$. Thus, we have

$$\mathbb{B}'_{max}(X_n) \subset \times_{i=1}^{n-1} \{x_{2i}, x_{2i+1}\},$$

and in particular
$$|\mathbb{B}_{max}(X_n)| \leq 2^{n-1}.$$
Consider now the set $\mathbb{B}_-(X_n)$ of internal trees. The definition of an internal tree implies directly that $x_{2n} \notin B$, hence that $x_{2n-1} \in B$, for every internal basis. Removing x_{2n-1} from each internal basis, we obtain the set $\mathbb{B}'_-(X_n)$. Now, consider the product
$$A := \times_{i=1}^{n-1}\{x_{2i-1}, x_{2i}\}.$$
If we append x_{2n-1} to any set in A, we obtain a basis $B \in \mathbb{B}(X_n)$; by induction on j, this follows from the assertion that every forest in $\times_{i=1}^{j}\{x_{2i-1}, x_{2i}\}$, $1 \leq j \leq n-1$ is a spanning tree on the subgraph that corresponds to the vertices $0, ..., j$.

Now, let $B = (b_1 \prec b_2 \prec \cdots \prec b_{n-1})$ be a tree in A. If $b_i = x_{2i-1}$, then $B \backslash b_i$ is completed to a spanning tree by x_{2i}, since $(b_1, ..., b_{i-1})$ connects the vertices $0, ..., i-1$ and each of x_{2i-1} and x_{2i} connects this vertex set to the vertex i.

If $b_i = x_{2i}$, since $J := (b_1, ..., b_{i-1})$ is a spanning tree of $0, ..., i-1$, the union $I \cup J \cup \{x_{2n-1}\}$ is full-rank, and hence b_i is not internally active in B. Thus, $A \subset \mathbb{B}'_-(X)$, and $|\mathbb{B}_-(X_n)| \geq 2^{n-1}$. This completes the proof, since the symmetry of the Tutte polynomial implies that $|\mathbb{B}_{max}(X_n)| = |\mathbb{B}_-(X_n)|$. $\square$

COROLLARY 2.3. *We have that*
$$\mathbb{B}_{max}(X_n) = \times_{i=1}^{n-1}\{x_{2i}, x_{2i+1}\} \times \{x_{2n}\},$$
and
$$\mathbb{B}_-(X_n) = \times_{i=1}^{n-1}\{x_{2i-1}, x_{2i}\} \times \{x_{2n-1}\}.$$

It is known [92] that the number of parking functions of any graph equals the number of spanning threes of that graph:
$$|S_n| = |\mathbb{B}(X_n)|.$$
The *central Hilbert series* $h_n := h_{X_n}$ is defined as
$$h_n(j) := |\{B \in \mathbb{X} : \text{val}(B) = j\}|.$$

The Tutte polynomial determines h_n; i.e h_n records the coefficients of $T_n(t, 1)$ (in reverse enumerations). Note that proposition 2.2 asserts thus that $h_n(n) = 2^{n-1}$. Parking functions could also be used to determine h_n:

PROPOSITION 2.4 (Holtz and Ron, [58]). *For each* $0 \leq j \leq n$,
$$h_n(j) = \left|\left\{s \in S(BW_n) : |s| := \sum_{i=1}^{n} s(i) = j\right\}\right|.$$
Thus there must be exactly 2^{n-1} *parking functions with* $|s| = n$.

COROLLARY 2.5. *The maximal parking functions* $S_{max}(BW_n)$ *are exactly the subset* N *of* $\mathbb{N}^n$ *of all sequences* s *that can be written as a sum*
$$s = e_1 + \sum_{j=1}^{n-1} a_j,$$
with $(e_i)_{i=1}^{n}$ *the standard basis for* $\mathbb{N}^n$, *and* $a_j \in \{e_j, e_{j+1}\}$ *for every* j.

PROOF. From proposition 2.2, we know that the number of parking functions s with $|s| = n$ is $h_n(n) = 2^{n-1}$. Since $|N| = 2^{n-1}$, we merely need to verify that $N \subset S_{max}(BW_n)$. The fact that $N \subset \{0, 1, 2\}^n$ is clear, and so is the fact that $s(n) \leq 1$ for $s \in N$. Now, suppose that $s \in N$ and $s(j) = 2$. Then $a_j = e_j$, and hence $\sum_{i=j+1}^{n-1} s(i) = |[j+1 : n-1]| < n-j$, which means that $s(k) = 0$ for some $k > i$. Finally, if $s(j) = s(i) = 2$ for some $j < i < n$, then $a_j = e_j$, while $a_{i-1} = e_i$. Hence $\sum_{k=j+1}^{i-1} s(k) = |[j+1 : i-2]| < j-i-1$, meaning that s must vanish in between j and i. Thus, s is a parking function, and our claim follows. $\square$

EXAMPLE 2.6. The maximal parking functions of BW_3 are

$$e_1 + e_1 + e_2 = (2,1,0), e_1 + e_1 + e_3 = (2,0,1), e_1 + e_2 + e_2 = (1,2,0), \text{ and } e_1 + e_2 + e_3 = (1,1,1).$$

Recall the set $\mathbb{B}_-(X_n)$ of internal bases. When restricting the valuation function to the internal bases, we obtain the *internal Hilbert series*

$$h_{n,-}(j) := |\{B \in \mathbb{B}_-(X_n) : \text{val}(B) = j\}|.$$

This function is also recorded by the Tutte polynomial and it is completely computable via the *internal parking functions* of BW_n. It is known that the cardinality of the set of internal parking functions agrees with the number of internal bases, hence

$$|S_-(BW_n)| = 2^{n-1}.$$

More concretely,

COROLLARY 2.7. *We have that* $S_-(BW_n) = \{s \in \{0,1\}^n : s(n) = 0\}$.

PROOF. Since both sets above have the same cardinality 2^{n-1}, we only need to check that every internal parking function must lie in $S_-(BW_n)$. Let s be internal. Since $d(n,n,n) = 2$, we conclude that $s(n) = 0$. Since $d(i,i,i) = 3$, for $i < n$, we conclude that $d(i) \leq 1$. $\qquad\square$

It is known, [59] that the internal Hilbert series is graded by the internal parking functions,

$$h_{n,-}(j) = \{s \in S_{n,-} : |s| = j\}.$$

We therefore conclude:

THEOREM 2.8. *The internal Hilbert series of* X_n *is binomial:*

$$h_{n,-}(j) = \begin{cases} \binom{n-1}{j}, & 0 \leq j < n \\ 0, & otherwise \end{cases}$$

We will now discuss zonotopal algebra in general, so that we have the framework for understanding the zonotopal algebra of the broken wheel graph, as well as the zonotopal algebra of the generalized broken wheel graph in section 4.

2.2. Zonotopal Spaces. Let X be a matrix whose columns lie in $\mathbb{R}^n \setminus 0$ and span $\mathbb{R}^n$. We can consider two families of variable convex (bounded) polytopes:

$$\Pi_r(t) := \{r : Xr = t, r \in \mathbb{R}_{\geq 0}\} \text{ and } \Pi_r^1(t) := \{r : Xr = t, r \in [0,1]^n\}.$$

The *box-spline* $B_r(t)$ is the volume of $\Pi_r^1(t)$. As discussed in [26], $B_r(t)$ is a piecewise polynomial. With $\mathbb{K}$ a field of characteristic zero, the *central Dahmen-Micchelli space*, or central $\mathcal{D}$-space, $\mathcal{D}(X)$ of $B_r(t)$ is the vector space in $\mathbb{K}[t_1, ..., t_n]$ generated by all polynomials in $B_r(t)$ and their partial derivatives.

Viewing X as a matroid whose ground set is the columns of X, $\mathcal{D}(X)$ can also be defined as the *Macaulay inverse system* [79] of a certain ideal $\mathcal{J}(X)$. To define this ideal, first note that a vector $r \in \mathbb{R}^n$ written in the basis $(t_1, ..., t_n)$ naturally defines the polynomial $p_r = \sum_{i=1}^n r_i t_i$ in $\mathbb{K}[t_1, ..., t_n]$; if R is a set of vectors, then let $p_R := \prod_{r \in R} p_r \in \mathbb{K}[t_1, ..., t_n]$. The ideal $\mathcal{J}(X)$ is generated by the polynomials in $\mathbb{K}[t_1, ..., t_n]$ defined by the cocircuits of X:

$$\mathcal{J}(X) := \text{ideal}\{p_C : C \subseteq X \text{ cocircuit}\} \subseteq \mathbb{K}[t_1, ..., t_n].$$

We then have that

$$\mathcal{D}(X) = \ker \mathcal{J}(X) := \{f \in \mathbb{K}[t_1, ..., t_n] : p(\frac{\delta}{\delta t_1}, ..., \frac{\delta}{\delta t_n})f = 0\},$$

where p runs over a set of generators of $\mathcal{J}(X)$. It was shown in [65] that the dimension of $\mathcal{D}(X)$ is $|\mathbb{B}(X)|$, where $\mathbb{B}(X)$ is the set of bases of $\mathbb{R}^n$ which can be selected from X. Note that we use the same notation here as we did in the section above for the spanning trees of a matrix define by a graph, as when dealing with a graphical matroid (as we are), these sets are the same.

The *central $\mathcal{P}$-space* of X is defined as

$$\mathcal{P}(X) := \text{span}\{p_R : R \subseteq X, X \setminus R \text{ has full rank}\} \subseteq \mathbb{K}[t_1, ..., t_n].$$

$\mathcal{P}(X)$ can also be expressed as a Macaulay inverse system of a *power ideal* generated by products of linear forms defining particular hyperplanes defined by X; see [27] for more details. As proven in [87], the central $\mathcal{D}(X)$ and $\mathcal{P}(X)$-spaces are dual under the pairing $\langle \cdot, \cdot \rangle : \mathcal{D}(X) \to \mathcal{P}(X)^*, f \mapsto \langle \cdot, f \rangle$, giving us that their Hilbert series are equal.

There are two more dual pairs which make up the zonotopal algebra of X. In order to define these pairs, we must define the set of *internal bases* $\mathbb{B}_-(X)$ and the set of *external bases* $\mathbb{B}_+(X)$ of X. Let $B_0 = (b_1, ..., b_n)$ be an arbitrary basis for $\mathbb{R}^n$ which is not necessarily contained in $\mathbb{B}(X)$. Let $X' = (X, B_0)$ and let

$$ex : \{I \subseteq X : I \text{ linearly independent}\} \to \mathbb{B}(X')$$

be the function mapping an independent set in X to its greedy extension in X'; i.e. for such an I, the vectors $b_1, ..., b_n$ are added successively to I unless the resulting set would be linearly dependent to get its image under ex. The set of *external bases* $\mathbb{B}_+(X)$ is then defined as

$$\mathbb{B}_+(X) := \{B \in \mathbb{B}(X') : B = ex(I) \text{ for some } I \subseteq X \text{ independent}\},$$

and the set of *internal bases* $\mathbb{B}_-(X)$ is defined as

$$\mathbb{B}_-(X) := \{B \in \mathbb{B}(X) : B \text{ contains no internally active elements}\}.$$

Note that the sets $\mathbb{B}_-(X)$ and $\mathbb{B}_+(X)$ as defined in the section above are equal to these sets for graphical matroids. We then have the following objects which define the *internal $\mathcal{D}_-$-space* and *external $\mathcal{D}_+$-space* of X:

$$\mathcal{J}_-(X) := \text{ideal}\{p_C : C \subseteq X \mathbb{B}_-(X)\text{-cocircuit}\} \subseteq \mathbb{K}[t_1, ..., t_n],$$

$$\mathcal{D}_-(X) := \ker \mathcal{J}_-(X) \subseteq \mathbb{K}[t_1, ..., t_n],$$

$$\mathcal{J}_+(X) := \text{ideal}\{p_C : C \subseteq X \mathbb{B}_+(X)\text{-cocircuit}\} \subseteq \mathbb{K}[t_1, ..., t_n],$$

$$\mathcal{D}_+(X) := \ker \mathcal{J}_+(X) \subseteq \mathbb{K}[t_1, ..., t_n],$$

where a $\mathbb{B}_-(X)$-cocircuit (or $\mathbb{B}_+(X)$-cocircuit) is a subset of X that intersects all bases in $\mathbb{B}_-(X)$ (or $\mathbb{B}_+(X)$), which is inclusion-minimal with this property. We then have that the *internal $\mathcal{P}_-$-space* and *external $\mathcal{P}_+$-space* of X are defined as:

$$\mathcal{P}_-(X) := \text{span}\{p_Y : Y \subseteq X\} \text{ and } \mathcal{P}_+(X) := \bigcap_{x \in X} \mathcal{P}(X \setminus x).$$

These three pairs of spaces make up the study of zonotopal algebras, and are discussed in great detail by Holtz and Ron in [59]. Now that we are familiar with their general definitions, we are ready to specialize our discussion to the case of the broken wheel graph.

2.3. The Zonotopal Spaces of the Broken Wheel Graph. We will now construct the zonotopal spaces associated to X_n. With $\mathbb{K}$ a field of characteristic zero, let $\mathbb{K}[t_1, ..., t_n]_j$ be the subspace of $\mathbb{K}[t_1, ..., t_n]$ consisting of homogeneous polynomials of degree j. Per [59], each graph is associated with three pairs of subspaces of $\mathbb{K}[t_1, ..., t_n]$: a central pair, an internal pair, and an external pair. As mentioned before, we will not need, and hence will not introduce, the external pair. We will first introduce the central and internal Dahmen-Micchelli zonotopal spaces $\mathcal{D}(X_n)$ and $\mathcal{D}_-(X_n)$, respectively. We would like to stress that the latter space depends on the ordering we impose on the edges of the graph. The definition we give below corresponds to ordering the edges of X_n in a reverse ordering. In fact, some of the proofs in this paper may be simplified once we use the reverse ordering. However, this reverse ordering is not inductive; the index of a given edge in the graph depends not only on

the vertices that are connected, but also on the rank of the graph. To this end, we single out, for $1 \le i \le j < n$, the following subset of X_n:

$$X_{i,j,n} := \{x_{2i}, ..., x_{2j}\} \cup \{x_{2i-1}, x_{2j+1}\}.$$

For $j = n$, the definition is as follows:

$$X_{i,n,n} := \{x_{2i}, ..., x_{2j}\} \cup \{x_{2i-1}\}.$$

The *central Dahmen-Micchelli space* $\mathcal{D}(X_n)$ is defined as the space of all polynomials in $\mathbb{K}[t_1, ..., t_n]$ that are annihilated by each of the following differential operators:

$$p_{X_{i,j,n}}(D), 1 \le i \le j \le n.$$

The *internal Dahmen-Micchelli space* $\mathcal{D}_-(X_n)$ is defined as the space of all polynomials in $\mathbb{K}[t_1, ..., t_n]$ that are annihilated by each of the following differential operators:

$$p_{x_{2i}}(D)p_{x_{2i+1}}(D), 1 \le i < n, \text{ and } p_{x_{2n}}(D).$$

Note that these definitions are derived by considering all polynomials p_C, where C is a cocircuit of X_n, and considering all differential operators which annihilate theses polynomials. This is the very construction of the central Dahmen-Micchelli space of X_n.

EXAMPLE 2.9. The differential operators which define $\mathcal{D}(X_2)$ correspond to the subsets

$$\{x_3, x_4\}, \{x_1, x_2, x_3\}, \{x_1, x_2, x_4\}.$$

Those which correspond to $\mathcal{D}_-(X_3)$ are

$$\{x_6\}, \{x_4, x_5\}, \{x_2, x_3\}.$$

Thus, while both spaces consist of polynomials in the variables t_1 and t_2 of degree not exceeding 2, the spaces themselves are different. Incidentally, the polynomial $t_2^2/2 + t_1 t_2$ lies in the first, while $t_1^2/2 + t_1 t_2$ lies in the second.

Next we will introduce the space dual to the central Dahmen-Micchelli space, called the $\mathcal{P}$-central space, and the space dual to the internal Dahmen-Micchelli space, called the $\mathcal{P}$-internal space. Here, and elsewhere, we denote by

$$p_x(D), x \in \mathbb{R}^n,$$

the directional derivative in the x direction. Also, for $Y \subset X$,

$$p_Y := \prod_{x \in Y} p_x.$$

The *$\mathcal{P}$-central space* $\mathcal{P}(X_n)$ is the space of all polynomials in $\mathbb{K}[t_1, ..., t_n]$ that are annihilated by each of the following differential operators:

$$p_{1_{i,j}}(D)^{j-i+3}, 1 \le i \le j < n,$$

and

$$p_{1_{i,n}}(D)^{n-i+2}, 1 \le i < n.$$

where $1_{i,j} := e_i + e_{i+1} + \cdots + e_j$, and $p_{1_{i,j}}(D)^k$ is k-fold differentiation in the $1_{i,j}$ direction. The *$\mathcal{P}$-internal space* $\mathcal{P}_-(X_n)$ is the space of all polynomials in $\mathbb{K}[t_1, ..., t_n]$ that are annihilated by each of the following differential operators:

$$p_{1_{i,j}}(D)^{j-i+2}, 1 \le i \le j < n,$$

and

$$p_{1_{i,n}}(D)^{n-i+1}, i \le i \le n.$$

Note that the set of differential operators given in the definition of the $\mathcal{P}$-internal space is redundant. However, we defined it in this way to demonstrate the parallels to the central case definition. This also makes it easier to check that the definition is consistent with the general definition of the internal space, as given in [**59**].

The Hilbert series of the broken wheel graph is captured by the homogeneous dimensions of the zonotopal spaces:

PROPOSITION 2.10 (Holtz and Ron, [59]). *For each $j \geq 0$, we have*

$$h_n(j) = \dim(\mathcal{P}(X_n) \cap \mathbb{K}[t_1, ..., t_n]_j),$$

and

$$h_{n,-}(j) = \dim(\mathcal{P}_-(X_n) \cap \mathbb{K}[t_1, ..., t_n]_j).$$

Recall that a polynomial space is *monomial* if it is spanned by monomials. The general theory of zonotopal algebra implies that once a $\mathcal{P}$-space of a graph is monomial, the corresponding parking functions yield a monomial basis for the space. This is exactly the case here.

THEOREM 2.11. *The zonotopal spaces $\mathcal{P}(X_n)$ and $\mathcal{P}_-(X_n)$ are monomial. Consequently, a basis for $\mathcal{P}(X_n)$ is given by the monomials*

$$m_s : t \mapsto t^s, s \in S_n,$$

while a basis for $\mathcal{P}_-(X_n)$ is given by the square-free monomials in the first $n-1$ variables.

PROOF. We simply verify that each of the aforementioned monomials is annihilated by each of the requisite differential operators. The rest follows from proposition 2.10.

Let $s \in S_-(BW_n)$, and choose $1 \leq i \leq n$. Since m_s does not involve the variable t_n, m_s is a polynomial of degree $\leq n-i$ in variables $t_i, ..., t_n$; hence, it is annihilated by $p_{1_{i,n}}(D)^{n-i+1}$. Now choose $1 \leq i \leq j < n$. Then m_s is a polynomial of degree $\leq n-i+1$ in the variables $t_i, ..., t_j$; hence, it is annihilated by $p_{1_{i,j}}(D)^{n-i+2}$. This completes the proof for the internal case.

Assume now that $s \in S_n$. Note that the characterization of s implies that $\sum_{j=i}^{n} s(j) \leq n-i+1$ (since the number of 2-entries on $[i:n]$ cannot exceed the number of 0 entries), while $\sum_{j=i}^{k} s(j) \leq n-i+2$. Thus, an analogous argument to the above yields the result. $\square$

We note in passing that the $\mathcal{P}$-external space is *not* monomial. In fact, external zonotopal spaces are never monomial unless the underlying linear matroid in the tensor of rank-1 matroids.

The general theory of zonotopal algebra tells us that the central spaces form a dual pair, and that the same is true for the internal pair. To this end, we make the following definition: Let X be a graph, and s a parking function of X. A polynomial $p \in \mathbb{K}[t_1, ..., t_n]$ is called **s**-*monic* in X if $p \in \mathcal{D}(X)$, the monomial m_s appears in the monomial expansion of p with coefficient 1, and all other monomials $m_{s'}$ that correspond to the other parking functions of X appear with coefficient 0 in this expansion.

Similarly, for an internal parking function s of X, $p \in \mathbb{K}[t_1, ..., t_n]$ is *internally* **s**-*monic* in X if $p \in \mathcal{D}_-(X)$ (for the fixed ordering of X that is considered), m_s appears in the monomial expansion of p with coefficient 1, and all other monomials $m_{s'}$ that correspond to the other internal parking functions appear with coefficient 0.

PROPOSITION 2.12 (Holtz and Ron, [59]). *Let X be a graphic matroid, and assume that $\mathcal{P}(X)$ is monomial. Then, for each parking function s of X there exists a unique s-monic polynomial in X. Similarly, if $\mathcal{P}_-(X)$ is monomial, and s is an internal parking function, there exist a unique internal s-monic polynomial in X. The collection of all s-monic polynomials in $\mathcal{D}(X)$ form a basis for $\mathcal{D}(X)$ (which is dual to the monomial basis of $\mathcal{P}(X)$); similarly for $\mathcal{D}_-(X)$.*

COROLLARY 2.13. *For each broken wheel graph BW_n, there is a unique basis for $\mathcal{D}(X_n)$ which is monic in X_n. Similarly, there is a unique basis for $\mathcal{D}_-(X_n)$ which is internally monic in X_n.*

EXAMPLE 2.14. In example 2.9, the polynomial $t_2^2/2 + t_1 t_2$ is (1,1)-monic in X_2 and $t_1^2 + t_1 t_2$ is internally (1,1,0)-monic in X_3.

3. The Stanley-Pitman Polytope

Pitman and Stanley [106] studied the n-dimensional polytope

$$Q_n(t) := \{ r \in \mathbb{R}_+^n : \sum_{i=j}^n r_i \leq \sum_{i=j}^n t_i, 1 \leq j \leq n \},$$

and outlined several of its properties as well as found an explicit expression for its volume

$$q_n(t) := \text{vol}(Q_n(t)).$$

In this section, we will draw a connection between the Stanley-Pitman polytope $Q_n(t)$ and zonotopal algebra of the broken wheel graph as well as prove theorems 0.2 and 0.3 from the introduction.

3.1. Connecting to the Zonotopal Algbra of the Broken Wheel Graph. We first need to introduce the additional variables $(u_1, ..., u_n)$ such that, for each j, we have

$$u_j + \sum_{i=1}^j r_i = \sum_{i=1}^j t_i.$$

Equivalently,

$$u_j + r_j - u_{j-1} = t_j, \ j = 2, ..., n,$$

and

$$u_1 + r_1 = t_1.$$

We then observe that these equations are equivalent to

$$X_n a = t,$$

with the $2n$-vector a obtained from the concatenated u, r by a suitable permutation: u_i corresponds to a_{21-1}, and r_i corresponds to a_{2i}. We also have the "side condition" that $a \in \mathbb{R}_+^{2n}$. With this, we have the conditions necessary to link the zonotopal algebra of the broken wheel graph with the Stanley-Pitman polytope. With this, we have that the volume polynomial $q_n(t)$ is a homogeneous polynomial of maximal degree n in the zonotopal space $\mathcal{D}(X_n)$:

THEOREM 3.1. *The Stanley-Pitman volume polynomial $q_n(t)$ is the monic polynomial in $\mathcal{D}(X_n)$ that corresponds to the parking function $(1, ..., 1) \in \mathbb{R}^n$. In addition, it is also the unique internally monic polynomial of maximal degree in $\mathcal{D}_-(X_{n+1})$ which corresponds to the unique internal parking function in X_{n+1} of maximal degree, viz $(1, 1, ..., 1, 0) \in \mathbb{R}^{n+1}$.*

PROOF. We have that $q_n(t)$ is the polynomial consisting of the sum of all the normalized monomials $\frac{m_s}{s!}$ of degree n which satisfy

$$\sum_{j=1}^i s(j) \leq i, 1 \leq i \leq n. \tag{IV.2}$$

This can be seen by applying our notation to proposition 0.1, the main theorem of Pitman and Stanley in [106]. Let C_n be the set of vectors s such that $\frac{m_s}{s!}$ is a term of $q_n(t)$. We notice that if $s \in C_n$ is a maximal parking function, then it must satisfy

$$i \leq \sum_{j=1}^i s(j) \leq i + 1. \tag{IV.3}$$

We can see this via corollary 2.5. Thus, we must have that $\sum_{j=1}^i s(j) = i$ for all j; in other words, $s = (1, ..., 1)$, making $q_n(t)$ the unique $(1, ..., 1)$-monic polynomial in $\mathcal{D}(X_n)$.

In order to show that $q_n(t)$ is the unique internally monic polynomial of maximal degree in $\mathcal{D}_-(X_{n+1})$ that corresponds to the unique internal parking function in X_{n+1} of maximal degree, we only need to show that $q_n(t) \in \mathcal{D}_-(X_{n+1})$, as our argument directly above gives us our correspondence between $q_n(t)$ and $(1,...,1,0)$, up to normalization.

We thus need to check that $q_n(t)$ is annihilated by the differential operators

$$p_{x_{2i}}(D)p_{x_{2i+1}}(D),\ 1 \le i < n+1,\ \text{and}\ p_{x_{2(n+1)}}(D).$$

We can quickly see that $p_{x_{2(n+1)}}(D)$ annihilates $q_n(t)$ as $p_{x_{2(n+1)}}(D)$ is differentiation in the t_{n+1} variable, of which there are none in $q_n(t)$. The other operators we need to consider are

$$D_{i+1}D_i - D_i^2, i = 1, ..., n.$$

When $i = n$, we have that $(D_{n+1}D_n - D_n^2)q_n(t) = D_{n+1}D_nq_n(t) - D_n^2q_n(t) = 0$, as the degree of t_{n+1} is 0 and the degree of t_n is either 0 or 1 for any term of $q_n(t)$.

For $i < n$, let's consider a term $m_s/s!$ of $q_n(t)$. If $s(i) \le 1$, we then have that $m_s/s!$ is annihilated by $D_{i+1}D_i - D_i^2$. If $s(i) \ge 2$, then let us prove that $s \in C_n$ if and only if $\hat{s} := s - e_i + e_{i+1} \in C_n$, as we will then see that the annihilation of $q_n(t)$ by the differential operators in question will directly follow from this statement. First, let's assume that $s \in C_n$. We can then see that

$$\sum_{j=1}^i s(j) = \sum_{j=1}^i \hat{s}(j) \le i.$$

Thus, $\hat{s}$ satisfies the inequalities (IV.2), meaning that $\hat{s} \in C_n$. Now, let us assume that $\hat{s} \in C_n$, and let us further assume for contradiction that $s \notin C_n$. Then there exists some i such that $\sum_{j=1}^i s(j) > i$. As $\hat{s} \in C_n$, we know that

$$\sum_{j=1}^{i+1} s(j) = \sum_{j=1}^{i+1} \hat{s}(j) \le i+1,$$

meaning that $i+1 \le s(1) + \cdots + s(i) \le s(1) + \cdots + s(i) + s(i+1) \le i+1$. This then means that $s(i+1) = 0$ and that $\sum_{j=1}^i s(j) = i+1$. But this then means that

$$\sum_{j=1}^i \hat{s}(j) = \sum_{j=1}^i s(j) = i+1 \le i,$$

a contradiction to our assumption that $\hat{s} \in C_n$. Thus, we must have that $s \in C_n$. Now, we can see, for $s \in C_n$ with $s(i) \ge 2$, that

$$D_i^2(m_s/s!) = D_{i+1}D_i(m_{\hat{s}}/\hat{s}!) = m_{s-2e_i}/(s-2e_i)!$$

and thus that the $D_i^2(m_s/s!)$ term and the $D_{i+1}D_i(m_{\hat{s}}/\hat{s}!)$ term in $(D_{i+1}D_i - D_i^2)q_n(t)$ cancel each other out. Furthermore, we know there exists a $t \in C_n$ (i.e. $t = s + e_i - e_{i+1}$) such that $s = \hat{t}$ and that $\hat{\hat{s}} \in C_n$. From this we know that the $D_i^2(m_t/t!)$ term and the $D_{i+1}D_i(m_s/s!)$ term cancel each other out, and that the $D_i^2(m_{\hat{s}}/\hat{s}!)$ term and the $D_{i+1}D_i(m_{\hat{\hat{s}}}/\hat{\hat{s}}!)$ term cancel each other out. Carrying on in this fashion, we have that all of the terms of $(D_{i+1}D_i - D_i^2)q_n(t)$ are cancelled and we have that $(D_{i+1}D_i - D_i^2)q_n(t) = 0$ as desired. We thus have that $q_n(t) \in \mathcal{D}_-(X_{n+1})$, giving us our result. $\square$

COROLLARY 3.2. *The polynomial space $\bar{q}_n(t)$ that is generated by the derivatives (of all orders) of the polynomial $q_n(t)$ is the zonotopal space $\mathcal{D}_-(X_{n+1})$. Thus, its homogeneous dimensions are binomial:*

$$\dim(q_n(t) \cap \prod_j^0) = \binom{n}{j},\ j = 0, ..., n.$$

PROOF. We know from theorem 2.11 that $\mathcal{P}_-(X_{n+1})$ is generated by the square-free monomials in the first n variables. Let's consider the generator of maximal degree, $t_1 \cdots t_n$. As we take partial derivatives of all orders of this monomial, we can see that we will generate all square-free monomials of degree $\leq n$. Thus, we have that $\mathcal{P}_-(X_{n+1})$ is the space generated by the derivatives (of all orders) of the monomial $t_1 \cdots t_n$.

Via proposition 2.12, we know that for every generator m_s of $\mathcal{P}_-(X_{n+1})$, there is a corresponding generator of $\mathcal{D}_-(X_{n+1})$ which is the unique internal s-monic polynomial in X_{n+1}.

Now, let's consider the polynomial $q_n(t)$, and let $q'(t) := D_1^{k_1} \cdots D_n^{k_n} q_n(t)$. We then know that $q'(t) \in \mathcal{D}_-(X_{n+1})$ and that the square-free monomial $D_1^{k_1} \cdots D_n^{k_n} t_1 \cdots t_n$ is a term of $q'(t)$. Let s be the exponent vector of $D_1^{k_1} \cdots D_n^{k_n} t_1 \cdots t_n$. Then we know that s is an internal parking function, meaning that $q'(t)$ must be the unique internal s-monic polynomial and thus is also a generator of $\mathcal{D}_-(X_{n+1})$.

Every generator of $\mathcal{D}_-(X_{n+1})$ is a derivative of $q_n(t)$, and every derivative of $q_n(t)$ is a generator of $\mathcal{D}_-(X_{n+1})$. Thus, we have that $\mathcal{D}_-(X_{n+1})$ is the polynomial space generated by the derivatives (of all orders) of the polynomial $q_n(t)$ as desired. $\square$

3.2. Proving Theorems 0.2 and 0.3 From the Introduction. From theorem 3.1 and corollary 3.2, the proofs of theorems 0.2 and 0.3 from the introduction become clear. Let us now prove these theorems. Recall that we denote partial differentiation with respect to t_i by D_i; i.e. with $p_i : \mathbb{R}^n \to \mathbb{R}^n, t \mapsto t_i$, we have $D_i = p_i(D)$, and $D_0 = 0$.

THEOREM 0.2. The polynomial $q_n(t)$ is the only polynomial (up to normalization) of degree n that is annihilated by each of the following differential operators

$$D_i(D_i - D_{i-1}), \ i = 1, ..., n.$$

Moreover, let $\mathcal{P}_{n,j}$ be the subspace of homogeneous polynomials (in n indeterminates) of degree j that are annihilated by each of the above differential operators. Then:

(1) $\mathcal{P}_{n,j}$ lies in the span of the translates of q_n.
(2) $\dim \mathcal{P}_{n,j} = \binom{n}{j}$.

PROOF. We show in the proof of theorem 3.1 that $q_n(t)$ is the unique internally monic polynomial of maximal degree in $\mathcal{D}_-(X_{n+1})$. We also have that $q_n(t)$ lies in the dual central zonotopal space, $\mathcal{D}(X_n)$, meaning that $q_n(t)$ is annihilated by $D_i(D_i - D_{i-1})$, for $i = 1, ..., n$, by definition. Corollary 3.2 of this note can be rephrased as saying that the space of translates of $q_n(t)$ is $\mathcal{D}_-(X_{n+1})$. We then can see that for a given degree j, we have that $\mathcal{P}_{n,j} \subset \mathbb{K}[t_1, ..., t_n]_j$, giving

$$(\mathcal{D}_-(X_{n+1}) \cap \mathcal{P}_{n,j}) \subseteq (\mathcal{D}_-(X_{n+1}) \cap \mathbb{K}[t_1, ..., t_n]_j). \tag{IV.4}$$

In other words, we have that $\mathcal{P}_{n,j} \subset \mathcal{D}_-(X_{n+1})$; i.e. we have that $\mathcal{P}_{n,j}$ lies in the span of the translates of $q_n(t)$. Furthermore, we can actually see that our inclusion (IV.4) is actually an equality, as the dimension of both $(\mathcal{D}_-(X_{n+1}) \cap \mathcal{P}_{n,j})$ and $(\mathcal{D}_-(X_{n+1}) \cap \mathbb{K}[t_1, ..., t_n]_j)$ is $\binom{n}{j}$.

The dimension of $(\mathcal{D}_-(X_{n+1}) \cap \mathbb{K}[t_1, ..., t_n]_j)$ is given to us by corollary 3.2. The dimension of $(\mathcal{D}_-(X_{n+1}) \cap \mathcal{P}_{n,j})$ is gotten by counting the number of internal parking functions of the broken wheel graph.

The uniqueness of $q_n(t)$ can then be quickly seen by the fact that $\mathcal{P}_{n,n} \subset \mathcal{D}_-(X_{n+1})$ and that $q_n(t)$ is the unique internally monic polynomial of maximal degree in $\mathcal{D}_-(X_{n+1})$. $\square$

EXAMPLE 3.3. Let's consider $n = 2$. We then have that $q_2(t) = t_2^2/2 + t_1 t_2$. The theorem above then tells us that $q_2(t)$ is the only polynomial which is annihilated by $D_2(D_2 - D_1)$ and D_1^2.

The following result gives another characterization of $q_n(t)$. It should be noted that while the following result resembles the theorem 0.2, it is the result of a rather different observation.

THEOREM 0.3. The polynomial $q_n(t)$ is the only polynomial $q(t)$ (in n variables) that satisfies the following two properties:

(1) With m the square-free monomial

$$m : t \mapsto \prod_{i=1}^{n} t_i,$$

the monomial support of $(q - m)(t)$ is disjoint of the monomial support of the polynomial

$$t \mapsto \prod_{i=1}^{n}(t_i + t_{i-1}), \ t_0 := 0.$$

(2) $q(t)$ is annihilated by each of the following differential operators:

$$(D_{j+1} - D_j)(\prod_{k=i}^{j} D_k)(D_i - D_{i-1}), \ 1 \leq i \leq < n$$

and

$$(\prod_{k=1}^{n} D_k)(D_i - D_{i-1}), \ 1 \leq i \leq n.$$

PROOF. For part (1), we can see that the polynomial $t \mapsto \prod_{i=1}^{n}(t_{i-1} + t_i)$ is exactly the polynomial $p_{n,0}(t)$, introduced in proposition 1.3. From proposition 1.3, we know that $S_{max}(BW_n) = \text{supp } p_{n,0}(t)$. In other words,

$$\text{supp } p_{n,0}(t) = \{s \in S(BW_n) : |s| = n\}.$$

We know from [106] that the only maximal parking function in C_n which gives rise to a term $m_s/s!$ of $q_n(t)$ is $s = (1, ..., 1)$. Thus, we have that $\text{supp } p_{n,0}(t) \cap \text{supp } q_n(t) = \{(1, ..., 1)\}$. And so, by subtracting the monomial m from $q_n(t)$, we can quickly see that

$$\text{supp } p_{n,0}(t) \cap \text{supp } (q_n - m)(t) = \emptyset.$$

For part (2), we again know that $q_n(t)$ must be annihilated by the differential operators in question as $q_n(t)$ lies in $\mathcal{D}(X_n)$. We can see that $q_n(t)$ is the only polynomial in n variables which satisfies both (1) and (2) because, as $q_n(t)$ is uniquely the polynomial in $\mathcal{D}(X_n)$ which corresponds to the monomial m in the basis of $\mathcal{D}(X_n)$, we have that $q_n(t)$ is the only polynomial satisfying (2) which also satisfies (1). $\square$

EXAMPLE 3.4. Considering $n = 2$, we have that $(q_2 - m)(t) = t_2^2/2$. We can then see that $\text{supp } (q_2 - m)(t) = \{(0, 2)\}$ and $\text{supp } t_1(t_1 + t_2) = \{(2, 0), (1, 1)\}$ are disjoint, and thus that condition (1) of the theorem above is satisfied. For condition (2), we can see that $q_2(t)$ is annihilated by both $D_1^2(D_2 - D_1)$ and D_1^2.

EXAMPLE 3.5. For $n = 3$, we have that $(q_3 - m)(t) = t_3^2/6 + t_3^2(t_1 + t_2)/2 + t_3 t_2^2/2$. For condition (1), we can see that $\text{supp } t_1(t_1 + t_2)(t_2 + t_3) = \{(2, 1, 0), (2, 0, 1), (1, 2, 0), (1, 1, 1)\}$ is disjoint from $\text{supp } (q_3 - m)(t) = \{(0, 0, 3), (1, 0, 2), (0, 1, 2), (0, 2, 1)\}$. For condition (2) we can see that $q_3(t)$ is annihilated by the operators

$$D_3(D_3 - D_2), \ D_3 D_2(D_2 - D_1), \ (D_3 - D_2)D_2(D_2 - D_1), \ (D_2 - D_1)D_1^2.$$

3.3. A Polyhedral Subdivision Relating to the Associahedron. Pitman and Stanley [106] describe a polyhedral subdivision of $Q_n(t)$ closely related to the *associahedron*. The *associahedron* $\mathfrak{A}_n$ is a polytope whose vertices correspond to the triangulations of the $(n+3)$-gon and whose edges correspond to *flips* of diagonal edges; i.e. removing one diagonal edge from a given triangulation and replacing it with another diagonal edge. This section is included as a review of this polyhedral subdivision of $Q_n(t)$ which Pitman and Stanley [106]
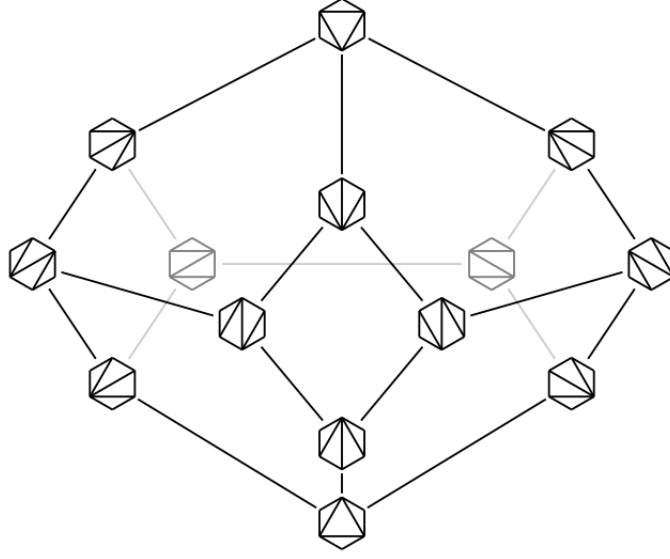
FIGURE 39. The associahedron $\mathfrak{A}_3$.

present and how the volume of each polytope in their subdivision is captured by the zonotopal algebra of the broken wheel graph. This connection was the main inspiration for the generalized broken wheel graph appearing in the coming sections.

Its dual is a simplicial complex whose vertices are diagonals of a convex $(n+3)$-gon, simplices are the partial triangulations of the $(n+3)$-gon, and whose maximal simplices are triangulations of the $(n+3)$-gon. Pitman and Stanley [106] construct a fan F_n whose chambers are indexed by *plane binary trees* with n internal vertices and prove the following result:

PROPOSITION 3.6 (Pitman and Stanley [106]). *The face poset of the fan F_n, with a top element adjoined, is isomorphic to the dual $dec(E_{n+2})^*$ of the face lattice of the associahedron.*

A *plane binary tree* is a plane tree such that each vertex has zero or two subtrees. If a vertex has zero subtrees, then we call it a *leaf*, and if a vertex has two subtrees, then we call it an *internal vertex*. The construction of the fan F_n is as follows. First consider a binary tree T. Do a depth-first search of T, labelling its internal vertices 1 through n in the order they are encountered from above. This labelling is referred to by Pitman and Stanley as the *binary search labelling*.
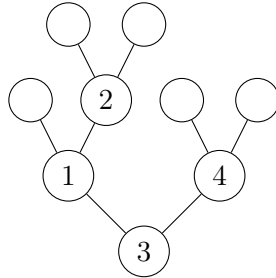
FIGURE 40. A plane tree with the binary search labelling.

If an internal vertex of T with label i is covered by j, then associate to the pair (i, j) the inequality

$$x_{i+1} + x_{i+2} + \cdots + x_j \leq 0$$

if $i < j$ and the inequality

$$x_{j+1} + x_{j+2} + \cdots + x_i \geq 0$$

if $i > j$. We then have a system of $n-1$ homogeneous linear equations which define a simplicial cone in $\mathbb{R}^{n-1}$. These cones, as they range over all plane binary trees with n internal vertices, form the chambers of a complete fan, denoted F_n, in $\mathbb{R}^{n-1}$.

Let $T \in \mathcal{T}_n$, where $\mathcal{T}_n$ is the set of binary trees with n internal vertices. Pitman and Stanley [106] then construct sets $\triangle_T(x)$ which form the maximal faces of a polyhedral decomposition Γ_n of $Q_n(x)$ whose set of interior faces, ordered by inclusion, is isomorphic to the face lattice of the dual associahedron. They also give the volume of these maximal faces.

PROPOSITION 3.7 (Pitman and Stanley [106]). *We have the following:*

(1) The sets $\triangle_T(x)$, $T \in \mathcal{T}_n$, form the maximal faces of a polyhedral decomposition Γ_n of $Q_n(x)$.

(2) Let $k(T) = (k_1, ..., k_n)$, $T \in \mathcal{T}_n$. Then $Vol(\triangle_T(x)) = \frac{x_1^{k_1}}{k_1!} \cdots \frac{x_n^{k_n}}{k_n!}$.

(3) The set of interior faces of Γ_n, ordered by inclusion, is isomorphic to the face lattice of the dual associahedron.

In order to understand this result, we must define the objects mentioned in it; let us do this. Given a plane tree T and E the set of edges of T, let's define a function $\ell : E \to \mathbb{R}_+$ sending every edge e of T to a positive real number $\ell(e)$. We will then call the pair (T, ℓ) a *plane tree with edge lengths*. Now fix a real number $s > 0$ which we would like to be the sum of the edge lengths of a plane tree. Let $x = (x_1, ..., x_n) \in \mathbb{R}_+^n$ be such that $\sum x_i < s$ and $y = (y_1, ..., y_n) \in \mathbb{R}_+^n$ with

$$y_1 + \cdots y_i \leq x_1 + \cdots x_i, \ 1 \leq i \leq n.$$

For each pair (x, y), we can assign a plane tree with edge lengths $\varphi(x, y) = (\overline{T}, \ell)$ as described in [106, p. 32]. We start with a root and traverse the tree in depth-first order:

(1) Go up distance x_i, then down distance y_i, for $1 \leq i \leq n$.
(2) Finish the tree by going up distance $x_{n+1} = s - x_1 - \cdots - x_n$ and down distance $y_{n+1} = s - y_1 - \cdots - y_n$.

We then have a planted (i.e. the root as one child) plane binary tree with edge lengths. Let T be the tree obtained by removing the roots and its incident edge from $\overline{T}$. Now let $x = (x_1, ..., x_n)$ be a sequence with $\sum x_i < s$ and let $T \in \mathcal{T}_n$ be a plane binary tree without edge lengths. We define

$$\triangle_T(x) := \{y \in \mathbb{R}_+^n : \varphi(x, y) = (\overline{T}, \ell) \text{ for some } \ell\}.$$

For $T \in \mathcal{T}_n$, with the binary search labeling of its internal vertices, let $k(T) = (k_1, ..., k_n) \in \mathbb{N}^n$ such that:

(1) $k_i = 0$ if the left child of vertex i is an internal vertex.
(2) If the left child of vertex i is an endpoint, then let k_i be the largest integer r such that there exists a chain $i < j_1 < \cdots j_r$ of internal vertices where j_h is a left child of j_{h+1} for $1 \leq h \leq r - 1$.

Proposition 3.7 tells us that the volume of every polytope in this particular subdivision of the Stanley-Pitman polytope $Q_n(t)$ is a term of $q_n(t)$, and that all terms of $q_n(t)$ appear as such volumes. So not only is the zonotopal algebra of the broken wheel graph capturing the volume of $Q_n(t)$, it is also capturing the volumes of the polytopes of a polyhedral subdivision of $Q_n(t)$ whose set of interior faces, ordered by inclusion, is isomorphic to the face lattice of the dual associahedron. This observation was our motivation for studying the volumes of polyhedral subdivisions in terms of zonotopal algebras and lead us to the generalized broken wheel graph.

4. The Zonotopal Algebra of the Generalized Broken Wheel Graph

While the zonotopal algebra of the broken wheel graph and its connection to the Stanley-Pitman polytope are rich in their own right, our study reaches even further. We will consider the zonotopal algebra of the *generalized broken wheel graph* $GBW_n(T)$ over a tree T with n vertices and how it relates to the regular simplex $\mathfrak{Sim}_n(t_1, ..., t_n)$ with positive parameters $(t_i)_{i \in [n]}$, defined by the inequalities

$$\sum_{i=1}^{n} r_i \leq \sum_{i=1}^{n} t_i, \ r_i \in \mathbb{R}_+^n,$$

where the $(r_i)_{i \in [n]}$ are variables. Since our set-up is homogeneous, we will assume without loss of generality that

$$\sum_{i=1}^{n} t_i = 1.$$

We will show how to partition $\mathfrak{Sim}_n(t_1, ..., t_n)$ into 2^{n-1} polytopes, where each polytope's volume is captured by the zonotopal algebra of $GBW_n(T)$. We begin by outlining the set-up necessary to define the generalized broken wheel graph.

4.1. Constructing the Generalized Broken Wheel Graph. Our first step in this process is to enumerate all rooted trees with n vertices. So, for example, there are two rooted trees with 3 vertices, which we will respectively call the "line tree" and the "fork tree", as illustrated in figure 41. For convenience, let's generally label the vertices of any rooted trees we consider 1 through n and always assume that the root of each tree is 1.
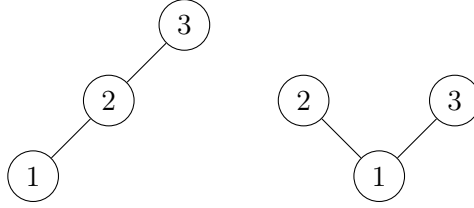
FIGURE 41. The line tree (to the left) and the fork tree (to the right).

There are 2^{n-1} different ways to direct the edges of a rooted tree T with n vertices. For $n = 3$, we have four directed trees from the line tree and four from the fork tree, as illustrated in figure 42.
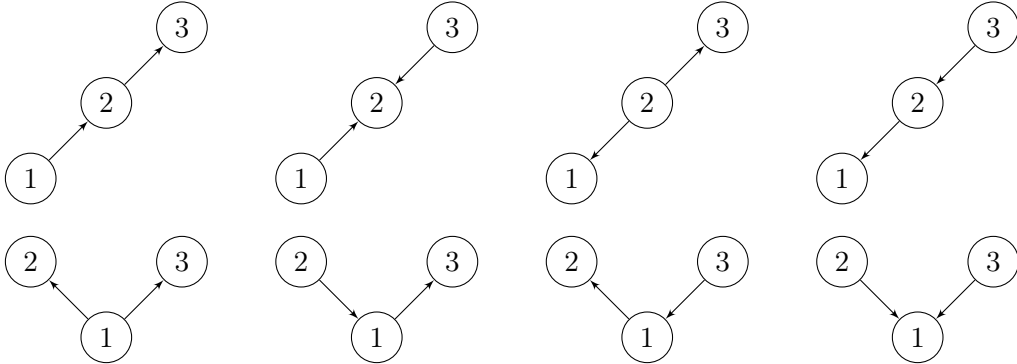
FIGURE 42. The possible ways of directing the edges of the line and fork trees.

We can identify each of the 2^{n-1} directed trees constructed via directing the edges of a rooted tree T with an n-tuple $k \in \{\pm 1\}^n$, where $k(1) := 1$ and, letting p be the parent vertex

of i,

$$k(i) := \begin{cases} 1 & \text{if the edge } (p, i) \text{ is directed towards } i \\ -1 & \text{if the edge } (p, i) \text{ is directed towards } p \end{cases}.$$

Let us denote all directed trees constructed via directing the edges of a root tree T according to k by T_k. Let $T_{k,j}$ be the subtree of T_k in which j is the root. For each directed tree T_k we define a corresponding polytope $Q_{T_k}(t_1, ..., t_n)$, which is the collection of all points $r \in \mathbb{R}_+^n$ that satisfy, for each $j \in T_k$, the set of inequalities,

$$\sum_{i \in T_{k,j}} r_i \ (\leq, \geq)_j \sum_{i \in T_{k,j}} t_i, \ j = 1, ..., n,$$

where

$$(\leq, \geq)_j := \begin{cases} \leq & k(j) = 1 \\ \geq & k(j) = -1 \end{cases}.$$

As $k(1) = 1$, we have that one of the above inequalities will always be

$$\sum_{i=1}^{n} r_i \leq 1,$$

which defines our regular simplex $\mathfrak{Sim}_n(t_1, ..., t_n)$. Thus the systems of inequalities for each of our 2^{n-1} directed trees together give a partition of $\mathfrak{Sim}_n(t_1, ..., t_n)$ into 2^{n-1} polytopes. For $\mathfrak{Sim}_3(t_1, t_2, t_3)$, the inequalities for the line tree are displayed in figure 43 and the inequalities for the fork tree are displayed in figure 44.

Now take a tree T with n vertices. For each directed tree T_k, we will complete it to a particular directed graph $GBW_n(T_k)$, which we will refer to as the *generalized broken wheel graph over T_k*. We construct $GBW_n(T_k)$ in the following way:

(1) Add one more vertex, labelled 0.
(2) Add two edges from 0 to the root vertex.
(3) Add one edge from 0 to each of the $n - 1$ vertices of T_k.
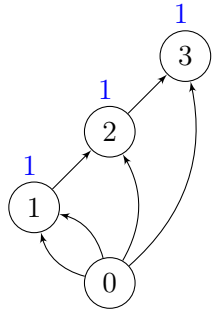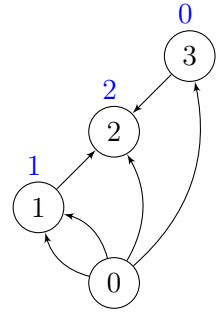
Let $GBW_n(T)$ denote the graph $GBW_n(T_k)$ without directed edges; $GBW_n(T)$ is the same for any k and will be referred to as the *generalized broken wheel graph over T*. In figure 43 we can see the graphs resulting from the line tree and in figure 44 we can see the graphs resulting from the fork tree. Once we have completed a directed tree T_k to $GBW_n(T_k)$, we will assign a weight to each of its vertices. The weight $w_{T_k}(v)$ of each vertex v of $GBW_n(T_k)$ will be equal to its indegree minus 1: $w_{T_k}(v) := \text{indeg}(v) - 1$. For instance, the weights of the $n = 3$ graphs are displayed in blue above each vertex in figures 43 and 44.

It is significant to note that $GBW_n(T)$, where T is the "line" tree on n vertices, is exactly the broken wheel graph BW_n; hence the name *generalized* broken wheel graph. In fact, the zonotopal algebra derived from BW_n is exactly the same as that which is derived from $GBW_n(T_k)$, where T is a line tree and $k = (1, ..., 1)$.

4.2. The Zonotopal Spaces of the Generalized Broken Wheel Graph. The weights of the vertices of $GBW_n(T_k)$ will guide us in constructing a polynomial $q_{T_k}(t) \in \mathbb{C}[t_1, ..., t_n]$, which will turn out to be the volume of the polytope $Q_{T_k}(t_1, ..., t_n)$. Each polynomial $q_{T_k}(t)$ has a distinguished monomial

$$\text{ref}_{T_k} : t \mapsto t^{w_{T_k}} := \prod_{i=1}^{n} t_i^{w_{T_k}(i)}, \ w_{T_k} := (w_{T_k}(1), ..., w_{T_k}(n)),$$

called the *reference monomial* of T_k. The polynomial $q_{T_k}(t)$ is constructed in the following way: the reference monomial ref_{T_k} is a term of $q_{T_k}(t)$. To get the exponent vectors of the other terms of $q_{T_k}(t)$, let's think of the weight at each vertex i of T_k as a sandpile of $w_{T_k}(i)$ grains of sand. Each grain of sand can be moved to a sandpile at another vertex j if there is an edge directed from i towards j.

k	(1,1,1)	(1,1,-1)
$GBW_n(T_k)$		
$Q_{T_k}(t_1,t_2,t_3)$	$\begin{aligned} r_1 + r_2 + r_3 &\leq t_1 + t_2 + t_3 \\ r_2 + r_3 &\leq t_2 + t_3 \\ r_3 &\leq t_3 \end{aligned}$	$\begin{aligned} r_1 + r_2 + r_3 &\leq t_1 + t_2 + t_3 \\ r_2 + r_3 &\leq t_2 + t_3 \\ r_3 &\geq t_3 \end{aligned}$
ref_{T_k}	$t_1 t_2 t_3$	$t_1 t_2^2$
$q_{T_k}(t)$	$t_1 t_2 t_3 + t_2^2 t_3 + t_3^3 + t_1 t_3^2 + t_2 t_3^2$	$t_1 t_2^2 + t_2^3$
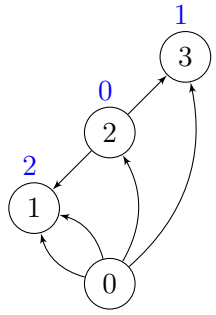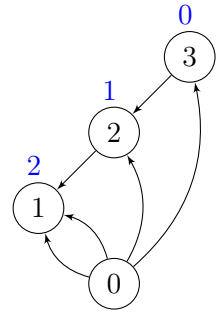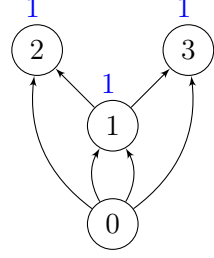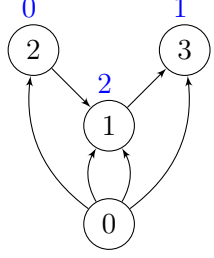
k	(1,-1,1)	(1,-1,-1)
$GBW_n(T_k)$		
$Q_{T_k}(t_1,t_2,t_3)$	$\begin{aligned} r_1 + r_2 + r_3 &\leq t_1 + t_2 + t_3 \\ r_2 + r_3 &\geq t_2 + t_3 \\ r_3 &\leq t_3 \end{aligned}$	$\begin{aligned} r_1 + r_2 + r_3 &\leq t_1 + t_2 + t_3 \\ r_2 + r_3 &\geq t_2 + t_3 \\ r_3 &\geq t_3 \end{aligned}$
ref_{T_k}	$t_1^2 t_3$	$t_1^2 t_2$
$q_{T_k}(t)$	$t_1^2 t_3$	$t_1^2 t_2 + t_1^3$

FIGURE 43. $\mathfrak{Sim}_3$ with the line tree.

More formally, a *move* can be made from i to j if $w_{T_k}(i) > 0$ and there exists an edge between i and j which is directed towards j. If a move is made from i to j, then the weight at i becomes $w_{T_k}(i) - 1$ and the weight at j becomes $w_{T_k}(j) + 1$. We then have that $w \in \mathrm{supp}\, q_{T_k}(t)$ if a series of moves can be made to get w from w_{T_k}.

EXAMPLE 4.1. Consider the top, leftmost graph in figure 44 with $k = (1,1,1)$. We know that $\mathrm{ref}_{T_k} = t_1 t_2 t_3$ is a term of $q_{T_k}(t)$. Remembering that we always start at $w_{T_k} = (1,1,1)$, we can see that a move can be made from 1 to 2 to get $(0,2,1)$, giving us the term $t_2^2 t_3$. We can also make a move from 1 to 3 to get $(0,1,2)$, giving us the term $t_2 t_3^2$. As there are no other tuples which can be reached by a series of moves, we have that $\mathrm{supp}\, q_{T_k} = \{(1,1,1),(0,1,2),(0,2,1)\}$ and $q_{T_k}(t) = t_1 t_2 t_3 + t_2^2 t_3 + t_2 t_3^2$.

We can construct zonotopal spaces from $GBW_n(T)$ in a similar fashion as we did for BW_n. For every edge (i,j) of $GBW_n(T)$ we associate the vector $e_i - e_j$ if (i,j) is directed towards i and $e_j - e_i$ if (i,j) is directed towards j. We take these vectors as columns of a matrix GX_n. From this matrix we can construct the central, internal, and external pairs of zonotopal spaces, as described in section 2.2.

k	$(1,1,1)$	$(1,-1,1)$
$GBW_n(T_k)$	graph with blue labels $1,1,1$ and nodes $2,3,1,0$	graph with blue labels $0,1,2$ and nodes $2,3,1,0$
$Q_{T_k}(t_1,t_2,t_3)$	$\begin{aligned} r_1+r_2+r_3 &\leq t_1+t_2+t_3 \\ r_2 &\leq t_2 \\ r_3 &\leq t_3 \end{aligned}$	$\begin{aligned} r_1+r_2+r_3 &\leq t_1+t_2+t_3 \\ r_2 &\geq t_2 \\ r_3 &\leq t_3 \end{aligned}$
ref_{T_k}	$t_1 t_2 t_3$	$t_1^2 t_3$
$q_{T_k}(t)$	$t_1 t_2 t_3 + t_2^2 t_3 + t_2 t_3^2$	$t_1^2 t_3 + t_1 t_3^2 + t_3^2$
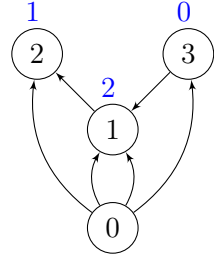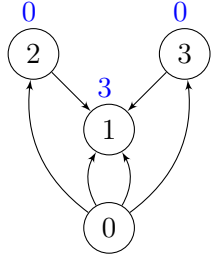
k	$(1,1,-1)$	$(1,-1,-1)$
$GBW_n(T_k)$	graph with blue labels $1,0,2$ and nodes $2,3,1,0$	graph with blue labels $0,0,3$ and nodes $2,3,1,0$
$Q_{T_k}(t_1,t_2,t_3)$	$\begin{aligned} r_1+r_2+r_3 &\leq t_1+t_2+t_3 \\ r_2 &\leq t_2 \\ r_3 &\geq t_3 \end{aligned}$	$\begin{aligned} r_1+r_2+r_3 &\leq t_1+t_2+t_3 \\ r_2 &\geq t_2 \\ r_3 &\geq t_3 \end{aligned}$
ref_{T_k}	$t_1^2 t_2$	t_1^3
$q_{T_k}(t)$	$t_1^2 t_2 + t_1 t_2^2 + t_2^3$	t_1^3

FIGURE 44. $\mathfrak{Sim}_3$ with the fork tree.

Let $\mathcal{P}_n(GX_n)$ be the space of all homogeneous polynomials of degree n that lie in the $\mathcal{P}$-central space $\mathcal{P}(GX_n)$, and let $\mathcal{D}_n(GX_n)$ be the space of all homogeneous polynomials of degree n that lie in the $\mathcal{D}$-central space $\mathcal{D}(GX_n)$. We will now show that the polynomials $q_{T_k}(t)$ form a basis for $\mathcal{D}_n(GX_n)$ and that the reference monomials ref_{T_k} form a basis for $\mathcal{P}_n(GX_n)$.

THEOREM 4.2. $\mathcal{P}_n(GX_n)$ is monomial and the monomials ref_{T_k} for each k together form a basis for $\mathcal{P}_n(GX_n)$.

PROOF. Benson, Chakrabarty, and Tetali prove in Theorem 3.1 of [9] that the set of weights,

$$\{w_{T_k} : k \in \{\pm 1\}^n, k(1) = 1\},$$

is exactly the set of maximal parking functions of $GBW_n(T_k)$. It was then shown in [92] that the set of parking functions of any graph G is the support of a monomial basis of the $\mathcal{P}$-central space associated to G. Thus the set of reference monomials, $\{\mathrm{ref}_{T_k} : k \in \{\pm 1\}^n, k(1) = 1\}$, is exactly the degree n basis elements of the $\mathcal{P}$-central space $\mathcal{P}(GX_n)$, which generate $\mathcal{P}_n(GX_n)$. $\qquad\square$

THEOREM 4.3. The polynomials $q_{T_k}(t)$ are contained in and form a basis for $\mathcal{D}_n(GX_n)$.

PROOF. A polynomial is contained in $\mathcal{D}_n(GX_n)$ if it is homogeneous of degree n and annihilated by all the operators defined by the cocircuits of $GBW_n(T_k)$. Let's consider any

cocircuit C of $GBW_n(T_k)$. We know that C is defined by a cycle in the dual graph of $GBW_n(T_k)$; let the set $\{v_1, ..., v_s\}$ be the set of vertices which are dual to C. The operator D_C defined by C is the product of operators of the form $(D_x - D_y)$ where (x, y) is an edge in $GBW_n(T_k)$ dual to an edge of C. We can see that the operator $D_{v_1} \cdots D_{v_s}$ is a factor of D_C, as all edges $(0, v_i), 1 \le i \le s$, are dual to an edge of C.

If $D_{v_1} \cdots D_{v_s}$ does not annihilate $q_{T_k}(t)$, then there must exist a vertex v_i in $\{v_1, ..., v_s\}$ such that all edges from v_i to a vertex in $\{v_1, ..., v_s\}\backslash\{v_i\}$ flow out of v_i, and such that all edges from v_i to a vertex in $\{v_{s+1}, ..., v_n\}$ flow into v_i. The product of all operators D_{v_j} such that v_j is adjacent to v_i and $v_j \in \{v_{s+1}, ..., v_n\}$ is a factor of D_C and annihilates $q_{T_k}(t)$ together with $D_{v_1} \cdots D_{v_s}$, giving us that $q_{T_k}(t) \in \mathcal{D}_n(GX_n)$. The polynomials $q_{T_k}(t)$ are then the unique s-monic polynomials, where s is the support of some reference monomial, which form a basis for $\mathcal{D}_n(GX_n)$ by proposition 2.12. $\qquad\square$

THEOREM 4.4. *The volume of* $Q_{T_k}(t_1, ..., t_n)$ *is* $q_{T_k}(t)$.

PROOF. The truncated power $Trn_X(t)$ is a function which records the normalized volume of $Q_{T_k}(t_1, ..., t_n)$. As defined in [**26**], it can specifically be identified as the function

$$Trn_X(t) := \text{vol}_{n-d}(X^{-1}\{t\} \cap \mathbb{R}_+^n)dt/|\det X|, \ t \in \text{ran } X,$$

where ran X is the range of X, d is the dimension of ran X, and X is any matrix in which 0 is an extreme point for the non-negative polytope M_X whose closed support is given by

$$\text{supp } M_X = \{Xa : 0 \le a \le 1\}.$$

It is piecewise in the $\mathcal{D}$-central space of $GBW_n(T)$, which is spanned by the 2^{n-1} polynomials $q_{T_k}(t)$. Since no edge of $GBW_n(T_k)$ ever lies in the interior of the positive octant for any k, the volume is one polynomial piece in the positive octant.

The positive octant has n facets. At least one of these facets is a part of the boundary of the support of the truncated power. The facets on the boundary depend on the k we choose. The volume polynomial $Q_{T_k}(t_1, ..., t_n)$ is thus divisible by $t_i^{w_i}$ whenever $t_i = 0$ is a boundary facet and $w_i + 1$ edges do not lie in the $t_i = 0$ facet. In our case, i will be a vertex which is a sink and w_i its corresponding weight.

For $n = 2$, there is one tree T with two possible orientations: $k_1 = (1, 1)$ and $k_2 = (1, -1)$. We then know that the polynomials $q_{T_{k_1}} = t_1 t_2 + t_2^2$ and $q_{T_{k_2}} = t_1^2$ form a basis for $\mathcal{D}(GX_2)$; so the volumes of $Q_{T_{k_1}}(t_1, ..., t_n)$ and $Q_{T_{k_2}}(t_1, ..., t_n)$ must be linear combinations of $q_{T_{k_1}} = t_1 t_2 + t^2$ and $q_{T_{k_2}} = t_1^2$, respectively. As these polynomials are divisible by t_2 and t_1^2, respectively, we can see from our observations about the truncated power that the volume of $Q_{T_{k_1}}(t_1, ..., t_n)$ must be $q_{T_{k_1}} = t_1 t_2 + t_2^2$ and the volume of $Q_{T_{k_2}}(t_1, ..., t_n)$ must be $q_{T_{k_2}} = t_1^2$.

Let's assume that the volume of $Q_{T_k}(t_1, ..., t_n)$ is $q_{T_k}(t)$ $n > 2$ for any k, and consider any tree T with $n + 1$ vertices, a k, and $GBW_{n+1}(T_k)$. We would like to find the volume of $Q_{T_k}(t_1, ..., t_n, t_{n+1})$. We can pick a leaf l of $GBW_{n+1}(T_k)$ with parent p, and consider the polytope $Q_{T_k}(t_1, ..., t_{l-1}, t_{l+1}, ..., t_{n+1})$ corresponding to the directed graph resulting from removing the edge between l and p and the edge between l and 0. We have two cases to consider: the case where the edge connecting l and p is oriented from p to l, and the case where the edge connecting l and p is oriented from l to p. For each case respectively, we have that:

(1) If the edge connecting l and p is oriented from p to l, then

$$(D_l - D_p)\,\text{vol}(Q_{T_k}(t_1, ..., t_n, t_{n+1})) = \text{vol}(Q_{T_k}(t_1, ..., t_{l-1}, t_{l+1}, ..., t_{n+1})).$$

(2) If the edge connecting l and p is oriented from l to p, then

$$(D_p - D_l)\,\text{vol}(Q_{T_k}(t_1, ..., t_n, t_{n+1})) = \text{vol}(Q_{T_k}(t_1, ..., t_{l-1}, t_{l+1}, ..., t_{n+1})).$$

Let us first begin with the case where the edge connecting l and p is oriented from p to l, as it is the quickest. In this case, as $\text{vol}(Q_{T_k}(t_1, ..., t_n))$ has all positive coefficients, we know

that

$$\mathrm{vol}(Q_{T_k}(t_1,...,t_n,t_{n+1})) = t_l \cdot \mathrm{vol}(Q_{T_k}(t_1,...,t_{l-1},t_{l+1},...,t_{n+1})) + t_l D_p \cdot \mathrm{vol}(Q_{T_k}(t_1,...,t_n,t_{n+1})).$$

Graphically this is the same as adding 1 to the weight of l, and then adding a monomial for each time you make a move from p to l. Or in other words, $\mathrm{vol}(Q_{T_k}(t_1,...,t_n,t_{n+1})) = q_{T_k}(t)$.

The second case, where the edge connecting l and p is oriented from l to p, is a bit more subtle. This is because we need to consider whether or not p is a sink. If p is a sink, then there is a t_p in every monomial of $q_{T_k}(t)$ and never a t_l. And so we can see that $\mathrm{vol}(Q_{T_k}(t_1,...,t_n,t_{n+1})) = t_p Q_{T_k}(t_1,...,t_{l-1},t_{l+1},...,t_{n+1})$, which is the same as adding 1 to the weight of p, showing us that $\mathrm{vol}(Q_{T_k}(t_1,...,t_n,t_{n+1})) = q_{T_k}(t)$.

When p is not a sink, we have to be careful because it is difficult to recover what we have lost after applying $(D_p - D_l)$ to $\mathrm{vol}(Q_{T_k}(t_1,...,t_n))$ from $\mathrm{vol}(Q_{T_k}(t_1,...,t_{l-1},t_{l+1},...,t_{n+1}))$, as we can no longer keep track of what moves out of p. So let's assume that $\mathrm{vol}(Q_{T_k}(t_1,...,t_n)) = q_{T_k}(t) + q_{T_{k'}}(t)$, where $k \neq k'$ and $q_{T_{k'}}(t)$ is divisible by a sink of T_k raised to the power of its weight. When applying $(D_p - D_l)$ to $\mathrm{vol}(Q_{T_k}(t_1,...,t_n))$, we can see that $(D_p - D_l)q_{T_k}(t) = D_p q_{T_k}(t) = \mathrm{vol}(Q_{T_k}(t_1,...,t_{l-1},t_{l+1},...,t_{n+1}))$, as there are no terms with t_l in $q_{T_k}(t)$.

We must then have that $(D_p - D_l)q_{T_{k'}}(t) = 0$. This means that either there are is no t_p or t_l as a factor of any term in $q_{T_{k'}}(t)$, which is not possible as the edge connecting p and l must be oriented towards either p or l, or there exists a pair of terms, $t_p \alpha$ and $t_l \alpha$, of $q_{T_{k'}}(t)$, where α is a monomial in $\mathbb{K}[t_1,...,t_n]$. This can only be the case if the edge connecting p and l is oriented towards l in $T_{k'}$, as that is the only way for there to even exist a term with a factor of t_l to begin with. This means, however, that $(D_p - D_l)q_{T_{k'}}(t) = -\mathrm{vol}(Q_{T_{k'}}(t_1,...,t_{l-1},t_{l+1},...,t_{n+1}))$ by the first case we considered in this proof. As $-\mathrm{vol}(Q_{T_{k'}}(t_1,...,t_{l-1},t_{l+1},...,t_{n+1}))$ is non-zero, this contradicts the fact that $(D_p - D_l)\mathrm{vol}(Q_{T_k}(t_1,...,t_n,t_{n+1})) = \mathrm{vol}(Q_{T_k}(t_1,...,t_{l-1},t_{l+1},...,t_{n+1}))$. We must then have that $\mathrm{vol}(Q_{T_k}(t_1,...,t_n,t_{n+1})) = q_{T_k}(t)$, as desired.   □

With these results we can see that the zonotopal algebra derived from a given rooted tree T completely describes a polyhedral subdivision of $\mathfrak{Sim}_n(t_1,...,t_n)$. Given how the zonotopal spaces in our study seem to capture the volumes of the polytopes and the polytopes appearing in their various subdivisions, it seems fair to suggest that the volumes of polytopes in general could be studied via their corresponding zonotopal spaces. Given a polytope, one would need to ask what the appropriate graphical matroid would be to derive the zonotopal spaces which capture its volume, and then analyze which polyhedral subdivisions come out of these spaces. This method could be a new and interesting approach towards studying volumes of polytopes.

Bibliography

1. D. Abramovich, L. Caporaso, and S. Payne, *The tropicalization of the moduli space of curves*, ArXiv e-prints (2012).
2. F. Ardila and A. Postnikov, *Combinatorics and geometry of power ideals*, ArXiv e-prints (2008).
3. N. Arkani-Hamed, J. L. Bourjaily, F. Cachazo, A. B. Goncharov, A. Postnikov, and J. Trnka, *Scattering Amplitudes and the Positive Grassmannian*, ArXiv e-prints (2012).
4. B. Assarf, E. Gawrilow, K. Herr, M. Joswig, B. Lorenz, A. Paffenholz, and T. Rehn, *Computing convex hulls and counting integer points with polymake*, ArXiv e-prints (2014).
5. M. Baker, *Specialization of linear systems from curves to graphs*, ArXiv Mathematics e-prints (2007).
6. M. Baker, Y. Len, R. Morrison, N. Pflueger, and Q. Ren, *Bitangents of tropical plane quartic curves*, ArXiv e-prints (2014).
7. M. Baker, S. Payne, and J. Rabinoff, *Nonarchimedean geometry, tropicalization, and metrics on curves*, ArXiv e-prints (2011).
8. A.T. Balaban, *Enumeration of cyclic graphs*, Chemical Applications of Graph Theory (A.T. Balaban, ed.) (1976), 63–105.
9. B. Benson, D. Chakrabarty, and P. Tetali, *G-Parking Functions, Acyclic Orientations and Spanning Trees*, ArXiv e-prints (2008).
10. Nantel Bergeron, Cesar Ceballos, and Jean-Philippe Labbé, *Fan realizations of subword complexes and multi-associahedra via Gale duality*, J. Algebraic Combin. (August 2014), 28 pages.
11. A. V. Borovik, I. M. Gelfand, and N. White, *Coxeter matroids*, Progress in Mathematics, vol. 216, Birkhäuser Boston Inc., Boston, MA, 2003.
12. S. Brannetti, M. Melo, and F. Viviani, *On the tropical Torelli map*, ArXiv e-prints (2009).
13. S. B. Brodsky, M. Joswig, R. Morrison, and B. Sturmfels, *Moduli of tropical plane curves*, Research in the Mathematical Sciences **2** (2015), no. 1, 1–31.
14. Sarah B. Brodsky, Cesar Ceballos, and Jean-Philippe Labbé, *Cluster algebras of type d_4, tropical planes, and the positive tropical grassmannian*, Beiträge zur Algebra und Geometrie / Contributions to Algebra and Geometry (2016), 1–22.
15. D. Cartwright, A. Dudzik, M. Manjunath, and Y. Yao, *Embeddings and immersions of tropical curves*, ArXiv e-prints (2014).
16. W. Castryck and J. Voight, *On nondegeneracy of curves*, ArXiv e-prints (2008).
17. Wouter Castryck, *Moving out the edges of a lattice polygon*, Discrete & Computational Geometry **47** (2011), no. 3, 496–518.
18. C. Ceballos, J.-P. Labbé, and C. Stump, *Subword complexes, cluster complexes, and generalized multi-associahedra*, J. Algebraic Combin. **39** (2014), no. 1.
19. C. Ceballos and V. Pilaud, *Denominator vectors and compatibility degrees in cluster algebras of finite type*, Trans. Amer. Math. Soc. **367** (2015).
20. Cesar Ceballos, Jean-Philippe Labbé, and Christian Stump, *Subword complexes, cluster complexes, and generalized multi-associahedra*, J. Algebraic Combin. **39** (2014), no. 1, 17–51.
21. Cesar Ceballos and Vincent Pilaud, *Denominator vectors and compatibility degrees in cluster algebras of finite type*, Trans. Amer. Math. Soc. **367** (2015), no. 2, 1421–1439.
22. Cesar Ceballos and Vincent Pilaud, *Cluster algebras of type D: pseudotriangulations approach*, preprint, `arXiv:1504:06377` (April 2015), 21 pp.
23. M. Chan, *Combinatorics of the tropical Torelli map*, ArXiv e-prints (2010).
24. _____, *Tropical hyperelliptic curves*, ArXiv e-prints (2011).
25. F. Chapoton, S. Fomin, and A. Zelevinsky, *Polytopal realizations of generalized associahedra*, Canad. Math. Bull. **45** (2002), no. 4.
26. C. de Boor, K. Höllig, and S.D. Riemenschneider, *Box splines*, Applied Mathematical Sciences, no. v. 98, Springer, 1993.
27. Carl de Boor, Nira Dyn, and Amos Ron, *On two polynomial spaces associated with a box spline.*, Pacific J. Math. **147** (1991), no. 2, 249–267.
28. C. De Concini and C. Procesi, *The algebra of the box spline*, ArXiv Mathematics e-prints (2006).
29. C. De Concini and C. Procesi, *Topics in hyperplane arrangements, polytopes and box-splines*, Universitext, New York : Springer, 2011.

30. C. De Concini, Claudio Procesi, and A. Björner, *Hyperplace arrangements and box splines*, Michigan Math. J. **57** (2008), 201–225.

31. J. De Loera, J. Rambau, and F. Santos, *Triangulations: Structures for algorithms and applications*, Algorithms and Computation in Mathematics, Springer Berlin Heidelberg, 2010.

32. C. Desjardins, *Monomization of Power Ideals and Parking Functions*, ArXiv e-prints (2010).

33. Deepak Dhar, *Self-organized critical state of sandpile automaton models*, Phys. Rev. Lett. **64** (1990), 1613–1616.

34. S. Di Rocco, C. Haase, B. Nill, and A. Paffenholz, *Polyhedral adjunction theory*, ArXiv e-prints (2011).

35. David Eisenbud, *Commutative algebra : with a view toward algebraic geometry*, Graduate texts in mathematics, Springer, New York, Berlin, Heildelberg, 1995, Réimpr. corr. en 1996. Autres tirages : 1999, 2004.

36. David Eisenbud, Daniel R. Grayson, Michael Stillman, and Bernd Sturmfels (eds.), *Computations in algebraic geometry with Macaulay 2*, Algorithms and Computation in Mathematics, vol. 8, Springer-Verlag, Berlin, 2002.

37. S. Fomin and A. Zelevinsky, *Cluster algebras I: foundations*, J. Amer. Math. Soc. **115** (2002).

38. _____, *Cluster algebras II: finite type classification*, Invent. Math. **154** (2003).

39. _____, *Cluster algebras IV: coefficients*, Comput. Math. **143** (2007).

40. Sergey Fomin, Michael Shapiro, and Dylan Thurston, *Cluster algebras and triangulated surfaces. I. Cluster complexes*, Acta Math. **201** (2008), no. 1, 83–146.

41. Sergey Fomin and Andrei Zelevinsky, *Cluster algebras. I. Foundations*, J. Amer. Math. Soc. **15** (2002), no. 2, 497–529 (electronic).

42. _____, *Cluster algebras. II. Finite type classification*, Invent. Math. **154** (2003), no. 1, 63–121.

43. _____, *Y-systems and generalized associahedra*, Ann. of Math. (2) **158** (2003), no. 3, 977–1018.

44. _____, *Cluster algebras. III. Upper bounds and double Bruhat cells*, Duke Math. J. **126** (2005), no. 1, 1–52.

45. _____, *Cluster algebras. IV. Coefficients*, Compos. Math. **143** (2007), no. 1, 112–164.

46. C. Fontanari and E. Looijenga, *A perfect stratification of M_g for g at most 5*, ArXiv e-prints (2007).

47. Ewgenij Gawrilow and Michael Joswig, *polymake: a framework for analyzing convex polytopes*, 1999.

48. _____, *polymake: a framework for analyzing convex polytopes*, Polytopes — Combinatorics and Computation (Gil Kalai and Günter M. Ziegler, eds.), Birkhäuser, 2000, pp. 43–74.

49. Ewgenij Gawrilow and Michael Joswig, *polymake: a framework for analyzing convex polytopes*, pp. 43–73, Birkhäuser Basel, Basel, 2000.

50. I.M. Gelfand, M. Kapranov, and A. Zelevinsky, *Discriminants, resultants, and multidimensional determinants*, Modern Birkhäuser Classics, Birkhäuser Boston, 2008.

51. Izrail Moiseevitch Gelfand, Mikhail M. Kapranov, and Andrei V. Zelevinsky, *Discriminants, resultants, and multidimensional determinants*, Mathematics : theory & applications, Birkhäuser, Boston, Basel, Berlin, 1994, Autre tirage de l'édition Birkhäuser chez Springer Science+ Business Media.

52. Aric A. Hagberg, Daniel A. Schult, and Pieter J. Swart, *Exploring network structure, dynamics, and function using NetworkX*, Proceedings of the 7th Python in Science Conference (SciPy2008) (Pasadena, CA USA), August 2008, pp. 11–15.

53. Douglas Hensley, *Lattice vertex polytopes with interior lattice points.*, Pacific J. Math. **105** (1983), no. 1, 183–191.

54. _____, *Lattice vertex polytopes with interior lattice points.*, Pacific J. Math. **105** (1983), no. 1, 183–191.

55. Sven Herrmann, Anders Jensen, Michael Joswig, and Bernd Sturmfels, *How to draw tropical planes*, Electron. J. Combin. **16** (2009), no. 2, Research Paper 6, 26.

56. Sven Herrmann, Michael Joswig, and David Speyer, *Dressians, tropical Grassmannians, and their rays*, Forum Mathematicum **26** (July 2012), no. 6, 1853–1881.

57. C. Hohlweg, C. E. M. C. Lange, and H. Thomas, *Permutahedra and generalized associahedra*, Adv. Math. **226** (2011), no. 1.

58. O. Holtz and A. Ron, *Zonotopal combinatorics*, (2011).

59. Olga Holtz and Amos Ron, *Zonotopal algebra*, Advances in Mathematics **227** (2011), no. 2, 847 – 894.

60. I. Itenberg, G. Mikhalkin, and E. Shustin, *Tropical algebraic geometry*, Oberwolfach Seminars Series, SPRINGER VERLAG NY, 2007.

61. I.V. Itenberg, G. Mikhalkin, and E. Shustin, *Tropical algebraic geometry*, Oberwolfach Seminars Series, SPRINGER VERLAG NY, 2007.

62. Lagarias J.C. and G. M. Ziegler, *Bounds for lattice polytopes containing a fixed number of interior points in a sublattice*, Canadian J. Math **43** (1991), 1022–1035.

63. Anders N. Jensen, *Gfan, a software system for Gröbner fans and tropical varieties*, Available at `http://home.imf.au.dk/jensen/software/gfan/gfan.html`.

64. _____, *Gfan, a software system for Gröbner fans and tropical varieties*, Available at `http://home.imf.au.dk/jensen/software/gfan/gfan.html`.

65. Rong-Qing Jia, *Local linear independence of the translates of a box spline*, Constructive Approximation **1** (1985), no. 1, 175–182.

66. V. Kaibel and G. M. Ziegler, *Counting Lattice Triangulations*, ArXiv Mathematics e-prints (2002).

67. _____, *Counting Lattice Triangulations*, ArXiv Mathematics e-prints (2002).

68. M. M. Kapranov, *Chow quotients of Grassmannians. I*, I. M. Gel′fand Seminar, Adv. Soviet Math., vol. 16, Amer. Math. Soc., Providence, RI, 1993, pp. 29–110.

69. A. Knutson and E. Miller, *Subword complexes in Coxeter groups*, Adv. Math. **184** (2004), no. 1.

70. _____, *Gröbner geometry of Schubert polynomials*, Ann. of Math. **161** (2005), no. 3.

71. R. Koelman, *The number of moduli of families of curves on toric surfaces*, Doctoral Dissertation (Proefschrift), Katholieke Universiteit te Nijmegen (1991).

72. D. Kostic and C. Yan, *Multiparking Functions, Graph Searching, and the Tutte Polynomial*, ArXiv Mathematics e-prints (2006).

73. A. G. Kouchnirenko, *Polyèdres de newton et nombres de milnor*, Inventiones mathematicae **32**, no. 1, 1–31.

74. A.G. Kouchnirenko, *Polyèdres de newton et nombres de milnor*, Inventiones mathematicae **32** (1976), 1–32.

75. J.C. Lagarias and G.M. Ziegler, *Bounds for lattice polytopes containing a fixed number of interior points in a sublattice*, Schwerpunktprogramm Anwendungsbezogene Optimierung und Steuerung: Report, Inst. für Mathematik, 1989.

76. J.-L. Loday, *Realization of the stasheff polytope*, Arch. Math. **83** (2004).

77. S. Ma, *The rationality of the moduli spaces of trigonal curves of odd genus*, ArXiv e-prints (2010).

78. _____, *The rationality of the moduli spaces of trigonal curves of odd genus*, ArXiv e-prints (2010).

79. F.S. Macaulay, *The algebraic theory of modular systems*, Cambridge mathematical library, Cambridge University Press, Cambridge, New York, Melbourne, 1994.

80. Diane Maclagan and Bernd Sturmfels, *Introduction to Tropical Geometry*, Graduate Studies in Mathematics, vol. 161, American Mathematical Society, Providence, RI, 2015.

81. _____, *Introduction to Tropical Geometry*, GTM, vol. 161, American Mathematical Society, Providence, RI, 2015.

82. _____, *Introduction to Tropical Geometry*, Graduate Studies in Mathematics, vol. 161, American Mathematical Society, Providence, RI, 2015.

83. G. Mikhalkin, *Real algebraic curves, the moment map and amoebas*, ArXiv Mathematics e-prints (2000).

84. _____, *Real algebraic curves, the moment map and amoebas*, ArXiv Mathematics e-prints (2000).

85. Ezra Miller and Bernd Sturmfels, *Combinatorial commutative algebra*, Graduate Texts in Mathematics, vol. 227, Springer-Verlag, New York, 2005.

86. G. Musiker and R. Schiffler, *Cluster expansion formulas and perfect matchings*, J. Algebraic Combin. **32** (2010), no. 2.

87. A. Ron N. Dyn, *Local approximation by certain spaces of exponential polynomials, approximation order of exponential box splines, and related interpolation problems*, Transactions of the American Mathematical Society **319** (1990), no. 1, 381–403.

88. J.G. Oxley, *Matroid theory*, Oxford graduate texts in mathematics, Oxford University Press, 2006.

89. V. Pilaud and C. Stump, *Brick polytopes of spherical subword complexes and generalized associahedra*, Adv. Math. **276** (2015).

90. _____, *Vertex barycenter of generalized associahedra*, Proc. Amer. Math. Soc. **153** (2015).

91. A. Postnikov, *Permutahedra, associahedra, and beyond*, Int. Math. Res. Not. **2006** (2009), no. 6.

92. A. Postnikov and B. Shapiro, *Trees, parking functions, syzygies, and deformations of monomial ideals*, ArXiv Mathematics e-prints (2003).

93. Alexander Postnikov, *Total positivity, Grassmannians, and networks*, preprint, `arXiv:math/0609764` (September 2006), 79 pp.

94. Jörg Rambau, *Topcom: Triangulations of point configurations and oriented matroids*, Tech. Report 02-17, ZIB, Takustr.7, 14195 Berlin, 2002.

95. Jörg Rambau, *Topcom: Triangulations of point configurations and oriented matroids*, 2002.

96. N. Reading, *Sortable elements and Cambrian lattices*, Algebra Universalis **56** (2007), no. 3-4.

97. N. Reading and D. Speyer, *Cambrian frameworks for cluster algebras of affine type*, Preprint, available at `arXiv:abs/1504.00260`, 2015.

98. Francisco Santos, *The Cayley trick and triangulations of products of simplices*, Integer points in polyhedra—geometry, number theory, algebra, optimization, Contemp. Math., vol. 374, Amer. Math. Soc., Providence, RI, 2005, pp. 151–177.

99. R. Schiffler, *A cluster expansion formula (A_n case)*, Electron. J. Combin. **15** (2008).

100. P.R. Scott, *On convex lattice polygons*, Bull. Austral. Math. Soc. **15** (1976), 395–399.

101. David Speyer and Bernd Sturmfels, *The tropical Grassmannian*, Adv. Geom. **4** (2004), no. 3, 389–411.

102. David Speyer and Lauren Williams, *The tropical totally positive Grassmannian*, J. Algebraic Combin. **22** (2005), no. 2, 189–210.

103. David E. Speyer, *Tropical linear spaces*, SIAM Journal on Discrete Mathematics **22** (2008), no. 4, 1527–1558.

104. _____, *A matroid invariant via the K-theory of the Grassmannian*, Adv. Math. **221** (2009), no. 3, 882–913.

105. Richard P. Stanley and Jim Pitman, *A polytope related to empirical distributions, plane trees, parking functions, and the associahedron*, Discrete Comput. Geom. **27** (2002), no. 4, 603–634.

106. _____, *A polytope related to empirical distributions, plane trees, parking functions, and the associahedron*, Discrete & Computational Geometry **27** (2002), no. 4, 603–602.

107. William A. Stein et al., *Sage Mathematics Software (Version 6.8)*, The Sage Development Team, 2015.

108. Christian Stump, *A new perspective on k-triangulations*, J. Combin. Theory Ser. A **118** (2011), no. 6, 1794–1800.

109. L. K. Williams, *Cluster algebras: an introduction*, ArXiv e-prints (2012).

Index